

UNCLASSIFIED

AD 265 941

*Reproduced
by the*

**ARMED SERVICES TECHNICAL INFORMATION AGENCY
ARLINGTON HALL STATION
ARLINGTON 12, VIRGINIA**



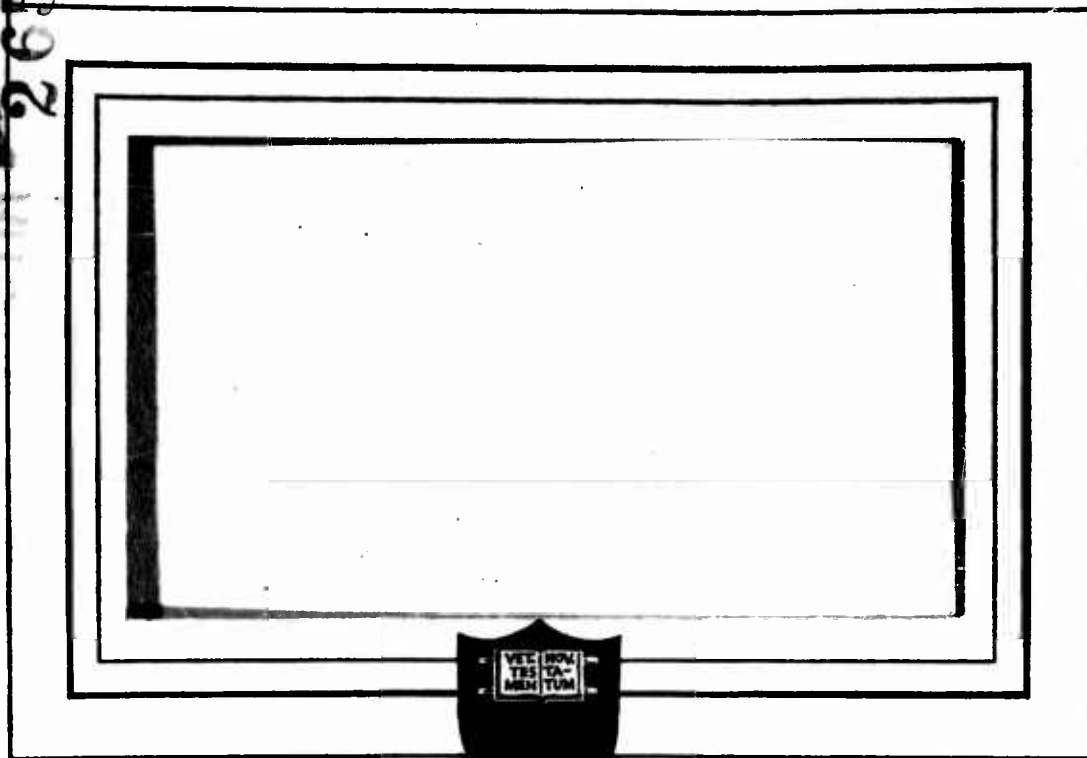
UNCLASSIFIED

NOTICE: When government or other drawings, specifications or other data are used for any purpose other than in connection with a definitely related government procurement operation, the U. S. Government thereby incurs no responsibility, nor any obligation whatsoever; and the fact that the Government may have formulated, furnished, or in any way supplied the said drawings, specifications, or other data is not to be regarded by implication or otherwise as in any manner licensing the holder or any other person or corporation, or conveying any rights or permission to manufacture, use or sell any patented invention that may in any way be related thereto.

265 941

10111

NOX
62-1-2



716300



PRINCETON UNIVERSITY

DEPARTMENT OF AERONAUTICAL ENGINEERING

U. S. Army Transportation Research Command
Fort Eustis, Virginia

Project No: 9-38-01-000, TK902
Contract No: DA44-177-TC-524

A NEW FACILITY FOR THE STUDY OF AIRCRAFT DYNAMICS

by

E. Martinez

Department of Aeronautical Engineering
Princeton University

Report No: 532

July 1961

Approved

C. J. Durbin

E. S. Durbin
Senior Research Associate

AA Nikolsky

A.A. Nikolsky
Project Leader

FOREWORD

The work covered in this report was conducted by the Department of Aeronautical Engineering of Princeton University under the sponsorship of the United States Army Transportation Research Command, as Phase 1 of work under the ALART Program. The development of the apparatus and a part of the experiments reported herein were conducted under the Office of Naval Research Contract Nonr - 1858 (11).

The work was performed under the supervision of Professor A. A. Nikolsky, Department of Aeronautical Engineering, Princeton University.

Mr. Theodor Dukes developed the associated electronic circuitry.

This work was administered for the United States Army by Mr. John Yeates.

TABLE OF CONTENTS

	Page
Summary	1
Introduction	2
List of Symbols	5
List of Illustrations	6
List of Photographs	7
Building	8
The Track and Electrical power system	12
The carriage	18
Data gathering and recording	30
Operating experience	41
a. Helicopter model	
b. Vertical take off model model	
c. Ground effect machine model	
Evaluation	53
References	58
Appendix I - Horizontal servomechanism	60
Appendix II - Vertical servomechanism	68
Appendix III - Ground effect model three-component strain gauge balance	72
Appendix IV - Method for equalization of travelling and lifted model mass	74
Illustrations	
Photographs	

SUMMARY

This report has a twofold purpose. The first is to acquaint the helicopter and vertical-take-off-and-landing engineer and designer with the use of this new model flight facility as an effective and practical tool by means of which he can economically evaluate, modify, and perfect his designs. The second one is to present the design philosophy and the experience accumulated during its development in order to provide the basis on which, in the future, other, perhaps more sophisticated facilities of this nature can be designed and constructed.

The physical plant and equipment are described in detail. A discussion on the design of the horizontal and vertical servomechanisms is presented. The design and construction of the models used in the facility are discussed briefly. Operating techniques used in the testing of a helicopter model, a vertical takeoff aircraft model, and a ground effect machine model are discussed and typical samples of the data obtained are included. A large number of photographs are shown to furnish a complete graphical description of the apparatus.

The preliminary information available from the facility has shown this new technique and apparatus to be highly effective in obtaining direct quantitative data on the dynamic stability of flying or proposed designs for helicopters, vertical or short takeoff craft.

INTRODUCTION

The successful completion of the basic forward flight facility installation marks the culmination of the program started by Princeton University in an effort to develop an effective tool to explore the dynamic behavior of rotary wing aircraft. These efforts have extended both into the realm of full scale flight testing and into the highly promising testing of dynamically similar models.

The inherent difficulties of full scale flight testing in measuring slow motions without a readily available frame of reference and the concern for pilot safety have continuously provided a strong motivation for the development of new techniques for obtaining information on the dynamic behavior of helicopters by means of easily instrumented and easily flown models designed on the basis of dynamic similitude.

The forward flight facility fills this heretofore existing gap by providing the means by which the dynamic response of a model can be obtained under controlled conditions. It allows separate evaluation of the effects of components by applying constraints as indicated by the computing techniques, thus providing simple and straightforward checks on theory.

The quasi-steady technique for stability analysis can be correlated from the response test data. The realization of the semi-free flight testing technique rests on the results of two essentially concurrent programs carried out by the Flight Mechanics Laboratories at Princeton University. One is the development of the design and construction methods of models that exhibit similar dynamic stability and control

characteristics of their full scale counterparts. The other one is the development of a servo-carriage-track system that would support the models but allow them to fly essentially free and at the same time would measure, transmit, record and present complete information on the models' motions.

Specifically, the free flight model testing technique consists of flying the models under their own power and restraining their flight to a certain vertical plane, within which the model is free to maneuver. A carriage, carrying the necessary instrumentation and providing an ever-present frame of reference to measure speeds, accelerations and attitudes, is enslaved to the models by means of horizontal and vertical servomechanisms. Position commands to the servomechanisms are generated by the model-supporting structure that allows limited freedom to the model motion without introducing disturbing forces. These signals are amplified to useful power levels and cause the carriage structure to move, following the model accurately. Within the operational range of the facility, no extraneous inputs are transmitted to the models by the carriage structure, thus insuring that only the inherent dynamics of the model are being observed.

The test area is completely enclosed in an economically constructed building, to prevent disturbing air currents and to provide weather protection.

Dynamic simulation of the aircraft is achieved by preserving in the model design the relationships between the inertial, gravitational and aerodynamic forces influencing the craft's motion. Due to the impossibility of satisfying all the conditions, the aerodynamic forces are not

rigorously simulated. However, the increased turbulence generated by the rotor wake, and the low speeds in consideration, respectively, reduce the possible discrepancies due to Reynolds number and Mach number differences. Scale factors have been chosen so as to yield models with a characteristic dimension of six feet, a size small enough to minimize building wall effects and large enough to ease somewhat the severe design restrictions imposed by the scaling down of the weight, inertia, and the blade and hub configuration.

A secondary use of the facility is to perform as a wind tunnel "in reverse". The air stands still and the model is powered through it, while the aerodynamic forces and moments acting upon it are measured. In this application its outstanding characteristics are an extremely accurate modulation of airspeed and a speed of response to control commands unattainable in conventional wind tunnels, thus allowing the exploration of transient phenomena and transition studies of vertical and short take off aircraft.

The ultimate goal of this program is to encourage the engineering approach to the design of rotary wing craft by substantiation of available theories and the development of new ones, and by providing an economical and powerful tool with which the engineer can explore, evaluate, modify, and perfect his design.

LIST OF SYMBOLS

- F_v = Force acting on vertical carriage in lbs.
 F_H = Horizontal force acting on total carriage in lbs.
 \dot{X}_v = Vertical velocity of carriage in ft./sec.
 \ddot{X}_v = Vertical acceleration of carriage in ft./sec²
 \dot{X}_H = Horizontal velocity of carriage in ft./sec.
 \ddot{X}_H = Horizontal acceleration of carriage in ft./sec²
 \dddot{X}_H = Rate of change of horizontal acceleration in ft./sec³
 M_i = Model counterweight in slugs.
 M_2 = Counterweight for M_i and M_H combined in slugs.
 M_v = Mass of vertical carriage in slugs.
 M_H = Total mass of carriage in slugs.
 M_M = Model mass in slugs.
 D_v = Diameter of vertical drive sprocket in in.
 D_H = Diameter of horizontal drive wheel in in.
 K_D = Overall drive constant in in. lb./volt.
 K_1 = Tachometer gain constant volts/rad/sec.
 K_A = Amplifier gain constant in amps/volt.
 K_P = Potentiometer gain constant volts/in.
 K_S = Hydraulic motor torque constant in in³.
 K_M = Hydraulic motor displacement constant in in³/rev.
 K_L = Hydraulic leakage factor in in⁵/sec. lb.
 K' = Vertical drive velocity constant in in. sec./volt
 K_{FB} = Feedback potentiometer constant volts/rad.
 K_v = Valve flow constant in in³/amp.sec.

K_E = Yoke drive constant in rad./in³.
 T = Time constant in sec.
 T' = Closed loop time constant in sec.
 T_2 = Effective time constant of tachometer network in sec.
 T_3 = Time lag constant in sec.
 T_5 = Closed loop yoke position effective time constant in sec.
 f = Mechanical viscous damping constant in lbs/in./sec.
 P = Model pitching moment in in. lb.
 L = Model lift in lbs.
 D = Model drag in lbs.
 F_M = Strain gage reading of pitching moment.
 F_L = Strain gage reading of lift.
 F_D = Strain gage reading of drag.
 m, n, p = As shown in Figure 18.
 a = Horizontal projection of line A B in Figure 18.
 b = Vertical projection of line A B in Figure 18.
 T_M = Hydraulic motor torque output in lb.
 P_F = Pressure of hydraulic fluid in lb./in².
 \dot{P}_F = Rate of change of hydraulic fluid pressure in lb./in² sec.
 F_D = Force transmitted by drive wheel in lb.
 N = Ratio of output rpm to input rpm through gear box.
 Q_p = Flow through pump in in³.
 Q_M = Flow through motor in in³.
 Q_L = Leakage flow in in³.
 Q_c = Volume change due to compressibility in in³.
 \dot{Q}_p = Rate of flow through pump in in³/sec.

\dot{Q}_m = Rate of flow through motor in in³/sec.
 \dot{Q}_L = Rate of loss due to leakage in in³/sec.
 \dot{Q}_c = Rate of loss due to compressibility in in³/sec.
 Θ_T = Yoke angle in rad.
 Ω_m = Motor output in rad./sec.
 V = Volume of hydraulic fluid in in³.
 B = Hydraulic fluid bulk modulus in lb./in².
 ω_n = Natural frequency of system in cycles/sec.
 ξ = Damping factor
 α = Compensating network lead time constant factor.
 v_i = Amplifier output in volts.
 $V(s)$ = Laplace transform of amplifier output.
 $E(s)$ = Laplace transform of servomechanism position error.
 $V_p(s)$ = Laplace transform of potentiometer voltage output.
 $\Theta(s)$ = Laplace transform of yoke motion.
 $G(s)$ = Forward loop transfer function.
 $H(s)$ = Feedback loop transfer function.
 $X_v(s)$ = Laplace transform of vertical motion.
 $X_h(s)$ = Laplace transform of horizontal motion.
 $X_m(s)$ = Laplace transform of model motion.

ILLUSTRATIONS

Figure

- 1 Typical time histories of fuselage variables of free oscillations during hovering test of a helicopter model
- 2 Horizontal position servomechanism
- 3 Horizontal position servomechanism - transfer functions of the various components
- 4 Approximate linear open-loop frequency responses of horizontal hydraulic position servomechanism
- 5 Approximate open-loop gain-phase plot of the horizontal position hydraulic servomechanism and the describing function of the non-linearity introduced by saturation and dead zone in the system
- 6 Velocity servo
- 7 Hydraulic drive schematic
- 8 Vertical servomechanism
- 9 Vertical servomechanism - Transfer functions of the various components
- 10 Schematic of the vertical magnetic fluid clutch drive
- 11 Approximate linear open-loop frequency response of vertical position clutch drive
- 12 Mechanical schematic of strain gauge balance
- 13 Variation of character of long period mode with horizontal link mass of a helicopter model
- 14 Method for equalizing lifted and traveling mass
- 15 Hovering carriage servomechanism with the transfer function of the various components
- 16 Constant velocity servomechanism with magnetic fluid clutch drive
- 17 Block diagram of static and dynamic data gathering system
- 18 Schematic drawing of the three-component strain gauge balance for ground effect models.
- 19 Typical transient response of helicopter model about forward flight trim condition.

PHOTOGRAPHS

Figure

- 26 Carriage and track -- general view
- 27 General rear view of the carriage
- 28 Error link
- 29 Model controls
- 30 Vertical servo
- 31 Vertical servo drive and carriage controls
- 32 Hydraulic drive installation
- 33 Hydraulic drive installation
- 34 Servo amplifiers
- 35 Telemeter
- 36 Power supply installation
- 37 Two-degree of freedom rig
- 38 Control console
- 39 Forty-five channel scope presentation of test data
- 40 Ground station and recording equipment
- 41 Boost system
- 42 Emergency Mechanical brake
- 43 Hovering track -- servo controls
- 44 Hovering track -- general view
- 45 Ground effect machine three-degree of freedom rig
- 46 Ground effect machine rig -- error links
- 47 General view of control room
- 48 Flight simulation equipment

BUILDING

In full scale testing disturbances in the aircraft motion due to random air motions are difficult to account for, especially at low flight speeds. In testing scaled down models these disturbances become magnified and if flight program schedules are to be independent of weather conditions, some type of shelter is required to insure that the model motion is the resultant of bona fide inputs.

The dimensions of the appropriate shelter are of considerable magnitude and its construction demands the expenditure of a significant fraction of the total cost of the facility. Keeping in mind cost considerations of the sheltering structure, it is logical to state the bare minimum requirements that will produce satisfactory results. First the cross sectional dimensions determine the maximum size of models that can be tested in the facility. Wind tunnel experience has shown that it is desirable to have wall clearances of the order of one and a half rotor diameters. Also the height of the building can be dictated by the desired altitude variations during the model's flight. These two combined requirements have to be evaluated in the light of the difficulties encountered in the model scaling-down process.

A satisfactory engineering compromise between the tendency to build larger models and the economic pressure to erect smaller buildings has been attained at this facility with models that are approximately six to eight feet in their largest dimensions and a building cross section of about thirty by thirty feet.

The length of the building is a function primarily of the top

speeds to be attained by the model during the experiments. Another consideration is the period of free oscillation of the model and the number of cycles required to yield meaningful information on the damping characteristics of the motion, limitations on assumptions of linearity, etc.

Scaling down the aircraft reduces both the required velocity and the period and is one of the factors that makes eminently practical the model free flight technique under controlled conditions.

If model flight speeds of the order of seventy feet per second are envisioned in such a facility (as they are at Princeton) and taking in account carriage traction limitations, the acceleration and braking phases of the run can use up as much as three hundred of track length. This estimate does not include time allowed for the settling out of acceleration transients nor possible emergency braking track length. A degree of improvement can be obtained by the use of an external power source to accelerate the carriage by positive means (independent of drive wheel-track friction) and an external braking system that can absorb safely the carriage kinetic energy at high rates. This approach was adopted in this facility. (see Figures 41 and 42)

A practical limit is reached as the structural strengths of the carriage and model are taxed by the stresses generated by the high accelerations.

Although the design has to be directed to the maximum specifications, an overwhelmingly large number of tests are performed at the lower speeds, and only in rare cases is the maximum potential of the facility called upon. This of course determines design concepts of the external boosting and braking equipment and consequently the total

building length.

Another question is what to do about interior temperature and temperature gradients in the building and their effects in the test results. The Princeton facility was built, for various reasons, in two stages. The original section of the building was effectively insulated but unheated. This prevents high rates of heat transfer, reducing correction currents, too fast temperature changes and gradients in the building atmosphere.

During hot summer months temperature gradients of approximately one half degree Fahrenheit per foot of altitude have been observed. It is to be noted, however, that no significant effects in test results have been recorded, possibly due to the thorough mixing by the model rotor flow after a few runs.

The second half of the building, which was built later, is not insulated at all. This has not noticeably influenced the test results. This simpler and more economical method of construction used in the second section of the building appears quite satisfactory for this type of installation, providing the necessary shelter for the minimum investment.

The climate inside the building is still quite rigorous and some measure of protection for the equipment is sometimes required.

Plans have been completed for the construction of an enclosure at the starting end of the building to maintain the carriage and the model including the electronic equipment at favorable temperature and humidity conditions while not in use. The control console, ground station and other electronic equipment in the control room require temperature control.

Details of the Princeton facility building construction are now given. Photographs in Figures 26 and 44 show the interior of this building.

The facility is enclosed in a low cost building of a minimum cross section of thirty by thirty feet and a length of seven hundred and sixty feet. The structure is made of steel trussless frames, for maximum internal clearance, spaced twenty feet apart. It is covered with light gauge corrugated aluminum sheets. The building was constructed in two separate stages, a few years apart. The first four hundred and sixty foot section is insulated by glass wool, and has a relatively elaborate lighting arrangement. A three hundred feet extension was added, without insulation and with minimum lighting. The floor throughout consists of a four inch concrete slab.

A small adjoining building houses the machine shop, model shop, control room and the analog computer installation.

The cost of the total building is approximately \$75,000.

THE TRACK AND THE ELECTRICAL POWER SYSTEM

The function of the track is to support and guide the carriage and to furnish the electric power required by the traveling apparatus. The operation principle of the facility makes it imperative that the basic carriage be restrained mechanically in all degrees of freedom except one: the horizontal direction; and the motions of the carriage in this dimension are accurately monitored and recorded at all times. It then fulfills the role of a frame of reference against which all model motions can be accurately measured.

The choice of track geometry is largely dictated by the basic geometry of the carriage. Its structural rigidity and strength influence strongly the performance of the carriage servomechanisms and limit the weight of the model and of the traveling instrumentation. Its accuracy in following a straight line determines the amplitude of unwanted disturbances to the motion of the model. These disturbances have to be kept down to an acceptable level throughout a wide range of temperature conditions; also, simple adjustments should correct long range deviations and misalignments.

Such considerations largely determined in general the construction of a monorail type of structure with special provisions to allow for thermal expansion (which otherwise would total as much as a foot). Special emphasis was placed in obtaining a large degree of longitudinal rigidity by means of the track's own structure. However, lateral stiffness was increased by attaching the track at regular intervals to the building frames; this proved only partially successful, because the main

building members in spite of their large size have shown surprisingly low stiffness. With the carriage placed in a given section of the track it is possible to excite a lateral track oscillation that will transmit itself to a sizeable portion of the building. These oscillations are of low frequency and rather heavily damped, but because of the carriage forward motion, no sustained lateral oscillations have been observed. The disturbances most deleterious to the servomechanism performance are those produced by areas of high resistance to the carriage motion. These sharp inputs produce instantaneous errors of a magnitude that excite the divergent non-linear mode of the servo.

The monorail design allows easy adjustments to be made within certain limits in the vertical and in the lateral alignment of the structure.

Another function of the track is to support the copper rails that deliver electric power to the carriage. (The choice between driving the carriage by a self-contained system carried along, or driving it by means of an outside motive power source will be discussed in the section dealing with the carriage design).

Each power rail consists of one continuous copper strip of such dimensions as to minimize the voltage drop along the length of the track. The normal current drawn by the idling carriage and instrumentation totals about thirty amperes, producing a drop of approximately five volts at the carriage with the maximum length of conductor rail.

During active servo operation or during acceleration, this current may go up to sixty amperes. At the starting portion of the track, which is the closest to the generator, the transient voltage drops have no

noticeable effects on the carriage dynamics. Yet, at the farthest sections of the track they can be of sufficient magnitude to decrease the input voltage to the Zener diode-controlled voltage sources, used as the servo references, below their effective regulating range. When this occurs, erratic output voltages from these power supplies may cause unstable servo operation.

Operating experience has shown that effects of this nature can be avoided most of the time by a moderate increase of the generator voltage above its normal rated output. Over-voltages may then occur at certain sections of the track with unfavorable results on the life of the equipment. It appears that a generator voltage regulating scheme with feedback from the actual track voltage may be the only fully satisfactory solution.

To fulfill the demand for compact and lightweight components, specially in the electric motors furnishing the motive power for the carriage, and to comply with the severe weight limitations in the design of the flying models propulsion units, a 400-cycle 3-phase electric power system was chosen. For use in equipment transported by the carriage whose weight must be kept, for dynamic consideration, as conservative as possible, the eminent suitability of lightweight aircraft type of motors and other components operating on this power, more than offsets their relatively higher cost and longer delivery schedules.

The dynamic testing of models in this facility can be divided into two phases: hovering dynamics and forward flight dynamics.

To examine the hovering dynamics of an aircraft model only a short track length is required; furthermore, since during the stick-fixed re-

sponse the altitude of the model remains essentially constant, no active vertical following is necessary: The limited vertical freedom allowed by the supporting linkages is sufficient for free-flight conditions.

These limited requirements have led to the erection of a short length of track outfitted with a simplified carriage for the purpose of conducting hovering experiments. The fact that experiments can be performed concurrently in both tracks adds significantly to the operating efficiency of the facility by permitting phasing in one model for hovering tests while studying another model's dynamics in the forward flight regime. The amount of time saved by a simplified hovering track can best be appreciated when one considers that at least seventy-five per cent of the time during which a model occupies the facility is spent in readying it for the runs. By overlapping both operations a smoother testing program of various models can be achieved.

Details of the track construction can be seen in Figures 26 and 27. A summary of pertinent details on the track and electric system is now presented.

THE TRACK is located at approximately five feet from a wave so that the model gyrations take place approximately in the center of the enclosure to insure maximum clearance.

The structural part of the track consists of a series of steel columns spaced ten feet apart and supporting twenty foot lengths of steel I-beams. An aluminum I-beam is mounted on the steel beam by means of adjustable jack screws. To allow for thermal expansion--which in a track of this length would be twelve inches for the aluminum beam--the steel I-beams were bolted down at their midpoint and the ends were re-

strained by sliding plates that allow longitudinal motion. The motion between the aluminum and steel beams was taken care of simply by oversize holes for the jack screws. Thus the track is essentially a series of twenty foot lengths separated by minimum clearances and free to expand without affecting the neighboring sections.

The transversal stiffness of the track has been increased by anchoring it to the building frames every twenty feet. The complete assembly has been constructed so that the deviations of the top member do not exceed the level plane by more than a quarter inch.

To restrain the carriage in "roll", a deep structural steel channel section is located at a lower level and is attached to the columns in such a way as to allow also for thermal expansion. To restrain the carriage in "yaw", an angle aluminum section is welded to the top aluminum beam.

A similarly constructed section, fifty feet in length, has been erected on the opposite side of the building for the sole purpose of handling hovering tests.

THE ELECTRICAL POWER is furnished by a motor generator set rated at 75 KVA. The output voltage is 3-phase 115 volts alternating current at 400 cycles in wye connection. The prime mover is a 3-phase 115 volts 60-cycle motor.

Field excitation is provided by a self-contained DC generator and the main generator voltage output is continuously variable throughout its entire range by controlling this field excitation.

The generator is connected to the rails at a point about one third from the starting end of the track. Electric power is drawn

by the carriage from four copper rails running the length of the track and supported by continuous clamps insulated from the rest of the structure. These clamps hold the copper strips in place, but allow them to slide; this prevents buckling due to thermal expansion. The dimensions of the rails, 1.25 inch in width and .125 inch in thickness, insure that the maximum voltage drop is no more than two volts for a load of 30 amperes, which is the current drawn during normal operation.

The electric rails are divided into two sections that can be powered either independently or simultaneously, to afford the possibility of two concurrent tests in the track.

THE CARRIAGE

The application of the concept of a servo-carriage following a flying model places automatically some stringent conditions on the weight, rigidity and drive characteristics of its design. The scope of the proposed tests to be performed further determines its basic geometry. Even within these bounds a large number of designs present themselves. However, these basic requirements are a good yardstick by which the merits of a given design can be evaluated.

The desired altitude excursions allowed the model have been a dominant factor in the present choice of carriage configuration. Another important requirement was that these variations in general must be made to occur at heights from the floor such that ground effect phenomena do not occur.

Specifically, it means removing the model at least one and a half rotor diameters from the floor in its lowest position and permitting an additional vertical freedom of approximately ten feet. Structurally the mechanical design of the vertical freedom forms the major portion of the overall carriage and was decided at the early stages of the planning. Various possibilities were brought up for consideration in this application: a telescoping vertical boom, a crane-type structure and a pantograph configuration, all three hydraulically operated.

VERTICAL FREEDOM. After examination of the stiffness of the above proposed schemes, and an estimate of the total carriage mass that each of these would entail, they were abandoned in favor of a

simple vertical track consisting of a large diameter tube 12 foot long, with the actual track located at one of the diameters. On their track a light weight cast aluminum carriage rides on a set of adjustable rollers. The working surfaces of this track have been accurately machined to provide low friction rolling action with the minimum clearance and play of the vertical carriage.

Attached to this carriage, there is a model-supporting six foot boom. This boom is constructed of sheet aluminum and it tapers from a broad base at the carriage end to a two-inch diameter at the model support linkages, so as to increase its stiffness and reduce possible interference effects at the model's rotor wake.

This assembly is driven by a fine pitch stainless steel chain. The chain forms a closed loop running over the drive sprocket and a number of guiding idler sprockets. The vertical carriage weight (not including the model that lifts its own weight during powered flight) is almost completely counterbalanced by a guided weight riding inside the vertical tube. This weight was necessary to remove a prohibitive constant load on the clutch drive. A net moderate unbalance is kept to insure that, in the case of a drive failure, the vertical carriage assembly will accelerate downwards where safe braking and shock absorbing devices have been installed. Shock absorbers of somewhat less capacity provide a safe stop on the top end of the tube when the model motions exceed the operating altitude range of the vertical servomechanism.

The vertical track is a seven-inch diameter aluminum tube with provisions for attaching it to the carriage at two points along its

length calculated to produce the maximum torsional and bending stiffness. Large torsional stresses are applied to the vertical structure during acceleration and braking when the full model inertia forces are transmitted through the large moment arm of the support boom. This has dictated the choice of a cylindrical shape for the basic track member. Excessive flexibility or play of this structure would be a direct cause of servo instability and response deterioration. The absence of oscillatory response of the servo traceable to structure flexibility has shown this design to be a sound approach to the vertical tracking of the model.

ERROR LINKAGES. The error linkage assembly allows the model to move horizontally and vertically for a limited distance with negligible friction. The relative position of the model to the center position of the linkage, once transformed into an electrical signal by means of potentiometers, is used as the input commands to the servomechanisms that position the carriage, so as to shift the link center to the model position.

To minimize friction, the sliding motions take place on linear ball bearings riding on hard chrome-plated polished rods. The friction level is extremely low since during flight, the model lifts its own weight, thereby unloading the bearings. Friction is further reduced by the vibration of the structure experienced during test runs.

A direct consequence of the orthogonal breakdown of the model motions is the change produced on the model mass by the error or servo linkage masses. On the horizontal component of the motion, the model carries besides its own mass, both the mass of the horizontal and vertical slides. But when it moves vertically, it carries only the vertical

slide, thus in effect exhibiting a lifted mass different from the horizontally traveling mass. This effect has been relatively small with the 25 pound models used. Ratios of traveling to lifted mass have been kept down to a moderate level by careful design and extensive use of magnesium and aluminum alloys in the linkage construction. However, to reduce further this discrepancy, rather difficult conditions are imposed on the mechanical design of the servo linkages. They must withstand the severe stresses generated by the model, especially during acceleration and braking and the possible untrimmed yawing moments. The link assembly provides plus-minus nine inches of horizontal travel and plus-minus three inches of vertical travel representing the limits for the allowable combined transient and steady state errors between the model and the carriage.

For most of the tests performed the servo linkages are mechanically locked as close as possible to the electrical null points of the error potentiometers during the acceleration phase. In this way no position command is applied to the carriage. The horizontal servo then is solely controlled by the velocity command potentiometer, until the carriage has reached the desired velocity (model trim velocity). A cam located in the track operates a switch on the carriage, releasing the locks, and allowing the now free flying model position to command the carriage motions.

Other designs for error linkages are possible. A promising approach would be to substitute the two orthogonal linkages by a single arm supporting the model. The model end of the arm would be free, within certain limits, to assume any position on the surface of an imaginary sphere of radius equal to the arm length. A gimbal or universal type of attachment to the carriage would be quite adequate for this mechanism. The

error signals to be applied to the servomechanism can then be derived from potentiometers that translate the horizontal and vertical angular displacement from an arbitrary reference into a suitable analog voltage.

MAGNETIC FLUID CLUTCH CARRIAGE. The first carriage was designed and built around the vertical track tube. By using it as the main structural element in addition to its guiding function, appreciable weight savings were attained. The rest of the carriage was a simple structure of square aluminum tubing supporting the servo drive and fitted with a number of guide rollers.

The horizontal servo drive of this carriage consisted of a bidirectional magnetic fluid clutch drive powered by a 3-horsepower synchronous motor. To obtain a large torque output four clutches were used: two for each direction of rotation. The principle of operation of this drive is similar to that of the vertical drive shown in Figure 10. It transmitted its motion to the carriage through a single Micarta drive wheel.

The drive itself shows an excellent response but its limited power output operating on a relatively large carriage mass resulted in poor response and low velocity capabilities.

Since at this stage the goal was to develop first the horizontal tracking capabilities, the vertical track structure was replaced by a minimum weight structure that provided only for horizontal following, improving its performance to a level sufficient to track effectively a helicopter model during stick-fixed oscillations in hovering.

This carriage also was used in spite of its limitations to

obtain some transition data on a tilt-wing vertical take-off model. A top speed of about 26 feet per second was obtained and at times some inverse transition maneuvers were examined by boosting the carriage speed through external application of power and then allowing its speed to decay.

The experience derived from operating this carriage clearly pointed out the need for much higher power levels to propel the carriage if a truly flexible facility was desired.

The inherent difficulties and limitations of the friction drive lie on the dissipation of the large quantities of heat generated during its operation. Being a non-conservative system, as most velocity or acceleration modulating systems tend to be, a large fraction of the energy input was transformed into useless heat. Convection and conduction were not sufficient to stabilize the temperature at a reasonable level, and eventually the electric coils buried in the clutches could not dissipate their own energy and burned out.

A higher power level system would present similar difficulties if not carefully chosen for this particular application. Also higher power in general means a reduction of the speed of response.

After a survey of the available sources of motive power for use in this facility it was decided that a variable displacement hydraulic pump and rotary motor system would fulfill the response requirements at the high power levels demanded by a fully flexible and adaptable facility.

THE HYDRAULIC SERVO CARRIAGE: The functions of the higher powered carriage are fundamentally unchanged: it supports the model

at rest and follows it while it is in flight, and it also restricts the model motions to the ones prescribed by the experiment. A major part of the instrumentation for gathering the data is borne by the carriage, which also carries its own complete servo drive and controls, the data amplification and telemetering equipment, a variety of power supplies for the excitation of the instruments and controls. It also contains a pneumatic system that provides power for actuating the model locking and releasing devices.

The flexibility required to use the apparatus for a wide variety of experiments has led to the design of a "basic" carriage which can perform the fundamental tasks common to all the experiments, i.e. horizontal tracking, data transmission, ground controls, etc. To adapt this basic carriage to a specific experiment, a series of "rigs" have been developed. Each rig is individually and permanently wired and instrumented to perform its particular job. The method of attachment to the basic carriage permits swift change from one experimental setup to another.

All the electrical connections at the model end and basic carriage end are made with suitable quick disconnect separated electric connectors.

Up to now, three rigs have been completed. One is used for two-degree of freedom operation, i.e., to allow the model to pitch and to move horizontally. This structure is also used for wind tunnel type experiments where the aerodynamic forces and moments acting on the model are measured.

Another rig has been designed and constructed to be used in the

steady state and dynamic testing of ground effect machines. Its design allows the flying of models a short distance from the floor, as compared to the other rigs that are used for flying models at an average distance of about twelve feet above the floor.

The third and most elaborate structure is the vertical track (discussed in a previous section of this chapter) which in conjunction with the basic carriage will permit the model to have three degrees of freedom. In this arrangement, models are attached to the servo link assembly which in turn is bolted at the outboard end of the horizontal boom.

From the point of view of its dynamic behavior, the hydraulic system consists basically of two major portions: the control circuit that positions the yoke and the power circuit that operates on the load through the hydraulic motor.

The transfer function of the hydraulic power circuit contains a quadratic term in the denominator, presenting the possibility of an oscillatory response. (See Appendix I.) This response has failed to materialize in the actual system, mainly due to the large ratio of fluid bulk modulus to the volume of fluid contained in the circuit and the existence of relatively large internal leakage in the system.

The inherently high response of the yoke control circuit can be improved further by the yoke position feedback with the result that its time lag is practically negligible. The corner frequency of the quadratic term in general determines the response of the system, and it occurs at a rather low frequency (12 radians per second). In an effort to shift this cross-over frequency to a higher value, a lead

term was introduced by installing a tachometer to generate a signal proportional to the relative speed between the model and the carriage. This in effect produces an error rate voltage in parallel with the error voltage. A gain potentiometer permits manipulation of the time constant of the resulting first order lead.

Further improvement was obtained by an additional lead term to neutralize more effectively the third order slope characteristics of the forward loop. This was accomplished by a R-C type lead lag network operating on the output of the error rate tachometer, and in parallel connection also with the error signal.

The compensations of the hydraulic dynamics discussed above have resulted in a satisfactory response for the present test programs with commensurate stability. However, it is possible that testing of models with much shorter periods of oscillation, or the need to investigate rapid maneuvers of aircraft, may demand further improvements in the carriage performance.

It is to be noted here that although the brief discussion above of the servomechanism was based on linear assumptions for the sake of simplicity, the actual dynamics of the complete system present a pronounced non-linear behavior. To be sure, this does not refer to the normal breakdown of linear assumptions found in all actual systems, at saturation levels but rather to the non-linearities purposefully introduced in the design as demanded by this specific application.

The most important non-linearity is produced by the use of a friction drive between the carriage and the track. The stainless steel drive wheel has been knurled in an effort to increase its traction on

the soft aluminum track. A coefficient of friction of about .6 has been attained by this simple method.

The torque capabilities of the hydraulic drive exceed the friction torque and special precautions have to be taken to prevent wheel slip. A direct solution to control the drive wheel torque was to limit the rate of change of the yoke angle by flow restrictions placed in the lines between the control valve and the yoke piston. Since the yoke position determines a certain carriage velocity, limiting its rate of motion is the equivalent of limiting the carriage acceleration.

The second type of non-linearity is a dead zone resulting from unavoidable track-carriage Coulomb friction. In Figure 5, the describing function N has been plotted in the form $-\frac{1}{N}$ in the gain-phase plane with the linear open loop transfer function of the system.

In reference to the same figure, it is possible to explain some of the phenomena observed during the operation and adjustment of the carriage. The optimum setting of the system parameters yields a frequency response curve, shown by the solid line, that produces a system of conditional stability with respect to K , the error rate tachometer gain. Increasing K (decreasing the time constant of the first lead) in essence shifts the curve upwards in a diagonal direction. The intersection of the open loop frequency locus with the describing function at point B gives rise to a high frequency limit cycle oscillation of small amplitude. Decreasing K moves the curve downwards and the intersection occurs at A in the lower frequency region of the open loop locus. At this point very small errors tend to produce a limit cycle oscillation of low frequency. Errors larger than those encountered at A give rise to a low

frequency divergent oscillation. An increase in the open loop gain moves the open loop curve vertically upwards producing a result similar to that of increasing K .

VERTICAL SERVO DRIVE. To follow the vertical component of the motion of a typical model's oscillation it was determined that the vertical servo drive must position the horizontal boom, a mass of about 50 pounds, at a maximum speed of 3 feet per second and at an acceleration of no less than one-half the acceleration of gravity. This performance was obtained by means of a special drive developed at this establishment, consisting of a set of two proportional magnetic fluid clutches powered by a constant speed, $1/4$ horsepower, 11,000 RPM motor.

The electric motor runs continuously at essentially synchronous speed, rotating the armature of the clutches in opposite direction at a reduced speed by means of gearing.

The output shafts of the clutches are geared down to a single shaft which is connected to a drive chain sprocket. The amount of torque transmitted to the output shafts of the clutches is proportional to the current input to the clutch coils. The direction of rotation of the drive sprocket is determined by which clutch is powered.

The horizontal boom is free to ride on the ten foot vertical track on a set of ball bearing rollers. It is driven up and down by a chain loop running through the drive sprocket at the bottom of the vertical track and an idler at the top.

The complete clutch drive assembly which also includes two tachometers, a boom position potentiometer, and a cooling fan is packaged in the 7 inch diameter vertical tube. The clutch coils are driven in push-

pull fashion to improve output linearity by means of a DC amplifier exactly the same as the one used in the horizontal drive. This arrangement has an excellent frequency response characteristic.

One disadvantage of using magnetic clutches is their limited capacity to dissipate the heat generated by slippage under load. The quiescent current in the clutches for zero output must be kept at a small fraction of full rated current to prevent overheating while the drive is idle. However, by careful design and by limited full loading to intermittent operation, the drive has shown good performance. The vertical error signal is generated in the same fashion as in the horizontal servo: a position potentiometer produces a voltage output proportional to the distance the model has moved from the center of the vertical servo-link. Its signal is amplified and fed into the clutch coils which will accelerate the horizontal boom up or down to align it with the model, reducing the error signal to zero. Full control of the damping is furnished by rate feedback from a tachometer geared to the drive output.

Due to the high response of the drive itself, no further stabilization was required to fulfill the expected performance. Similarly to the horizontal servo, it is possible by opening the major or position loop to generate a constant velocity of ascent or descent by the application of a calibrated voltage to the amplifier inputs.

DATA GATHERING AND RECORDING

The instrumentation of dynamic investigations has been kept as simple as possible consistent with the requirements of the minimum number of variables to produce useful and significant results.

The data gathering system consists of a number of transducers such as potentiometers, tachometers, strain gauge beams and accelerometers, an amplifier to bring small transducer outputs up to useful levels and a multichannel transmitter and ground station, which are covered in detail later in this paper.

The raw data is recorded in magnetic tape and it is also transformed into an analog voltage normally recorded in filtered or unfiltered form on a 4-channel paper recorder. A scope presentation of all the channels is also available.

In general it is required to measure the following model fuselage quantities: pitch angle, pitch rate, horizontal velocity, vertical velocity. Also (but of less interest), normal acceleration and pitch angular acceleration. The vertical position is also available.

Pitch angle - The model has a pitch angle freedom of about $\pm 30^\circ$ before it is limited by the structural members of the error link. A low friction potentiometer with the wiper directly connected to the model and the card attached to the structure of the vertical climb link provides the accuracy and resolution necessary without disturbing the model motion.

Pitch rates - The maximum pitch rates are of the order of about 2 radians per second and it is desired to obtain a resolution of about

.05 radian. To obtain an output of .5 volt for the tachometers used, a gear ratio of the order of 50 is needed. This will magnify the tachometer inertia by a factor of 2500. This represents an inertia increase that must be taken in consideration.

Horizontal velocity - The horizontal velocity of the model is obtained by the algebraic summation of two components. One is the carriage velocity as it moves on the track. The other is the velocity of the model relative to the carriage. The sum of these two components is the true model velocity. This last quantity sometimes called "error rate" in servomechanism terminology is also used for the stabilization of the hydraulic horizontal drive. Physically it is obtained by a take-off from the position error potentiometer rack and pinion drive. Its gearing level has been determined mainly by the servo stability requirements. It adds to the forward or traveling inertia of the model.

Vertical velocity - The vertical velocity of the model is obtained in a manner similar to the horizontal velocity. The vertical carriage velocity is obtained from a tachometer included in the output side of the vertical drive. The vertical velocity of the model relative to the carriage is measured by a tachometer driven by a rack and gear arrangement sensing the motion of the climb link. This again increases the effective lifted mass of the model, and also introduces some damping.

Normal accelerations - They are sensed by a Statham unbonded strain gauge accelerometer with an output requiring amplification. Angular pitch accelerations are not obtained directly at present. When needed they are obtained by means of graphical derivations from the pitch

rate.

Vertical position - It is available from a potentiometer geared to the output of the vertical drive.

A transmitter accepting input signals from 0 to 15 millivolts was originally used. It was found that it was very difficult to keep a favorable signal-to-noise ratio under the circumstances in which the carriage operates. The presence of the power rails and the various drive motors and other electronic equipment in the carriage generates strong electric and magnetic fields in the neighborhood of the carriage. The relatively high output of the position and velocity transducers requires large voltage dividing resistors, further increasing the noise and complexity of the circuitry.

The output of strain gauge devices fell more in line within the 0-15 millivolt range. However, it was often the case that to obtain enough resolution and sensitivity without amplification required designing strain gauge beams to operate at high levels of strain. This resulted in rather "soft" beams with the corresponding low natural frequencies and large deflections under loads. It was possible to calibrate out the "droop" due to loads such as the change in pitch angle due to pitching moment, but the undamped low natural frequencies were not easily filtered out electrically without endangering the legitimate data. In an effort to filter the data mechanically and to avoid resonance effects in the model strain gauge systems, a simple type of hydraulic damper with variable orifice was developed. Silicon fluids and kerosene were used as damping fluids. The dampers were very effective and reliable and optimum time constants were

easily obtained by the variable throttle adjustments. To increase the effectiveness of the dampers, strain gauge beams of very low apparent stiffness were used. A composition beam was developed to provide large deflections and still keep the strain on the gauges within specification. With deflections of the order of $\pm 1/8$ inch the applications of stops to limit the stresses in the beams becomes feasible.

The measurement of forces and moments in the Forward Flight Facility presents unique problems, and special techniques have been applied towards their solution.

The most difficult problem is that the carriage and the restrained model are subjected to vibrations and random motions in all planes of a relatively high acceleration.

Under normal circumstances the ratio of the inertial forces acting on the model to the aerodynamic forces is about 10 to 1. It is seen that special precautions have to be taken to separate their action. Two approaches are used:

- a) One is based on the fact that the inertial forces are of a fluctuating nature and their average is zero while the aerodynamic forces are essentially constant, and in general have non-zero value during a constant speed run.
- b) The second rests on the possibility of mass balancing the model in all directions.

Method (a) makes use of the low natural frequencies resulting from "soft" strain gauge beams and the mass of the model. This method depends on designing a mass-spring-damper system with a resonance frequency well below the forcing frequencies and also on the use of criti-

cal or supercritical damping ratios. The low natural frequency results from the mass of the model and the use of "soft" strain gauge beams. High damping forces are required and can be produced by means of hydraulic dampers. High frequency inputs or rapidly fluctuating random forcing are effectively "shunted out" by the damper. And the strain gauge beams are not subjected to large strains.

Constantly applied forces will not "see" the dampers and will produce deflections on the strain gauge beam. Therefore from the point of view of the strain gauges the system is a mechanical low pass filter. A large time constant is acceptable since the aerodynamic forces do not vary or they do so at very low rates; such as during quasi-steady testing.

The mass-balancing method (b) cancels out the inertia forces in all directions by accurately adding suitable masses to generate equal and opposite forces under accelerations. The strain gauges then sense the net moment produced by the aerodynamic forces. This method appears more advantageous for use in this facility. It gives a higher response to data variations. It appears that for relatively stiff beams and high resonant frequencies, once accurate balance has been attained to minimize inputs, very little damping is necessary.

Pitch balancing offers little difficulty. since the models are supported by their center of gravity axis, and exciting inputs are essentially non-existent.

Drag and lift measurements require balancing the model on the horizontal and vertical direction respectively.

It is of course desirable to keep the balancing masses to a

minimum. This involves high leverage ratios between the model and the mass. Space considerations sometimes do not allow a straightforward lever system: in those cases a low friction gearing stage may be suitable.

A three-component strain gauge system for ground effect models is discussed in detail in Appendix III.

TELEMETRY AND RECORDING. The method for bringing the data from the carriage to the ground was chosen on the basis of practicability, reliability, capacity and flexibility of operation. The weight of the transported equipment is a serious consideration beyond certain limits.

In general three solutions are possible:

- (a) Recording model data and interpreting it after the test run,
- (b) Transmission of the transducer output to the ground by means of a cable or track.
- (c) Transmission of the information to the ground by means of a radio link using the various modern telemetering methods.

The recording method appears feasible for use in this type of facility when a limited number of variables are of interest, and a short range program is in view. One of its main difficulties is in the interpretation of the recorded traces and the fact that in some cases there is quite a lag between the experiment and the availability of the data in useful form. A typical example are those recorders using photosensitive films that require development before the recorded data can be interpreted. Even in those recorders when no processing is required to obtain records, the data is cold at the end of the run and

calibration and adjustment of the various transducers can be a laborious and time-consuming operation.

The use of cabling (method b) or a track was considered in the preliminary stages of the facility development. A cable was used successfully in a short hovering track to carry three or four transducer outputs to ground. The hovering tests were performed with maximum excursions of the order of 30 feet and the drag of the cable was reduced by a simple on-off servo drum that paid out the cable as required by the position of the carriage. A cable system for use in the full length of the facility would involve lengths of about 400 feet minimum. The drag effects on the carriage performance are prohibitive and carriage velocities of 60 or 70 feet per second would introduce some extremely difficult problems.

Some investigations were carried out to explore the possibility of sending out the model information by means of a track. It was concluded from the results of these experiments that a satisfactory signal-to-noise ratio would be difficult to achieve by means of a straight track and brush arrangement. A straight track and brush system had the disadvantage of not wearing in with use; therefore it does not improve its noise characteristics with operation.

The present ASCOP telemeter system (method c) specially with the high level inputs has shown excellent accuracy and flexibility. Telemetering the information appears, in the light of the Princeton operating experience, to be ideal for a facility of this type.

The operation of this system will now be discussed. The carriage telemetering set consists of a commutator to switch the input circuit

to a number of different transducers, a keyer to form the pulses, and a transmitter to generate the radio frequency signal used to transmit the pulses. Primary power of 28 volts DC are furnished from carriage power supplies.

The commutator is a high speed rotating switch used to sample in turn the outputs of a number of transducers. The design of the commutator determines the maximum number of transducers that can be telemetered from one set and the basic rate at which each transducer is sampled.

The total samples per second, which is the number of channels time the sampling rate, is 900; therefore the segment of time allotted for each transducer sample is equal to approximately 1100 milliseconds. A second row of contacts on the commutator provides trigger signals to rotor. The commutated signals are then supplied to the input of the keyer, and each sample in turn determines the width of one pulse.

The pulses are formed electronically using a multivibrator circuit. They are initiated by a Schmitt trigger circuit in conjunction with the timing signals from the commutator. The keyer includes an electronic voltage regulator which reduces the ± 150 volts for use in the keyer and transmitter.

The keyer output pulses by themselves are not in a form that could be radiated from the antenna to a receiving station, so it is necessary to use them to modulate a radio-frequency signal in the transmitter; this signal is generated by a crystal-controlled oscillator, which is modulated by the keyer pulses. The transmitter operates in the telemetering frequency band of 214 to 236 megacycles. The

effect of the frequency modulation is that the output frequency is at one value when there is no positive pulse present at the keyer output; and it is shifted by some value, usually 100 kilocycles, during a keyer pulse. This frequency deviation can be detected by the receiving station and used to regenerate the pulse.

To mark the end of one pulse train and the start of the next, two pulses are omitted. These missing pulses are sometimes referred to as synchronization pulses. Two of the remaining channels are the calibration channels normally used to transmit the zero and full scale instrument voltages. The self-calibrating feature results from the transmission of these calibration channels. The ground station utilizes these two channels as reference channels, against which the outputs of all the data channels may be compared. In this way the data may be shown as a percentage of full scale instrument voltage instead of absolute volts, which is preferable as it automatically compensates for any fluctuation of the instrument supply voltage or any unknown variations in the electronic transmission line. Since the calibration pulses and the data pulses all travel through the same circuits, they will be affected alike by any variations, and their relative magnitudes will be preserved.

The high input impedance prevents loading the transducers electrically which could otherwise affect their calibrations. This allows greater flexibility in its use.

Frequency response may be defined as the highest frequency that can be transmitted by the system without distortion. A good rule of thumb for any sampled data system is that five samples per cycle are

required to permit visual interpolation of output records with an accuracy of ± 1 per cent of full scale. This defines the frequency response of one data channel as approximately 4 cycles per second for a 45 by 20 system. Higher frequency data may be transmitted by doubling up the numbers of channels used for one measurement, but a practical limit of around 25 cycles per second is reached.

In the ground station, the Channel Selector decommutates the incoming signal and provides a separate gating pulse for each data channel. Patch boards permit connection of gating pulses singly or in multiple to the desired translators.

Each output translator converts the pulse-width data samples of its assigned channel to a proportional DC voltage. Channel selector pulses are used to gate on the translator circuit for the duration of the selected channel to allow the operation of a triangular wave generator. The output voltage of the circuit rises to a level which is proportional to the duration of the data pulse. The final voltage level, reached at the end of the pulse, represents the desired information.

The translator output voltage is of high amplitude, normally 0 to 100 volts with a linearity of better than one per cent. The translator output is at high impedance, capable of driving a DC amplifier, micro-meter or oscilloscope.

In order to obtain the proper DC control voltages, two translators, operating in the zero and full scale reference channels, are provided. Each of these translators converts the pulse width modulation of the selected channel into a DC voltage whose level is proportional to the width of the incoming pulse. By controlling the initial voltage level

and triangular slope of all translator units by the DC control voltages, continuous correction is made for changes in zero and full scale pulse width of the telemetered data.

The tape recorder used is an Ampex model 309, which is designed to record pulse-width data; it records the received output on magnetic tape where it is available for playback at any time. During a tape playback the received signals are duplicated exactly and the conditions of the telemetered flight are reproduced completely so far as the ground station can tell.

The Monitor Scope provides a visual display of the pulse width input signals to the ground station. The display is a series of vertical traces. The height of each trace is proportional to the duration of the corresponding data signal, there being a vertical trace for each data channel. Time markers are provided in the form of small horizontal pips on the vertical traces at 50 microsecond intervals.

OPERATING EXPERIENCE

TECHNIQUES AND OPERATING PROCEDURE USED IN THE TESTING PERFORMED WITH A DYNAMICALLY SIMILAR HELICOPTER NEAR HOVERING FLIGHT

In general, the dynamic similarity between the model and the full scale machine was accomplished by preserving the relationships between the gravitational, inertial and aerodynamic forces. The helicopter is a $1/6.625$ scaled version of a single rotor service helicopter having a three-bladed, fully articulated rotor 53 feet in diameter.

A scaling process requiring constant Froude number, constant thrust coefficient, and scaled linear dimensions was used, introducing a compromise in reduced Reynolds and Mach numbers. The only significant effect of a reduced Reynolds number on the stability and control characteristics is a change in the blade section lift curve slope that can be nullified by modifying the airfoil section. The Reynolds number effect on the blade profile drag coefficient influences performance and was of no interest in this test. The effect of the reduced Reynolds number on the fuselage aerodynamics was probably offset by the turbulence generated by the rotor wake, but little data is available at the present.

Mach number effects were not considered significant in this experiment.

Model: The model was designed by using the rotor drive transmission as the basic structural component. The transmission containing a 23.1 reduction gear train was housed in a magnesium casting providing attachment points for the rest of the fuselage. Power was provided by a 1 horsepower, 400 cycle, 200 volt, 3-phase electric motor

and a power take-off for the tail rotor.

The forward fuselage shell was fabricated from high-impact vacuum-formed polystyrene plastic sheets, reinforced with plywood and balsa frames. The tail boom was a 1/16th-inch magnesium sheet monocoque structure. The model tail rotor consisted of an aluminum hub and adjustable-pitch cast Lockfoam blades.

The only significant problem encountered with the model was in the scaling of gross weights and inertia. The transmission was located above and to the rear of the full scale center of gravity position as were the tail boom, hub, and blades. This was counterbalanced by the drive motor and lead weights forward and below the full scale center of gravity. The model was balanced at a center of gravity position, with the equivalent maximum gross weight identical to that used in service acceptance stability test flights. The balanced solution obtained in this manner gave a higher moment of inertia than true scale value. Experience with this model indicates that scaling inertia in models with simple construction can be a difficult problem. However, later on, by careful redesign, true scaled values were obtained. The model rotor blades were cast from Lockfoam in a heated aluminum mold, with an integral meter spar and root fitting.

The blade section was changed from the full scale NACA 0012 to the NACA 0015 on the model to compensate for the effects of the reduction of Reynolds number.

Dynamic similarity of the rotor blades was obtained by scaling weight per foot, moment of inertia, mass moment about the flapping hinge, stiffness, chord-wise center of gravity and shear center. Mass

moment of inertia about the flapping hinge and blade weight per foot were closely scaled, as they are the most significant properties of the blade affecting stability and control.

Accurate simulation of the full scale helicopter required scaled hub and pitch changing mechanisms. The full scale helicopter hub bi-directional universal for flap and lag hinges was simulated on the model with a conventional rod end accurately located in the hub for a scaled hinge offset. The pitch link mechanism was accurately scaled, except for the pitch link length, which was slightly longer on the model, lowering the swashplate position. This results in a decrease of the rate of change of pitch angle with lag angle, which has a desirable stabilizing effect on blade pitch lag oscillations and partially offsets the increased pitch coupling from lag angle due to Reynolds number effect. An accurate analysis of the entire hub coupling would be required to evaluate the effect of these changes, but with most of the hub scaled, the analysis was not developed, as the non-scaled items affect primarily the rate of change of pitch with lag angle, which should have little effect on stability.

Test and test procedure: The static and dynamic stability of the helicopter model was evaluated near hovering flight by force measurements and semi-free flight tests. Static forces were measured during constant velocity runs, with the model mounted on a strain gauge balance fixed to the servo-carriage. Essentially a wind tunnel type testing, this technique was used to determine the variation of thrust, drag, and pitching moment with velocity near hovering. With the fuselage fixed at the hovering trim pitch angle, the force measure-

ments gave a direct measurement of static stability with velocity.

The stick-fixed transient response of the helicopter model was determined near hovering flight from limited degree-of-freedom tests. Constrained by a linkage assembly to constant altitude, the model had freedom in fuselage pitch angle and horizontal velocity. The horizontal position of the model was followed by the servo carriage during the oscillation. As the instability of the helicopter model would rapidly amplify minute disturbances, the maximum length of data run was obtained with self-excited responses. Tests were also performed at zero velocity with freedom only in fuselage pitch angle. The magnetic fluid clutch servo carriage was used for these tests.

Dynamic testing procedure: The model was mounted on the carriage approximately center in the 30 by 30-foot building with the rotor two diameters above the floor. The rotor had been previously tracked on a thrust stand by adjusting the length of the pitch link of each blade.

The initial force and moment balance of trim of the model was achieved by adjusting collective pitch so thrust equalled weight, and adjusting cyclic pitch control for moment balance. Fuselage pitch angle was then adjusted for zero horizontal force. This trimmed the model longitudinally.

Obtaining steady, unaccelerated trim conditions required considerable care and adjustment as the model force and moment balance were very sensitive to small variations in thrust, horizontal force, and cyclic pitch control. However, with care, the model could be trimmed quite accurately and would hover motionless for 1 to 4 seconds before be-

ginning a self-excited oscillation. Free or self-excited oscillations were used since a minimum input was necessary to obtain a sufficient number of cycles to permit determination of the period and damping of the oscillation. With a good trim, 1 1/2 cycles of data were obtained before the model hit the pitch limits. To start the test, the model rotor was rapidly brought up to speed and its RPM determined with the strobotac. The model was then trimmed for a steady hover and launched. After launching, the model began a self-excited oscillation which continued until the amplitude of the oscillation built up to the available pitch freedom of the model, at which time the test was stopped.

Instrumentation: A simple instrumentation system permitting direct real-time read out of the data, was used for the dynamic tests. The electrical signals from the transducers were wired directly to a four-channel Sanborn recorder. Enough slack was left in the wiring between the carriage and the recorder to permit sufficient excursion for the hovering oscillations. The sensitivity of the system was set by matching the maximum output of the problem variable to the width of the Sanborn paper. The system was noise-free, and its resolution was estimated to be within the accuracy of the reading of the records.

Evaluation and reduction of the dynamic response data required the model output in fuselage pitch angle and horizontal velocity. Error position was also necessary to determine if the model hit the error limit stops. The measured velocity was made up of two parts, the velocity of the model and horizontal excursion link with respect to the carriage (error velocity), and the velocity of the carriage. Error velocity was measured with a DC tachometer fixed to the horizontal link and geared to a rack on the horizontal error platform.

Carriage velocity was transduced similarly with the tachometer fixed to the horizontal link and driven by the error velocity tachometer gear train. Pitch angle was measured with a low torque potentiometer mounted on the model with the wiper fixed to the vertical excursion link. Model RPM was determined with a strobatac prior to each run as preliminary experiments indicated no significant variation during an oscillation. The hub was not instrumented for blade measurements, but blade angles were determined statically with a propeller protractor as necessary.

A more complete discussion of this experiment can be found in Reference No. 1.

STATIC AND ONE DEGREE PARTIAL TRANSITION TESTS OF A VERTICAL TAKE OFF AIRCRAFT MODEL.

The model is a 1/5.2 scale dynamically-similar powered model of the Vertol V-76 tilt wing craft. In general, no attempt was made to scale the elastic properties of the aircraft as a whole. However, rotor blade mass, mass distribution, and bending and torsional properties were preserved as closely as possible to those values simulating the full scale rotor blade. In design and construction of the model particular attention was given to avoiding natural frequencies close to the one per revolution and three per revolution rotor forcing frequencies. Obvious success in this endeavor was demonstrated in the complete absence of any vibration problems throughout both test programs.

The model main drive system consists of a single 1.5 horsepower, three-phase 400 cycle electric motor driving the two three-bladed rotors through a geared-down transmission and a timing belt and

sprocket arrangement. The timing belts transmit the power from the fuselage-located transmission, out the wing, to the rotor shafts, and are centered about the wing tilt hinge to allow the wing to tilt through the required limits. Such a drive system proved quite light and trouble-free under all power and wing-tilt conditions.

The model rotors are semi-articulated with full flapping but no lag freedom, and the hub geometry and blade static moment are exactly scaled to the full scale aircraft's values. The primary structural member of the wing construction is a thin-walled aluminum tube to which are attached the wing hinge points, rotor shaft housings and welded magnesium ribs. The aerodynamic surface is formed of .010 inch aluminum sheet to which is bonded 1/32 inch balsa sheet for stiffening. The covering is bonded and screwed to the wing with a resulting surface that is quite free of wrinkles, waves and other irregularities.

The demand for light weight construction for dynamic similitude required a welded thin-wall aluminum tubing fuselage and a thin vacuum-formed polystyrene plastic bubble.

The power for the tail fan is taken from the main rotor drive system and transmitted along the fuselage and up through the vertical fin by means of a flexible cable drive. The horizontal stabilizer may be set at any desired incidence, but no rudder surface or yaw fan is provided as this model was originally intended for longitudinal testing only.

A small DC motor drives the rotor collective pitch adjustment, and a potentiometer is used to measure model collective pitch for

telemetering to the ground. A similar DC motor drives a spring-loaded cable arrangement to rotate the spoiler plate above the tail pitch fan. This drive system is designed to have adequate response characteristics to apply a one second pulse input in model scale time for dynamic control response tests.

The wing tilting mechanism is driven by a 400 cycle synchronous motor through a high-reduction planetary gear box. Several combinations of motor speeds and gear ratios are available to allow different scaled time transitions to be accomplished. This same mechanism drives the links by which the model is supported and which allow the model supports to follow the center of gravity travel of the aircraft during wing rotation.

Instrumentation: One of the major problem areas associated with conducting static tests on the Forward Flight Facility is concerned with model force and moment measuring instrumentation. The difficulties encountered arise primarily due to the peculiar nature of the testing facility, in that the forces to be measured are those acting on a moving model rather than on one with the flow moving past it, as previously discussed.

The first approach to the problem of vibration noise in the strain gauge system involved the use of very soft beams allowing sizeable deflections under load. The resulting finite motions were then damped by including oil-filled bellows arrangements in parallel with the spring of the strain gauge beams. Results using this scheme with battery-excited gauges were compatible with the accuracies allowed by other parts of the data-gathering system, with noise in the lift and

drag readings of the order of six to 8 per cent of full scale values. Pitching moment readings were particularly noise-free, due mostly to the fine balancing of the model about its support points and the relative absence of carriage pitch attitude forcing. Noise levels of the order of two per cent were easily achieved in the pitch gauge with quite low damping ratios, whereas the unbalanced model inertial forces required large supercritical damping ratios in both lift and drag.

Instrumentation requirements in the one-degree-of-freedom tests were somewhat different from those of the static tests in that no horizontal restraint was desired and the wing was not fixed in position but allowed to tilt. Solutions to the problems associated with a soft pitching moment beam were made possible through the provision of additional instrumentation equipment--AC excited strain gauge carrier amplifiers. Use of an amplified strain gauge output signal allowed a vast increase in the stiffness of the pitch beam at the expense, however, of motions large enough to permit damping. It was found in the one-degree-of-freedom tests that, with a sufficiently well-balanced model, it was not necessary to damp the pitching freedom, and these tests were conducted without benefit of any damping. The direct pitching moment data obtained in these tests exhibited no noise that could be directly attributed to carriage vibratory excitation of the model.

The other longitudinal force to be measured during the transition runs is lift, or vertical force. This is probably the most difficult freedom to instrument, in that small variations in a rather large force are desired, and normal excitation of the model by track and carriage disturbances can be quite severe. The first of these problems was

avoided in the static tests by engaging the lift beam only after the model was lifting its own weight less the equivalent of half of the full scale reading. The procedure allowed any desired sensibility with fifty per cent output when the model was lifting gross weight. Carriage normal excitation is a severe problem and an attempt was made to eliminate these inputs by counterbalancing the model in such a way that normal accelerations of the end of the boom would produce no strain in the lift beam gages.

A complete static test program was performed during which the lift, drag, and pitching moments of the model were obtained for various values of fuselage, angle of attack and wing tilt angle for velocities up to 30 feet per second.

The one-degree-of-freedom tests recorded the lift, pitching moment and forward velocity of the model for various fuselage angles of attack as the wing attitude was changed from its hovering position to its forward flight position.

These transition tests were carried out only up to approximately 30 feet per second due to the limited length of track available at the time of the tests.

GROUND EFFECT MACHINE

A limited testing program on a ground effect model was instituted to extend the capabilities of Princeton Forward Flight Facility to static and dynamic testing of this type of machines. The model used in these experiments was a 4 foot diameter circular "flying saucer" design (see Figure 46). The model can be considered a scaled-down (although not exactly) version of a 20-foot diameter Princeton ground

effect machine of similar design. Its simple construction consists of a large number of radial ribs covered with balsa wood on the top, with the exception of a central intake for the propeller. The bottom consists of a balsa wood disk slightly raised with respect to the rim, covering the lower surface except for an annular clearance through which the air exhausts in the form of a peripheral jet.

The model is powered by a 2 horsepower, 3-phase, 115 volts, 11,000 RPM motor that can raise it .6 inches off the ground. The instrumentation for static tests consisted of a strain gauge balance system that measured lift, drag, and pitching moment of the model. This was a mass-balanced scheme designed to reduce the strain gauge noise readings due to track irregularities and misalignment. A discussion of this balance can be found in Appendix III.

Dynamic testing was limited to two-degree-of-freedom runs up to 40 feet per second during which the altitude and pitch angle response of the model was measured as it went over an abrupt descending change in ground level.

A three-degree-of-freedom apparatus was constructed (see Figure 45), but due to a change in testing schedule, has not yet been put to use.

This brief series of tests outlined above has proven the feasibility of the use of this facility for testing ground effect craft under realistic conditions that cannot be easily duplicated in a wind tunnel. One of the problems encountered during this experience was that the distance from the floor to the carriage-supported model varied approximately 2 inches throughout the 700-foot length of the track.

This amounted to a gradual change in altitude of the model but, since it is predictable, it can be subtracted from the altitude data. Occasionally, sharp changes in altitude occur; they can be smoothed down by judicious placing of inexpensive plywood boards on the uneven areas.

EVALUATION

During the development of a new type of testing facility, the designer is confronted with a multitude of decisions and choices. The obvious difficulties encountered in predicting the major potential problems and in developing practical solutions without the benefit of parallel experience, constitute a challenging engineering endeavor and encourage a careful analysis of the various possible design concepts. Of course, there is no guarantee that the chosen approach is the best one of the lot. Final success provides an encouraging indication that at least certain minimum requirements have been satisfied and supplies a qualified figure of merit on the apparatus developed.

The optimum choice of hardware at a given time is influenced to a significant degree by the state of the art in the various technical fields touched by the development. Therefore an evaluation of the apparatus must necessarily be made in the light of the best available components and on the stated goals of the development.

In a facility whose fundamental purpose is to perform dynamic experiments, the dynamic behavior of the apparatus in general and of its various components is of primary importance.

The first of the various components is the carriage. Its dynamic response is the resultant of its mass, its drive power output and the nature of this drive. Experience has shown that it is better to assume a large carriage mass since most weight estimates tend by their nature to be conservative. For a drive with power modulation capabilities a variable delivery hydraulic pump-motor system presents the advantage over a non-conservative friction drive that only relatively small

amounts of heat are generated in its operation. The superior response of a hydraulic drive over an electrical one can best be understood by comparing the large effective spring constant derived from the bulk modulus of a fluid to the spring constant of the magnetic lines of forces in an electrical motor.

The track may be injected in the results of the experiments mainly through its negative characteristics, such as too much flexibility and misalignment; those can induce servo instability and also introduce, through the carriage structure, various types of forcing inputs into the model.

During three-degree-of-freedom tests, the model is flying under its own power and it is essentially decoupled from the carriage. Under these circumstances, the model, with a period of several seconds, acts as an effective filter in response to the high-frequency content of the forcing due to the track, and no noticeable effects are recorded in the model motion data. In the static type of tests, however, when the model is restrained and the aerodynamic forces are measured, track irregularities can produce a high level of noise in the force-measuring apparatus.

Three approaches to the solution of this problem are apparent. First, a reduction of track misalignment and irregularities; second a more sophisticated force-measuring scheme that would discriminate between extraneous inertial forces and aerodynamic forces; & third, a properly designed platform can be installed between the track and the force measuring instrumentation to alleviate the forcing disturbances.

The first solution can only attain limited success since it

appears difficult to maintain a tolerable alignment for any extended period of time. The second solution is more attractive because it would concentrate the design efforts to a limited portion of the equipment rather than on large numbers of track sections. This concept has been put into practice with encouraging results in the Forward Flight Facility. It operates on the principle of balancing the model to cancel out the inertia forces generated by its mass, thereby isolating the aerodynamic forces. The reduction of the disturbances measured by the strain gauges is a direct function of the accuracy of balance, introducing the practical limits of this approach.

The third solution is worthwhile investigating in combination with the second one above. It appears that the double effect of reducing the magnitude of the disturbance plus a decrease in sensitivity to those disturbances by the force-measuring instrumentation can effectively eliminate track noise from the static data.

The last component in the facility that can affect the data is the transmitting and recording equipment. Among the various methods of gathering and recording data produced in a moving vehicle, telemetering has gained wide acceptance in the last few years, with the advent of accurate, reliable, and flexible systems. In the telemetering system used in this facility, the weight of the traveling equipment has been kept at a minimum. This system provides immediate availability of the information in various forms of presentation, such as meter, scope, and paper recordings. These can be done in more elaborate forms since the equipment does not have to be borne in the moving vehicle, and a large amount of information can be conveyed through the forty-odd data channels.

Such a data collecting and recording system has proven ideally suited for the operation of the Princeton Forward Flight Facility.

The present normal operating crew of the facility during dynamic testing consists of two men. One runs the recording equipment in the control room and coordinates the experiment; the other is needed for model adjustments and resetting of the model locking devices at the start of the run. Further development of the track will allow one man to carry out a series of experiments without extra help.

It is worthwhile to consider that an increase in usefulness of a facility of this type may be accomplished by applying its basic concepts and capabilities to areas beyond the dynamic testing of aircraft at hovering and moderate forward speeds, into the investigation, for example, of landing and take-off maneuvers, gusts disturbances, hydrofoil craft dynamics and others. This can be accomplished with a minimum of expenditure and construction.

The cost of a similar facility, to be constructed on the basis of the experience obtained is estimated to be \$200,000. An approximate breakdown of this figure is: building, \$75,000; carriage and track, \$85,000 (auxiliary equipment included); instrumentation and recording, \$40,000. The cost of designing and constructing a dynamically similar model may vary between \$25,000 and \$75,000.

The above figures compare favorably with the cost of developing and constructing a wind tunnel of comparable dimensions which of course would have to be limited to static measurements.

The question of the validity of the results obtained at this facility can be answered, at least in principle, by comparing the data

available on an operational aircraft with that obtained from the facility. A correlation program instituted with a helicopter model is in progress. In practice such correlation efforts encounter some inherent difficulties, ironically due to those same problems that the facility is designed to overcome: In full scale testing, because of extraneous disturbances and understandable pilot limitations, the input to the control system is not well defined and even subsequent correcting action may occur. The inputs applied to the model in the Forward Flight Facility are on the contrary almost mathematically exact. Therefore, some variation of the responses may be expected and perhaps are unavoidable. Indirect correlation may be achieved by an analog computer investigation that will apply to the simulated model the actual time history of a pilot input.

On the other hand, the data obtained from the facility presents excellent repeatability and correlates satisfactorily with available theory.

BIBLIOGRAPHY

1. Bennett, Robert M., and Howard C. Curtiss, Jr., An Experimental Investigation of Helicopter Stability Characteristics Near Hovering Flight Using A Dynamically Similar Model, Report No. 517, Department of Aeronautical Engineering, Princeton University, July 1960.
2. Gebhard, David F., An Economical Technique for the Construction and Hovering Flight Evaluation of Dynamically Similar Helicopter Models, Report No. 373, Princeton University Aeronautical Engineering Laboratory, November 1956.
3. Goland, Leonard, On the Design of Models for Helicopter Research and Development, Report No. 240, Princeton University Aeronautical Engineering Laboratory, October 1953.
4. Gray, McCaskill, Gebhard, and Goland, Model Study of Helicopter Dynamic Stability and Control, Phase II, Comparison of Theoretical and Experimental Results Near Hovering Flight, Report No. 230, Princeton University Aeronautical Engineering Laboratory, May 1953.
5. Hadekel, R., "Complex Servos," Hydraulic and Pneumatic Servos, Part 6, Reprinted from Automation, October 1954 through March 1955, pp. 53-62.
6. Murphy, Glenn, Similitude in Engineering, The Ronald Press Company, New York, 1950.
7. Proceedings of Conference on Hydraulic Servomechanisms, Institution of Mechanical Engineers, London, 1953: (a) H. G. Conway and E. G. Collinson, "An Introduction to Hydraulic Servomechanism Theory," (b) N. F. Harpur, "Some Design Considerations of Hydraulic Servos of the Jack Type," (c) T. E. Beacham, "Variable-stroke Pumps for Power Transmission--Some Design Considerations," (d) J. M. Ford, Discussion, (e) P. F. Foreman, Discussion.
8. Proceedings of Conference on Hydraulic Servomechanisms, Institution of Mechanical Engineers, London, 1953, P. J. Palmer, "The Force of the Piston Track of a Variable Capacity Type of Hydraulic Pump."
9. Newton, G. C., "Hydraulic Variable Speed Transmissions as Servo Motors," Journal of Franklin Institute, Volume 243, London, 1947.
10. Sayre, D. C., A Proposed Model Track Facility for Dynamic Studies of Helicopters in Forward Flight, Report No. 247, Princeton University Aeronautical Engineering Laboratory, January 1954.
11. Truxal, John G., Automatic Feedback Control System Synthesis, McGraw-Hill Book Company, Inc., New York, Toronto, London, 1955.

BIBLIOGRAPHY

12. Putman, William F., Results of Experiments on a Tilt-wing VTOL Aircraft using the Princeton University Forward Flight Facility, Report No. 542, Princeton University Aeronautical Engineering Department, May 1961.
13. Murphy, Gordon J., Basic Automatic Control Theory, D. Van Nostrand Company, Inc., Princeton, N. J. 1957.

APPENDIX I

HORIZONTAL SERVOMECHANISM

The horizontal servomechanism consists of a position sensing linkage, an amplifier, and a hydraulic drive system. Its major loop is closed through the carriage structure. Fig. 2 is a block diagram of the system.

The dynamics of the hydraulic drive are the dominant factor in the behavior of the carriage. Specifically, the most critical dynamics in the system are those of the power circuit, that is, that portion of the drive from the yoke to the load.

In order to write the transfer function describing the horizontal servomechanism, the power circuit transfer function will be determined first.

The load consists of a carriage of M_H and a viscous friction coefficient f_H . The output torque of the hydraulic motor is applied to a drive wheel of a diameter D through a gear reducer of ratio N .

The force or thrust generated in this manner by the drive must be equal to the force demanded by the carriage motion.

$$F_H = M_H \ddot{x}_H + f \dot{x}_H \quad (1)$$

The torque produced by the hydraulic motor is proportional to the pressure drop across it.

$$T_M = K_S P_F$$

and this torque applied to the drive wheel results in a force:

$$F_D = \frac{2 K_S N}{D_H} P_F = M_H \ddot{x}_H + f \dot{x}_H$$

and conversely the pressure drop at the motor is:

$$P_F = \frac{D_H}{2K_S N} [M_H \ddot{x}_H + f \dot{x}_H] \quad (2)$$

The output flow of the pump must supply the flow through the motor, the interval leakage and the volume variations due to fluid compressibility.

$$Q_P = Q_M + Q_L + Q_C$$

and the rates of flow are given by:

$$\dot{Q}_P = \dot{Q}_M + \dot{Q}_L + \dot{Q}_C \quad (3)$$

The output rate of flow of the pump is proportional to the yoke angle:

$$\dot{Q}_P = K_T \dot{\theta}_T \quad (4)$$

The rate of flow through the motor is proportional to the motor shaft rate of rotation:

$$\dot{Q}_M = K_M \Omega_M$$

or in terms of the carriage motion:

$$\dot{Q}_M = \frac{K_M N}{D_H} \dot{x}_H \quad (5)$$

The rate of flow due to leakage is proportional to the pressure P.

$$\dot{Q}_L = K_L P_F$$

and from Equation (2)

$$\dot{Q}_L = \frac{K_L D_H}{2K_S N} [M_H \ddot{x}_H + f \dot{x}_H] \quad (6)$$

The change in volume of the fluid is proportional to the change in pressure. If B is the bulk modulus of the fluid and V is the volume under consideration, then:

$$Q_C = \Delta V = \frac{V}{B} \Delta P_F$$

and

$$\dot{Q}_c = \frac{V}{B} \dot{P}_F$$

Differentiating Equation (2) with respect to time and substituting \dot{P} in the above equation gives:

$$\dot{Q}_c = \frac{V D_H}{2 B K_S N} [M \ddot{x}_H + f \dot{x}_H] \quad (7)$$

By equating these various flows to the output flow of the pump as expressed by Equation (3) we have:

$$K_T \Theta_T = \frac{K_M N}{D_H} \dot{x}_H + \frac{K_L D_H}{2 K_S N} [M \ddot{x}_H + f \dot{x}_H] + \frac{V D_H}{2 B K_S N} [M \ddot{x}_H + f \dot{x}_H]$$

Regrouping the terms:

$$K_T \Theta_T = \frac{V D_M}{2 B K_S N} \ddot{x}_H + \left[\frac{K_L D_M}{2 K_S N} + \frac{V D_F}{2 B K_S N} \right] \ddot{x}_H + \left[\frac{K_M N}{D_H} + \frac{K_L D_F}{2 K_S N} \right] \dot{x}_H$$

In terms of the Laplace operator:

$$K_T \Theta_T(s) = s \left[\frac{V D_M}{2 B K_S N} s^2 + \left(\frac{K_L D_M}{2 K_S N} + \frac{V D_F}{2 B K_S N} \right) s + \left(\frac{K_M N}{D_H} + \frac{K_L D_F}{2 K_S N} \right) \right] X_H(s)$$

And the transfer function directly obtained

$$\frac{X_H(s)}{\Theta_T(s)} = \frac{K_T / \left(\frac{K_M N}{D_H} + \frac{K_L D_f}{2 K_S N} \right)}{s \left[\frac{\frac{V D_M H}{2 B K_S N}}{\left(\frac{K_M N}{D_H} + \frac{K_L D_f}{2 K_S N} \right)} s^2 + \frac{\left(\frac{K_L D_M H}{2 K_S N} + \frac{V D_f}{2 B K_S N} \right)}{\left(\frac{K_M N}{D_H} + \frac{K_L D_f}{2 K_S N} \right)} s + 1 \right]}$$

or in the standard form:

$$\frac{X_H(s)}{\Theta_T(s)} = \frac{K_D}{s \left[\frac{s^2}{\omega_N^2} + \frac{2 \xi}{\omega_N} s + 1 \right]} \quad (8)$$

where

$$K_D = \frac{K_T}{\left(\frac{K_M N}{D_H} + \frac{K_L D_f}{2 K_S N} \right)}$$

$$\omega_N = \sqrt{\frac{B}{V M_H} \left(\frac{2 K_S K_M N^2}{D_H^2} + K_L f \right)}$$

$$\xi = \frac{V f + K_L M_H B}{2 \sqrt{B V M_H} \left(\frac{2 K_M K_S N^2}{D_H^2} + K_L f \right)}$$

Substituting the following values:

$$B = 2 \times 10^5 \quad \frac{\text{lb}}{\text{in}^2}$$

$$K_S = .1 \quad \text{in}^3$$

$$K_M = 10 \quad \frac{\text{in}^3}{\text{rev}}$$

$$N = 2$$

$$D_H = 4 \text{ in}$$

$$M_H = 36 \text{ slugs} = 3 \quad \frac{\text{lb}}{\frac{\text{in}}{\text{sec}^2}}$$

$$V = 150 \text{ in}^3$$

$$K_L = .02 \text{ in}^5/\text{sec}$$

$$f = \frac{.1 \text{ lb sec}}{\text{in}}$$

$$K_T = 130 \text{ in}^3$$

Yields:

$$K_D = \frac{130}{\left(\frac{10 \times 2}{4} + \frac{.02 \times 4 \times .1}{2 \times .1 \times 2}\right)} = \frac{130}{5.02} \approx 26 \text{ in/sec.}$$

$$\omega_N = \sqrt{\frac{2 \times 10^5}{150 \times 3} \left(\frac{2 \times 10 \times .1 \times (2)^2}{4^2} + .02 \times .1 \right)} = \sqrt{440 (.5 \times .002)}$$

$$\approx 14.8 \text{ rad/sec}$$

$$\xi = \frac{150 \times .1 + .02 \times 3 \times 2 \times 10^5}{2 \sqrt{2 \times 10^5 \times 150 \times 3 \left(\frac{2 \times 10 \times .1 \times 2^2}{4^2} + .02 \times .1 \right)}}$$

$$= \frac{15 + 1.2 \times 10^4}{2 \times 10^4 \sqrt{.9 (.502)}} \approx \frac{1.2 \times 10^4}{2 \times 10^4 \sqrt{.45}} = \frac{1.2}{1.34} = .9$$

Substituting these values back gives the final power circuit

transfer function:

$$\frac{X_H(s)}{\Theta_T(s)} = \frac{26}{s \left(\frac{s^2}{219} + \frac{s}{8.2} + 1 \right)}$$

The servo valve response is high enough to be considered an amplifier without time lag. The stroking piston that drives the yoke also had excellent response and can be closely approximated as an ideal integrator. Other components in the system with negligible time lags are the error-sensing potentiometer, the yoke position feedback potentiometer and the error rate tachometer.

To obtain the open loop transfer function of the complete system, the two inner loops will now be eliminated.

In reference to Figure 3 the combined output voltage of the error potentiometer, tachometer and the lead network is:

$$V_i(s) = \left[(K_P + K_T s) \frac{1 + \alpha \tau_3 s}{1 + \tau_3 s} \right] E(s)$$

and its transfer function is:

$$\frac{V_i(s)}{E(s)} = K_P \left[(1 + \tau_2 s) \frac{1 + \alpha \tau_3 s}{1 + \tau_3 s} \right]$$

where

$$\tau_2 = \frac{K_T}{K_P}$$

substituting

$$K_T = .15 \text{ volt/sec/in}$$

$$K_P = 10 \text{ volt/in}$$

gives

$$\tau_2 = \frac{.15}{10} = .015 \text{ sec}$$

also

$$\tau_3 = .0167$$

$$\alpha = 1$$

therefore

$$\frac{V_i(s)}{E(s)} = \frac{10(1 + .015s)(1 + .066s)}{(1 + .0167s)}$$

In the second inner loop (yoke position feedback)

$$G(s) = \frac{K_A K_V K_2}{s} \quad \text{and} \quad H(s) = K_{FB}$$

and its closed-loop transfer function is:

$$\frac{\Theta_T(s)}{V_i(s)} = \frac{G(s)}{1 + G(s)H(s)} = \frac{1}{K_{FB}} \frac{1}{1 + \tau_5 s}$$

where

$$\tau_5 = \frac{1}{K_A K_V K_2 K_{FB}}$$

substituting:

$$K_{FB} = 200 \frac{\text{volts}}{\text{rad}}$$

$$K_A K_V K_2 = 5 \frac{\text{rad}}{\text{sec-volt}}$$

gives

$$\tau_5 = \frac{1}{5(200)} = .001 \text{ sec.}$$

$$\frac{\Theta_T(s)}{V_i(s)} = \frac{1}{200} \left(\frac{1}{1 + .001s} \right)$$

Assuming that the dynamics of the carriage structure are negligible, the open loop transfer function of the system is:

$$\frac{X_H(s)}{X_M(s)} = \left[\frac{\Theta_T(s)}{V_i(s)} \right] \left[\frac{V_i(s)}{E(s)} \right] \left[\frac{X_H(s)}{\Theta_T(s)} \right]$$

$$= \left[\frac{1}{200} \left(\frac{1}{1+.001s} \right) \right] \left[\frac{10(1+.015s)(1+.066s)}{(1+.0167s)} \right]$$

$$\left[\frac{26}{s \left(\frac{s^2}{219} + \frac{s}{8.2} + 1 \right)} \right]$$

or simplifying:

$$\frac{X_H(s)}{X_M(s)} = \left[\frac{(1+.015s)(1+.066s)}{(1+.001s)(1+.0167s)} \right] \left[\frac{1.3}{s \left(\frac{s^2}{219} + \frac{s}{8.2} + 1 \right)} \right]$$

This transfer function is shown in Figure 4 for its maximum stable gain.

APPENDIX II

VERTICAL SERVOMECHANISM

The components of the vertical servomechanism show a very good response. The inductive time constant of the clutch coils has been made negligible by the use of a high output impedance amplifier.

The main dynamic contribution is made by the load. The vertical carriage mass including the horizontal boom, error linkages, and counterweights, is approximately 50 lbs. A number of ball bearing guide rollers generate a certain amount of viscous friction.

A block diagram of the components is shown in Fig. 8.

The transfer function of the drive and load will now be determined by assuming that the vertical carriage has a mass M and a viscous damping coefficient f .

The force output of the clutch drive is directly proportional to the voltage applied to the clutch. This force must be equal to the force required by the carriage.

$$F_v = \frac{K_D}{D_v} V_i = M \ddot{x}_v + f \dot{x}_v$$

where D is the chain drive sprocket diameter.

In terms of the Laplace operator:

$$\frac{K_D}{D_v} V_i(s) = s [Ms + f] X_v(s)$$

And the transfer function is readily obtained as:

$$\frac{X_v(s)}{V_i(s)} = \frac{K_D / f D_v}{s(\tau s + 1)}$$

where $\tau = M/f$

The feedback tachometer is assumed to be an ideal differentiator at the frequencies of interest. Its transfer function is:

$$\frac{V_T(s)}{X_V(s)} = K_T s$$

Fig. 9 is a schematic diagram showing the servo loop with the individual component transfer functions.

To obtain the open loop transfer function the inner loop will now be eliminated.

The forward portion of the inner loop is:

$$G(s) = \frac{K_A K_D / f D_v}{s(\tau s + 1)}$$

and the tachometer feedback loop is:

$$H(s) = K_T s$$

The closed loop transfer function of the inner loop is now:

$$\begin{aligned} \frac{X_V(s)}{V_p(s)} &= \frac{G(s)}{1 + G(s)H(s)} = \frac{\frac{K_A K_D / f D_v}{s(\tau s + 1)}}{1 + \frac{K_A K_D / f D_v}{s(\tau s + 1)} K_T s} \\ &= \frac{\frac{K_A K_D}{f D_v (1 + \frac{K_A K_D K_T}{f D_v})}}{s \left[\frac{\tau s}{1 + \frac{K_A K_D K_T}{f D_v}} + 1 \right]} \end{aligned}$$

Putting in standard form we have:

$$\frac{X_v(s)}{V_p(s)} = \frac{K'}{s(\tau's+1)}$$

where the new time constant is:

$$\tau' = \frac{\tau}{(1 + \frac{K_A K_D K_T}{f D_v})}$$

and the new gain constant is:

$$K' = \frac{K_A K_D}{f D_v (1 + \frac{K_A K_D K_T}{f D_v})}$$

With the potentiometer gain constant K_p , the open loop transfer function of the complete system is:

$$\frac{X_v(s)}{X_M(s)} = \frac{K' K_p}{s(\tau's+1)}$$

Using the following values:

$$K_A = 100$$

$$K_D = .5 \quad \frac{\text{in. lb.}}{\text{volt}}$$

$$K_T = 1 \quad \frac{\text{volt. sec.}}{\text{in.}}$$

$$f = .1 \quad \frac{\text{lb. sec.}}{\text{in.}}$$

$$D_v = 1 \quad \text{in.}$$

$$\tau = 20 \quad \text{sec.}$$

$$K_p = 30 \quad \frac{\text{volts}}{\text{in.}}$$

We get:

$$\tau' = \frac{20}{1 + \frac{100 \times .5 \times 1}{.1 \times 1}} = .04 \text{ sec}$$

$$K' = \frac{100 \times .5}{.1 \left[1 + \frac{100 \times .5 \times 1}{.1 \times 1} \right]} = 1$$

And for the final open loop transfer function:

$$\frac{X_v(s)}{X_M(s)} = \frac{30}{s(.04s + 1)}$$

The approximate frequency response for the open loop is shown in Fig. 11 at its maximum stable gain.

APPENDIX III

GROUND EFFECT MODEL

THREE-COMPONENT STRAIN GAUGE BALANCE

A strain gauge balance has been developed to obtain the data on the longitudinal aerodynamic forces and moments acting on the model, i.e. lift, drag and pitching moment.

To reduce or eliminate the disturbances caused by the track irregularities and by the servo operation the model mass has been fully balanced by masses calculated to cancel out the inertia forces generated by the model.

Track-induced inputs components are assumed to be present in both horizontal and vertical direction. It is therefore required to balance the model mass in all directions in the longitudinal plane. In reference to Figure 18, the model is suspended by a pivot at point A through its center of gravity. The supporting arm is pivoted at point B. The mass M_1 exactly balances the model mass M_M . The second supporting arm is pivoted at point C; this pivot is attached to the carriage structure. The mass M_2 balances the combined model mass M_M and M_1 . Another way to describe this balancing process is to visualize the effect of mass M_1 shifting the center of gravity of the assembly from the model to point B. Mass M_2 in turn displaces the center of gravity from point B to point C. This system will not respond to accelerations in the longitudinal plane (the plane of the drawing).

To measure the forces and moments the system will be restrained by strain gauge beams in the locations shown in the drawing. The strain

gauge beams are beams of rectangular cross section, constrained at both ends with the load applied at its midpoint. A four strain-gauge bridge is used on every beam to compensate for changes in ambient temperature. Two beams separated by a given distance are used to measure lift and also rolling moment.

Considering the relative positions of the various components restrained by the strain gauge beams as shown in Figure 18, it can be seen that only the pitch gauge will record directly the desired force, in this case the pitching moment. The drag and lift gauge readings will include effects due to the other forces and moment.

To determine the actual forces acting on the model the following relationships are required

$$P = p F_M$$

$$D = \frac{n}{m} F_D - \frac{mp}{m+n} F_M$$

$$L = F_L + \frac{bn}{am} F_D + \frac{p}{a} \left[1 - \frac{bm}{m+n} \right] F_M$$

where P , D , and L are the pitching moment, drag and lift respectively and F_M , F_L , and F_D are the forces read by the gauges. Distances are as shown in Figure 18.

APPENDIX IV

METHOD FOR EQUALIZATION OF LIFTED AND TRAVELING MODEL MASS

The error link design introduces a difference in the traveling and lifted mass of the model. The effect of this difference on the dynamic behavior was small for the helicopter model tested. See Figure 13. However, it is possible that for models of different configuration and mass this effect becomes significant. A suggested method for equalizing the two masses is given here in reference to Figure 14. The model traveling mass including linkages is M_T and the model lifted mass also including linkages is M_L .

The installation of a rack-and-gear-driven flywheel of rotational inertia J to the lifted link will produce an effective increase in lifted mass with a relatively small increase in traveling mass. Some additional mass besides the flywheel installation mass M_W will be included in both the traveling and the lifted mass and is also included in the analysis. Assuming that the additional traveling mass due to the rack and the rack support installation is M_R and that the apparent increment in lifted mass due to the flywheel is $\frac{J}{F^2}$, then the new traveling and lifted masses are:

$$M_{T1} = M_T + M_R + M_W$$

$$M_{L1} = M_L + M_W + \frac{J}{F^2}$$

M_{T1} must be equal to M_{L1} :

$$M_T + M_R + M_W = M_L + M_W + \frac{J}{F^2}$$

therefore the design condition is:

$$\frac{J}{r^2} = M_r$$

A successful design must include the effects of the sensing transducers attached to both the traveling and lifted masses. It is to be noted that this approach increases the inertial coupling between the model and the carriage.

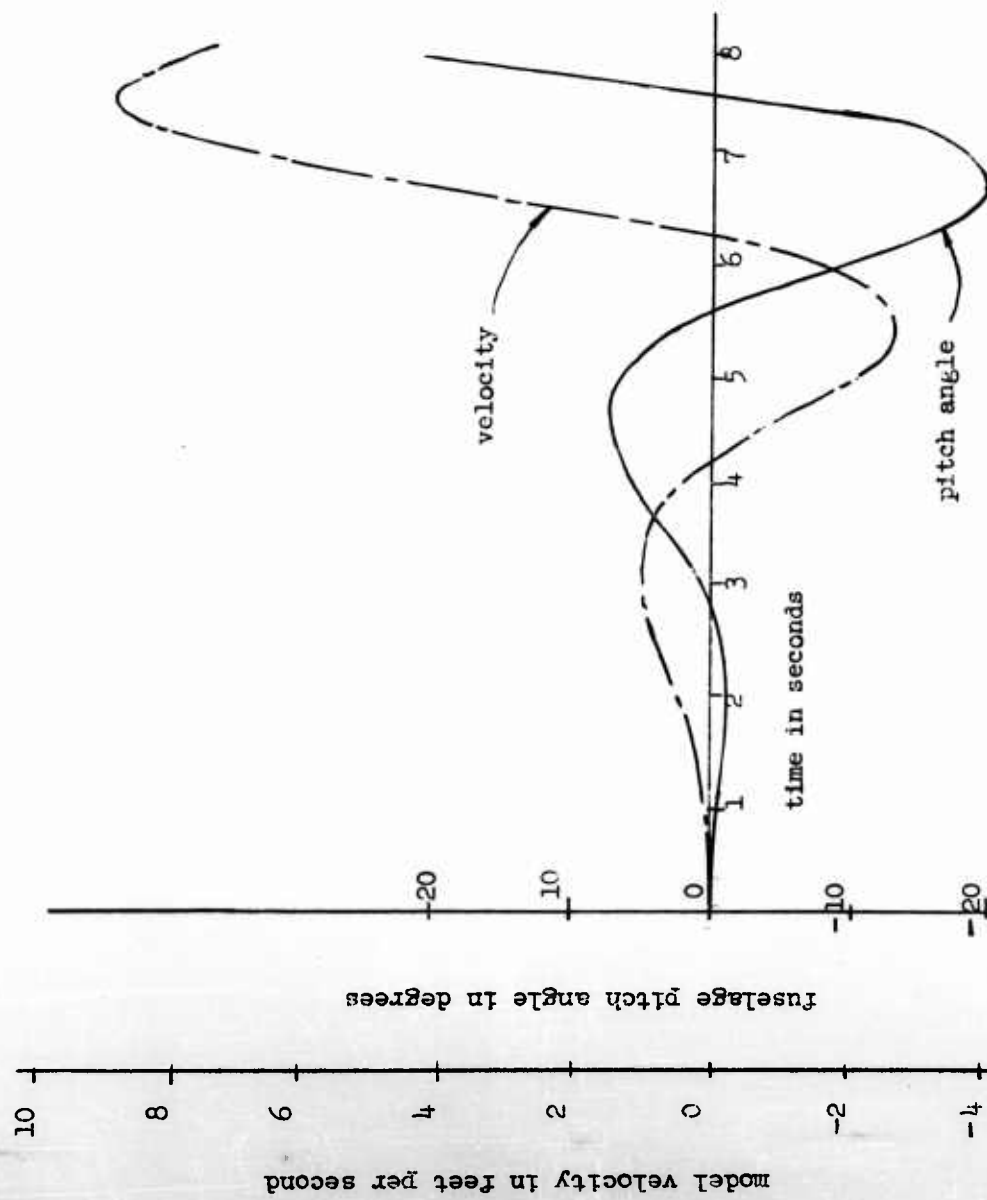


Figure 1. Typical time histories of fuselage variables of free oscillations during hovering test of a helicopter model

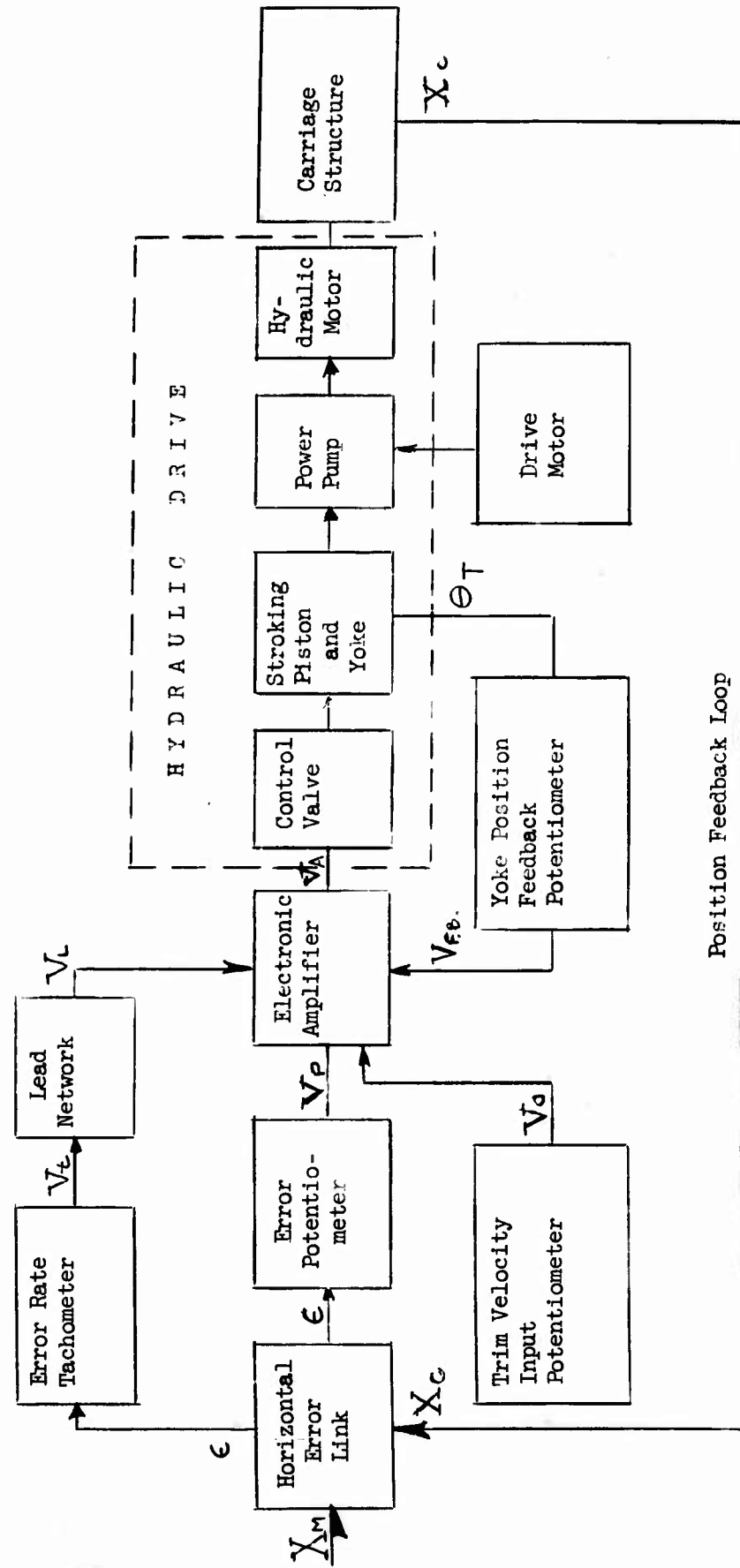


Figure 2 Horizontal position servomechanism

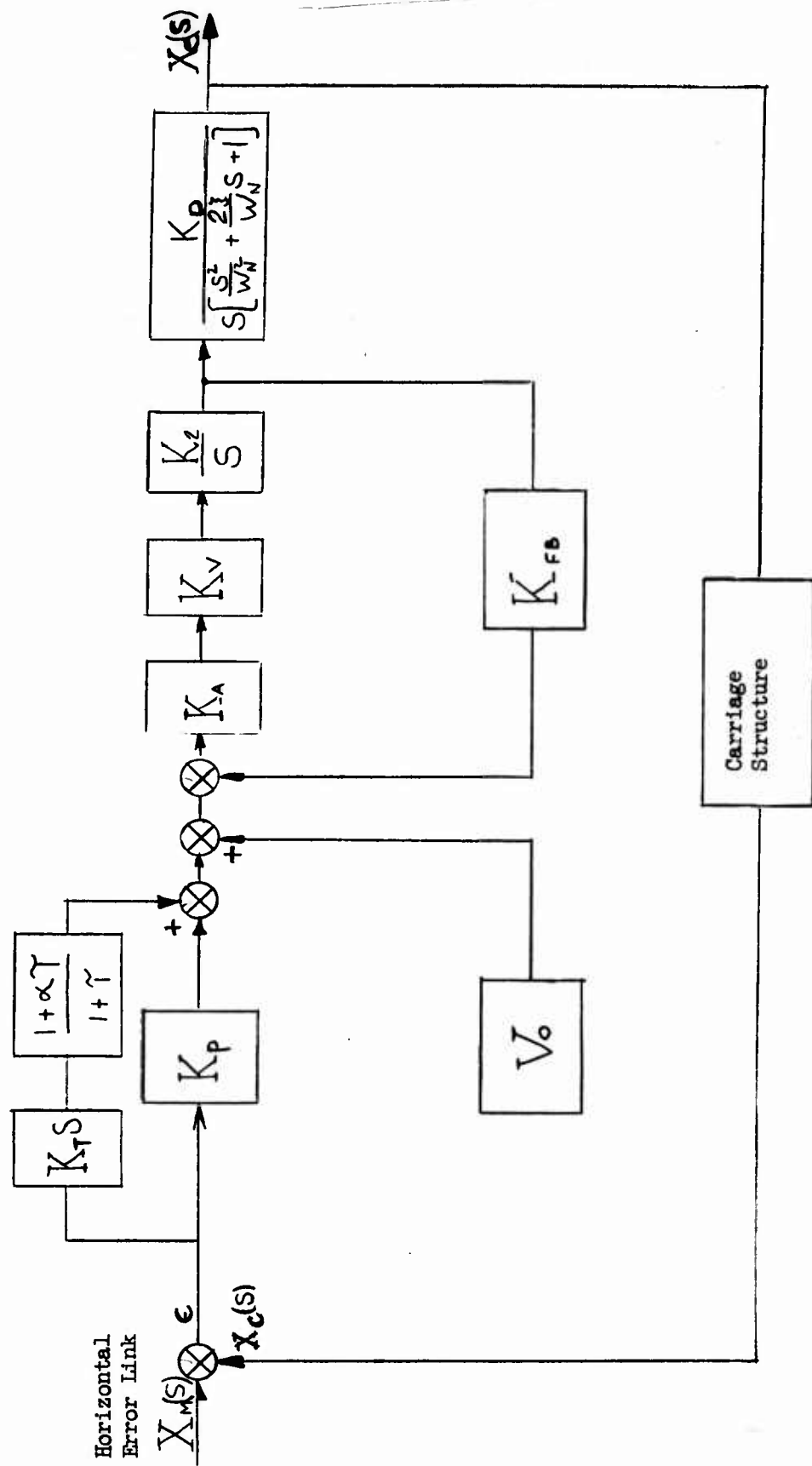


Figure 3 Horizontal position servomechanism - transfer functions of the various components

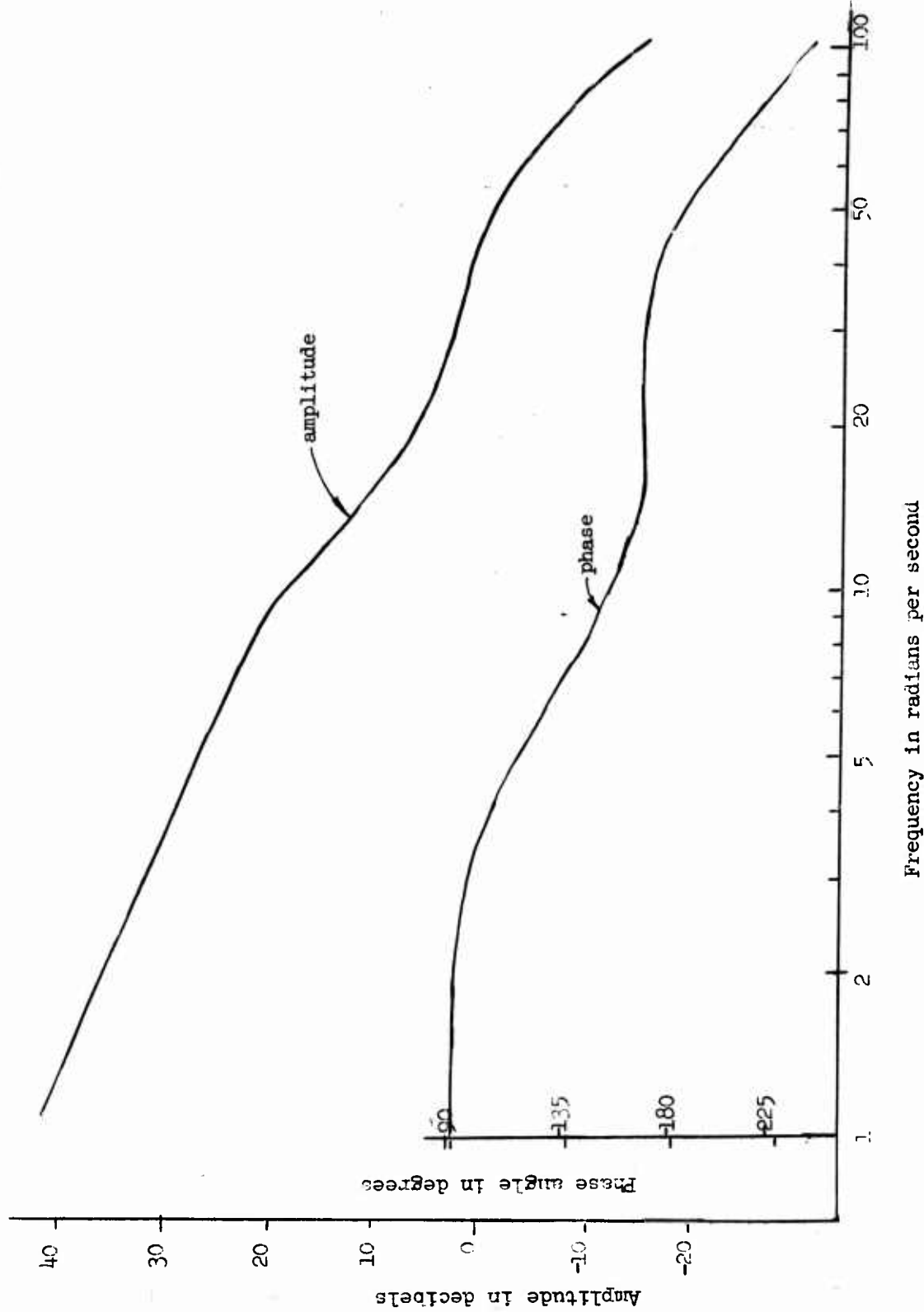


Figure 4 Approximate linear open-loop frequency responses of horizontal hydraulic position servomechanism

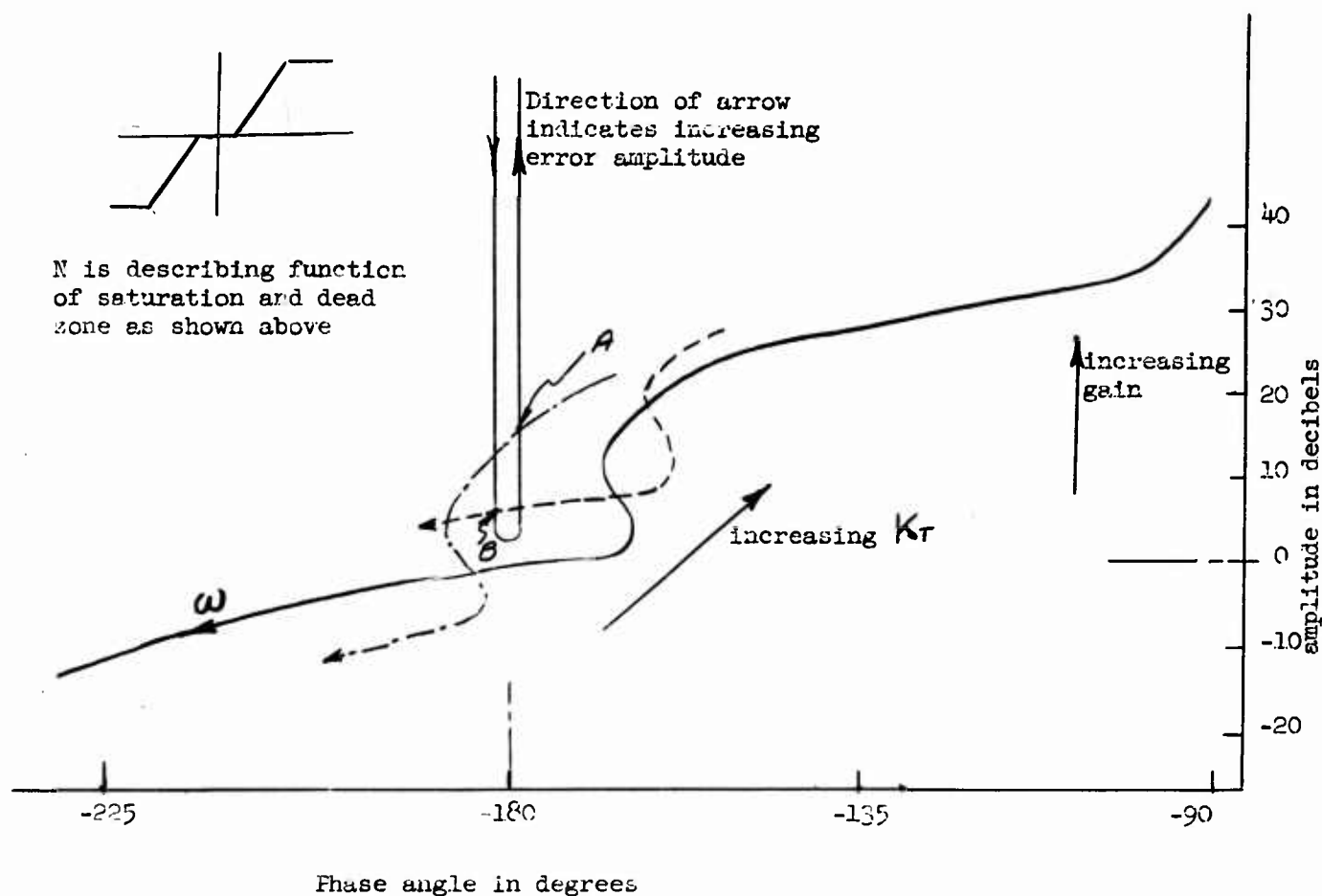


Figure 5 Approximate open loop gain-phase plot of the horizontal position hydraulic servomechanism and the describing function of the non-linearity introduced by saturation and dead zone in the system

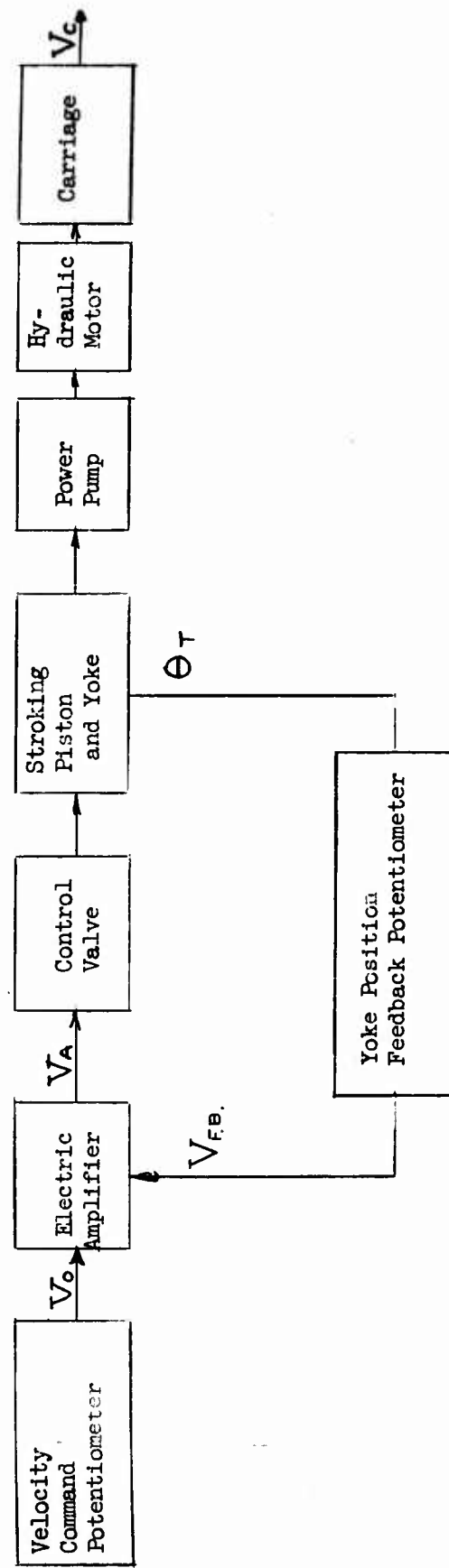


Figure 6 Velocity servo

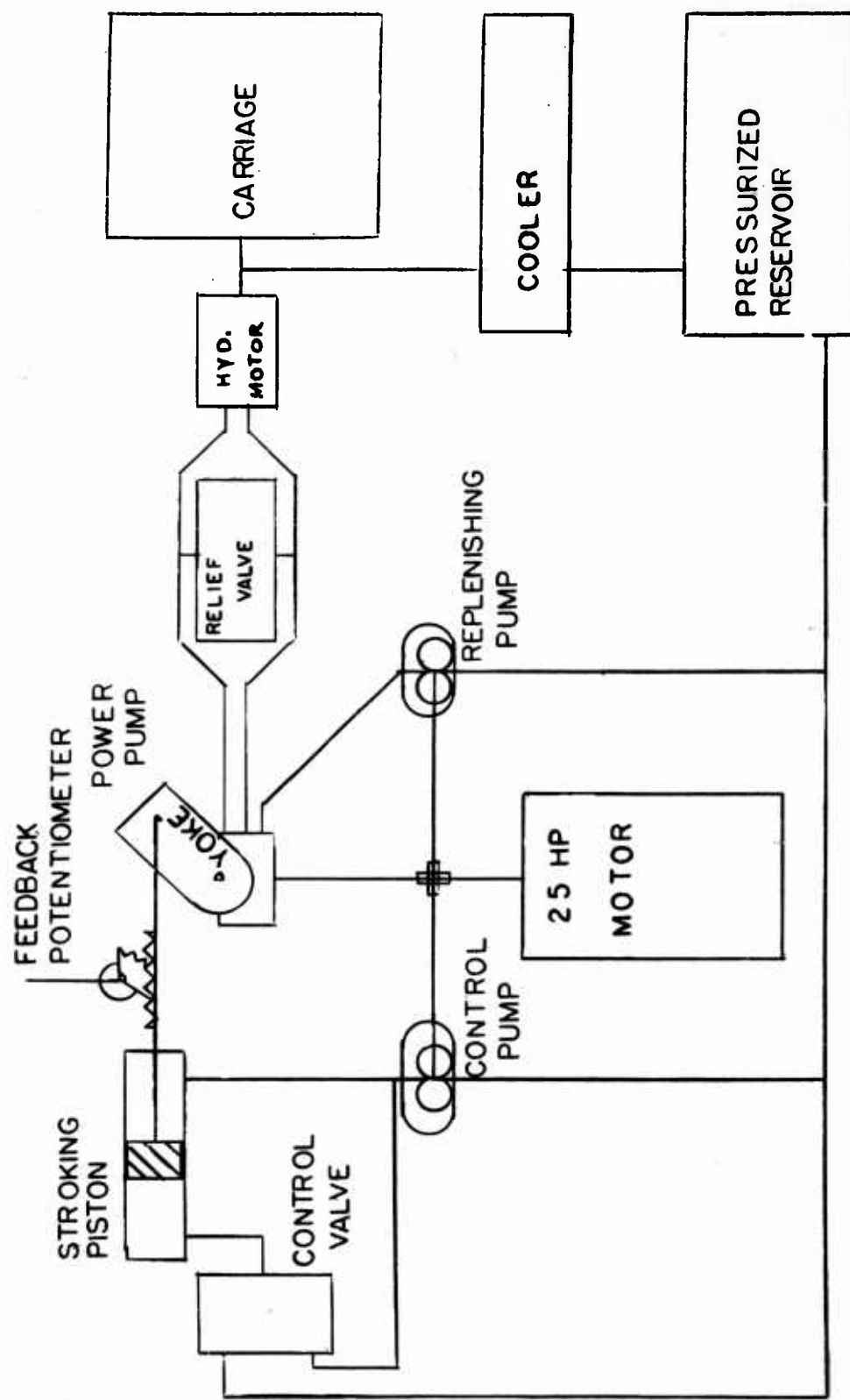


Figure 7 HYDRAULIC DRIVE SCHEMATIC

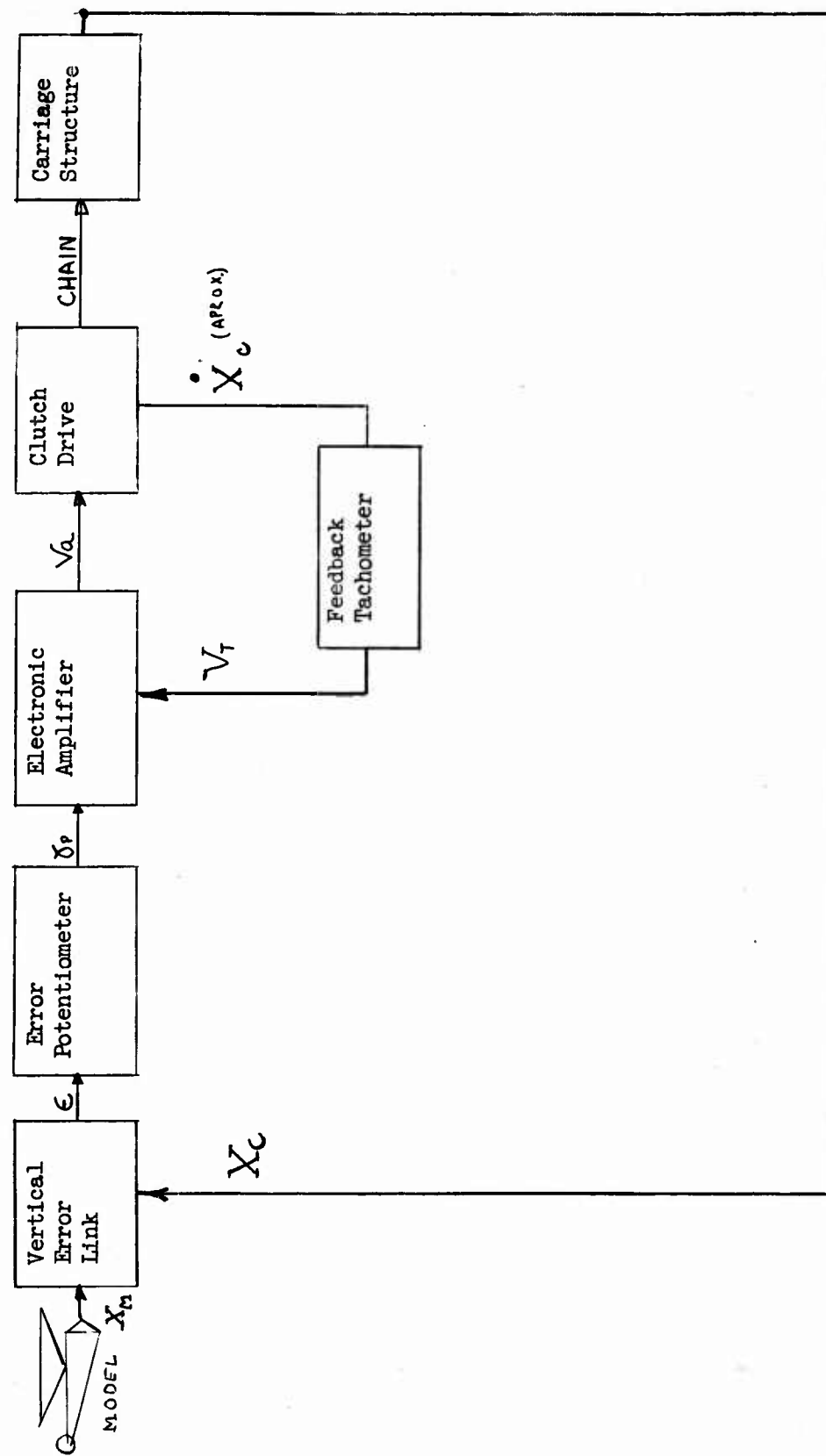


Figure 8 Vertical servomechanism

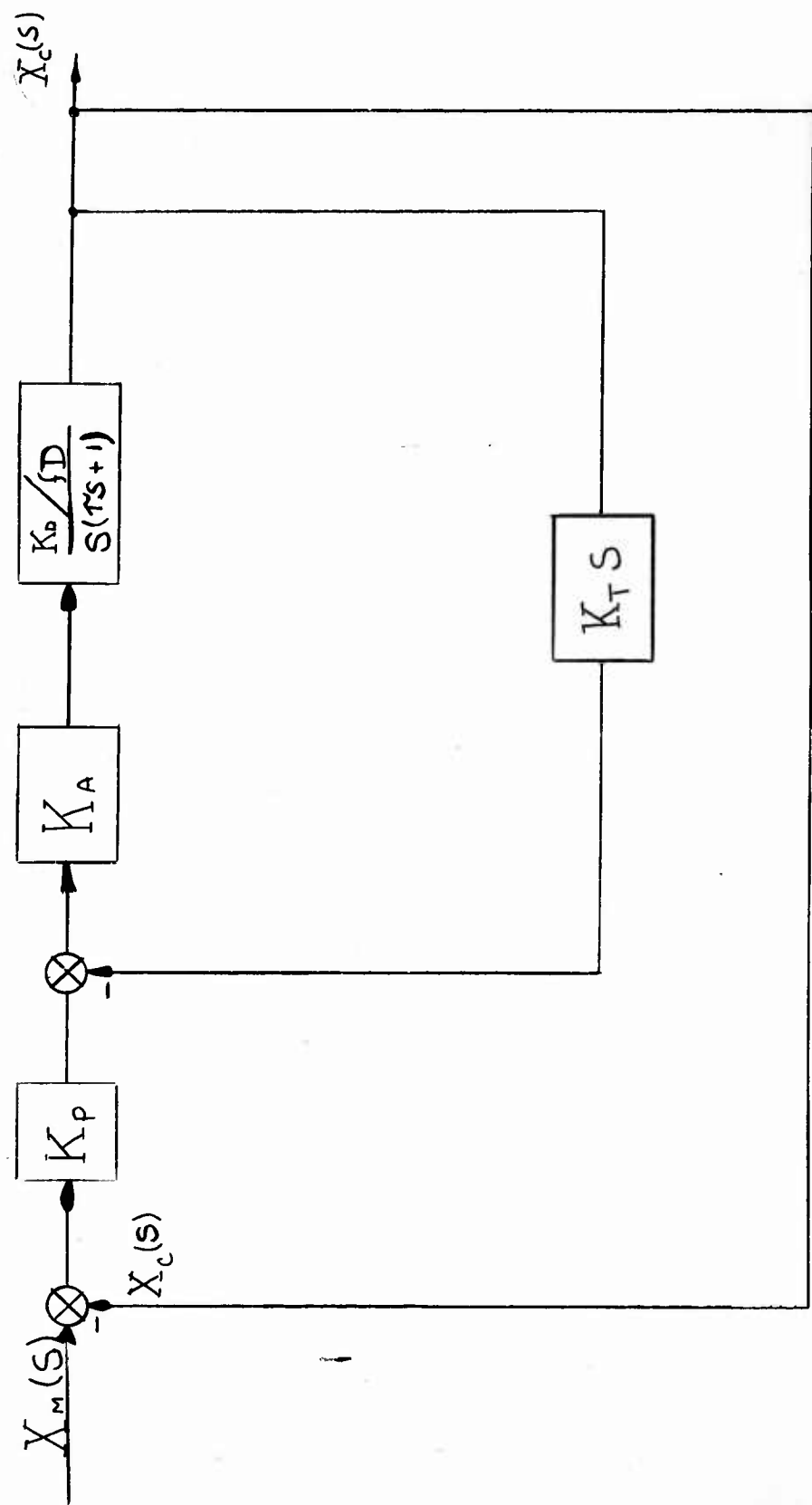


Figure 9 Vertical Servomechanism - Transfer functions of the various components

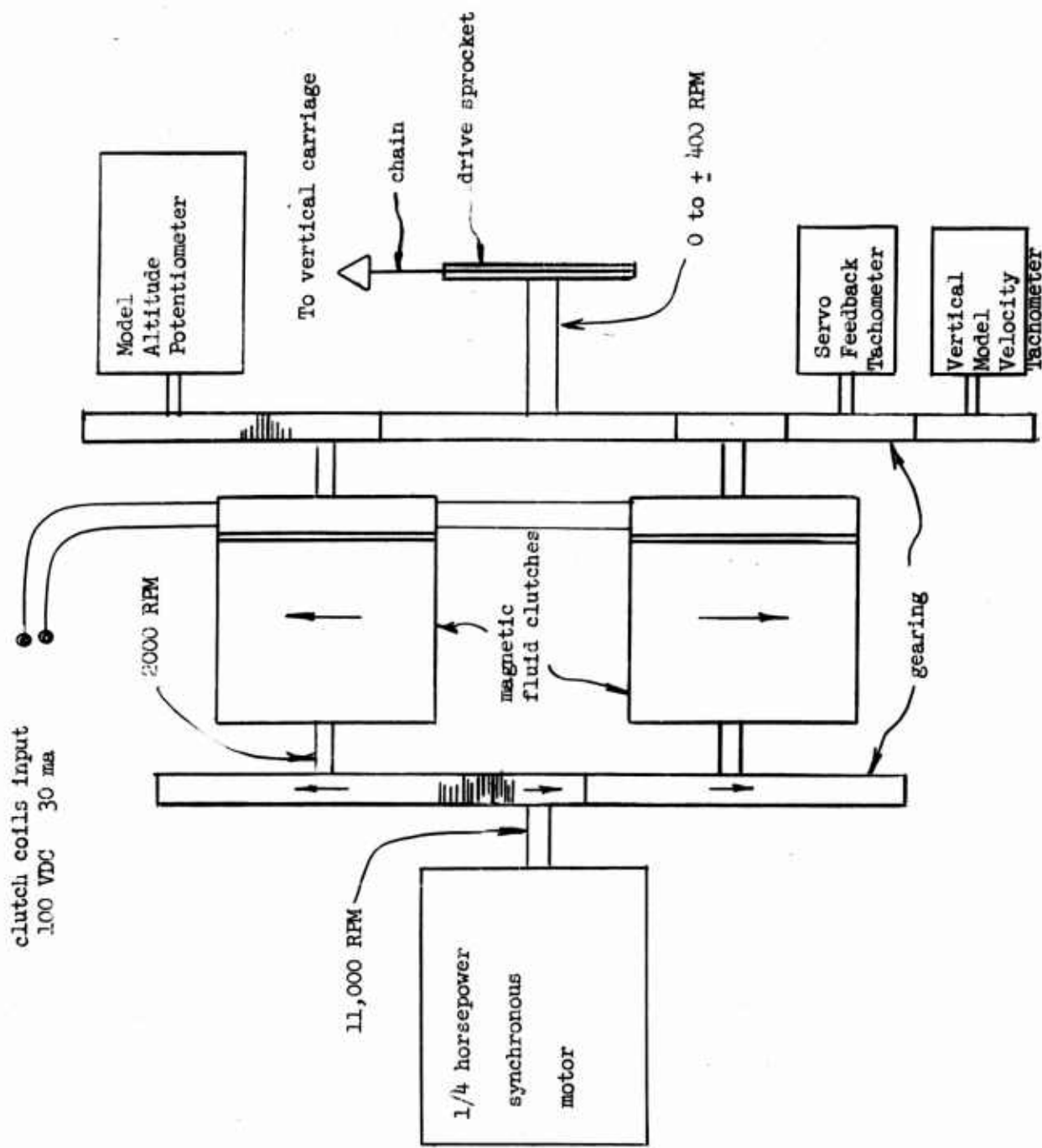


Figure 10 Schematic of the vertical magnetic fluid clutch drive

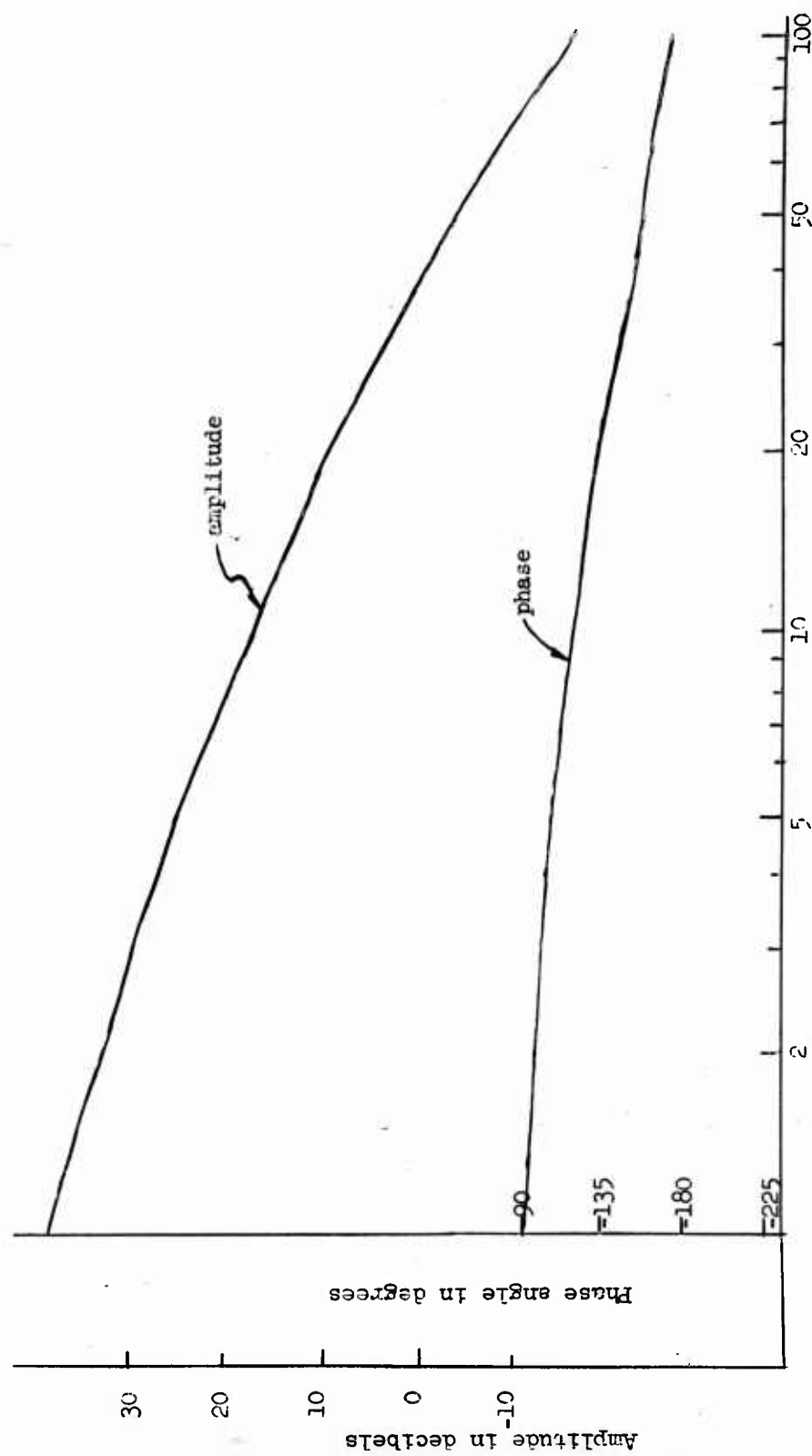


Figure 11 Approximate linear open loop frequency response of vertical position clutch drive

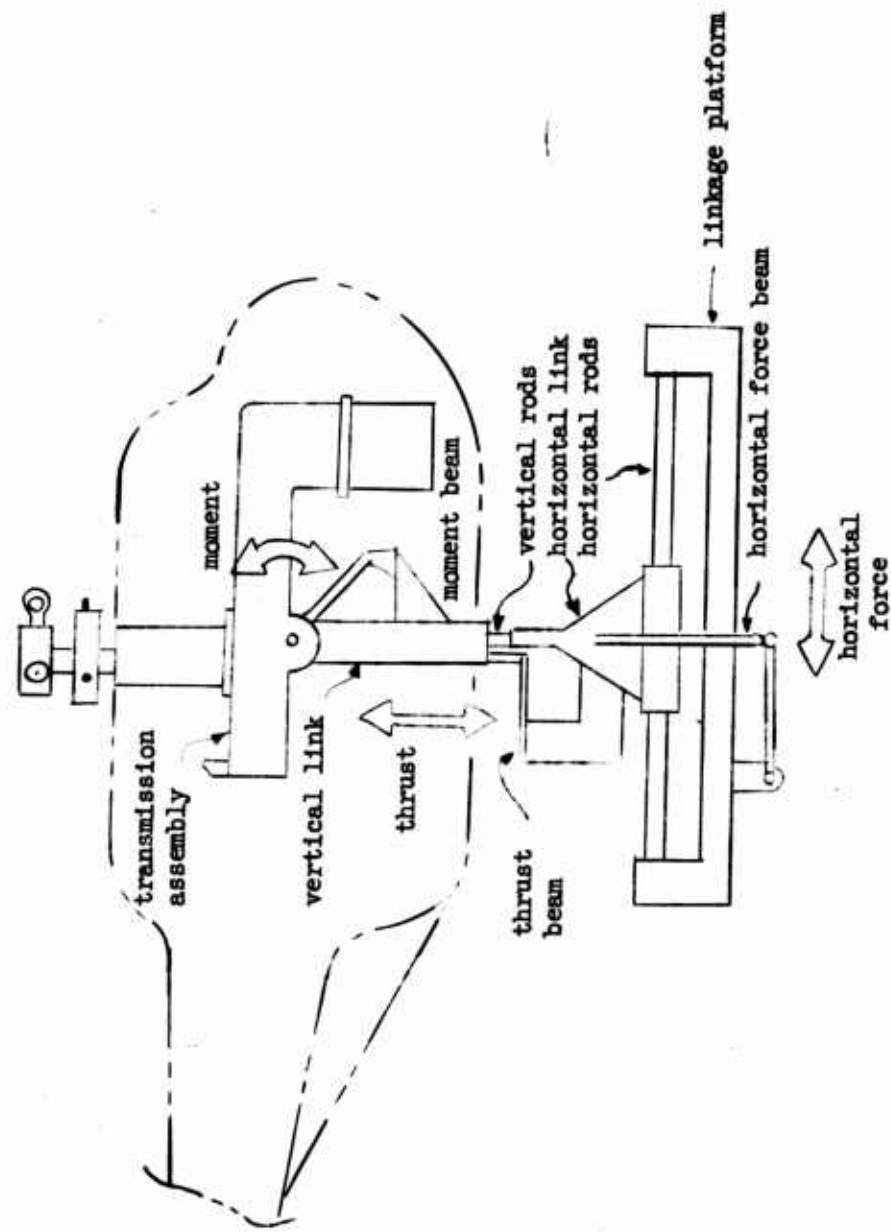


Figure 12. Mechanical schematic of strain gage balance.

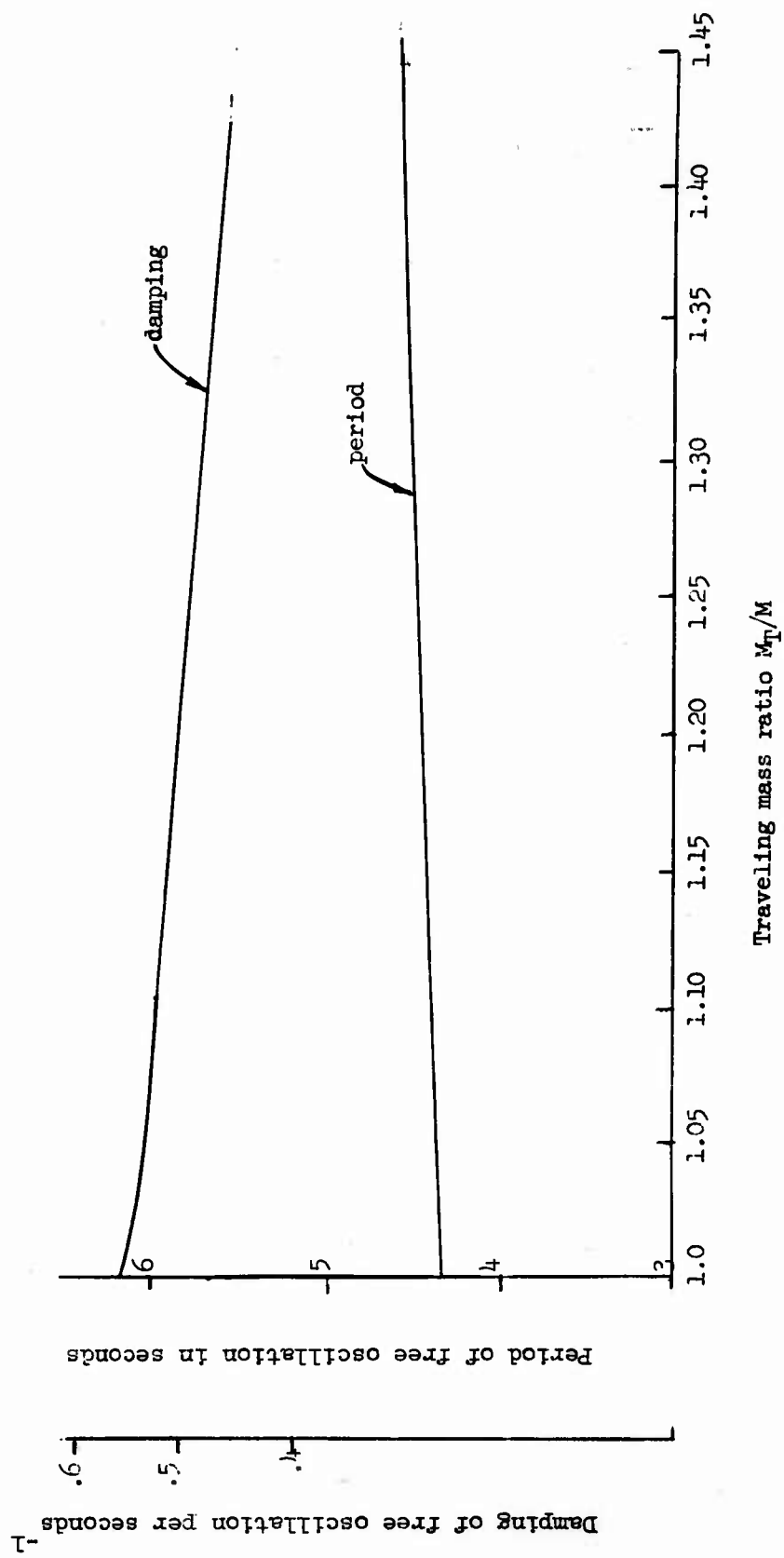


Figure 13 Variation of character of long period mode with horizontal link mass of a helicopter model

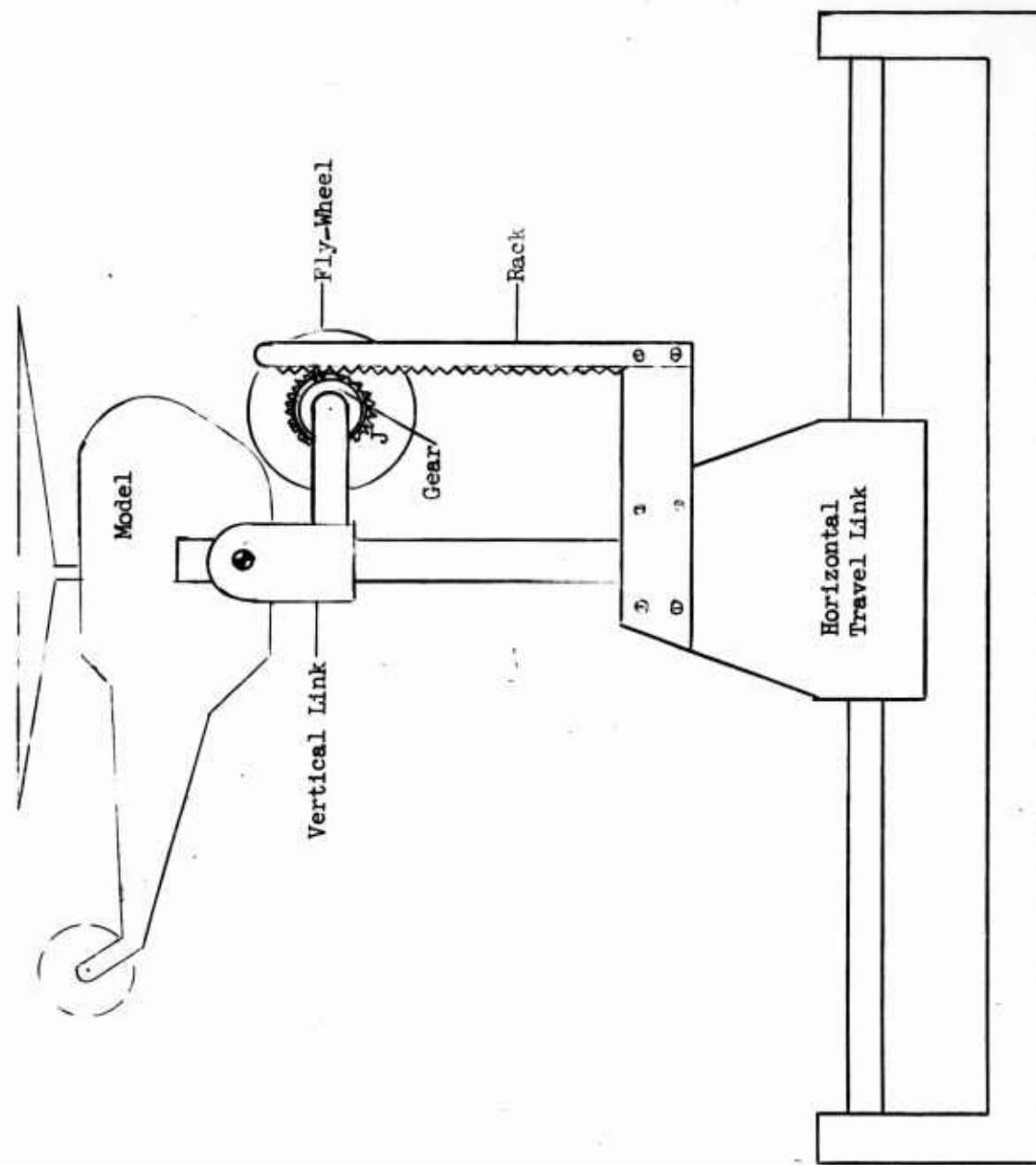


Figure 14 Method for equalizing lifted and traveling mass

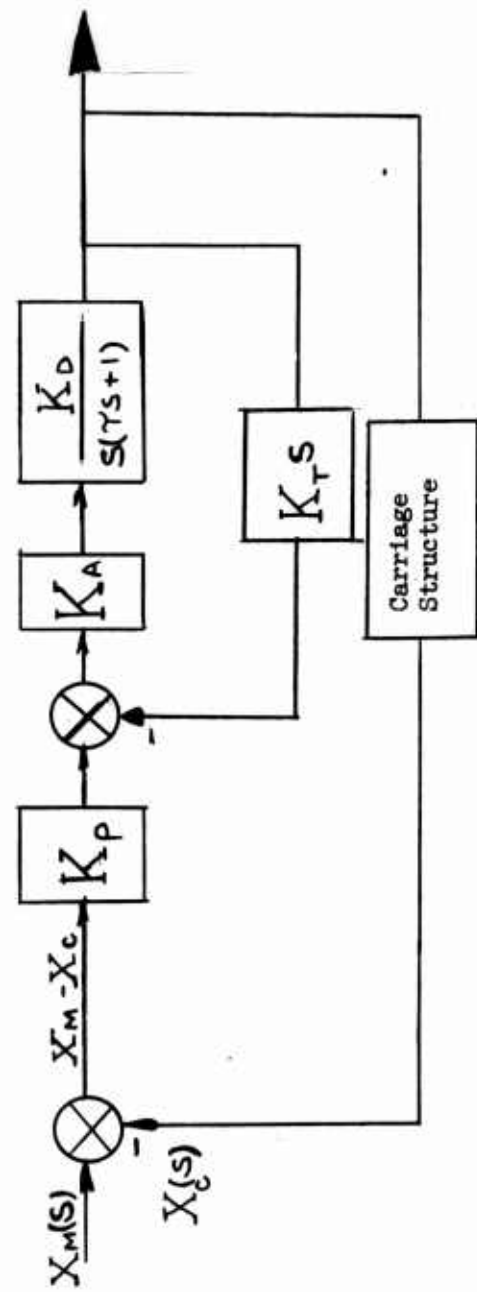
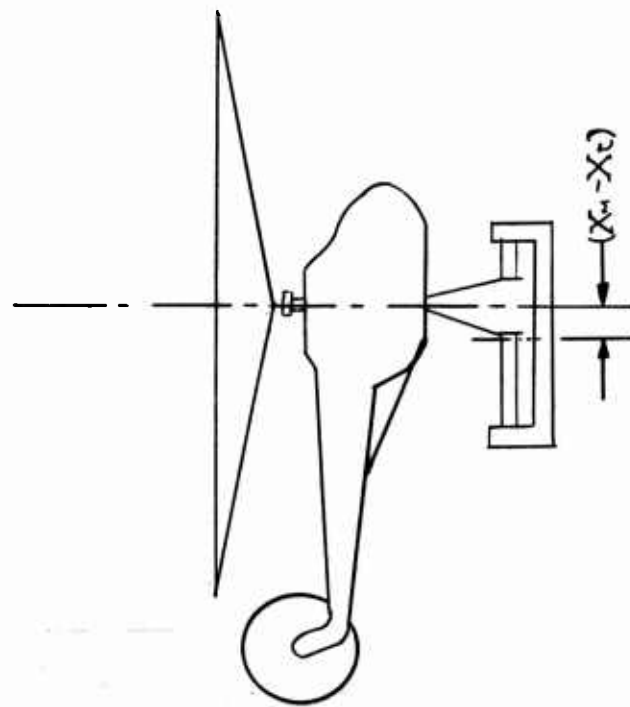


Figure 15 Hovering carriage servomechanism with the transfer function of the various components

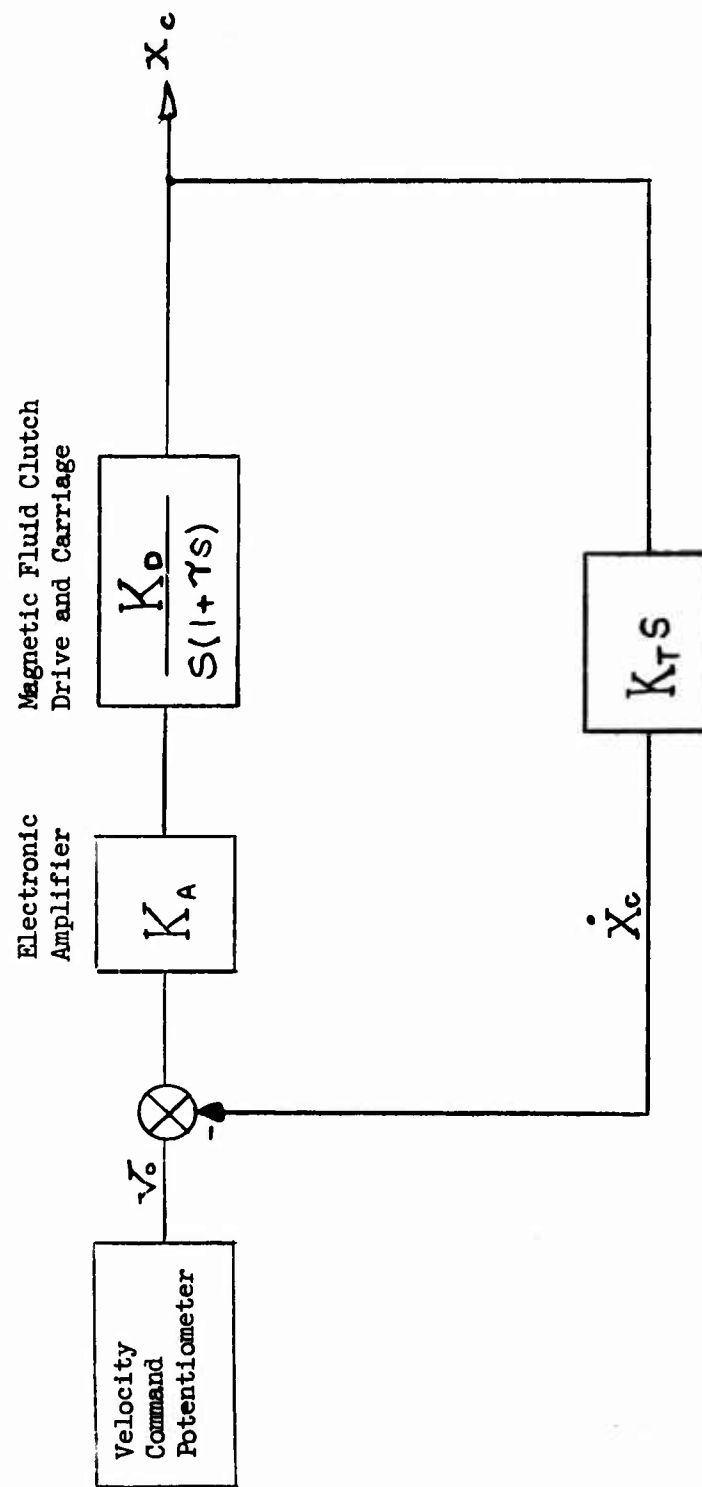


Figure 16 Constant velocity servomechanism with magnetic fluid clutch drive

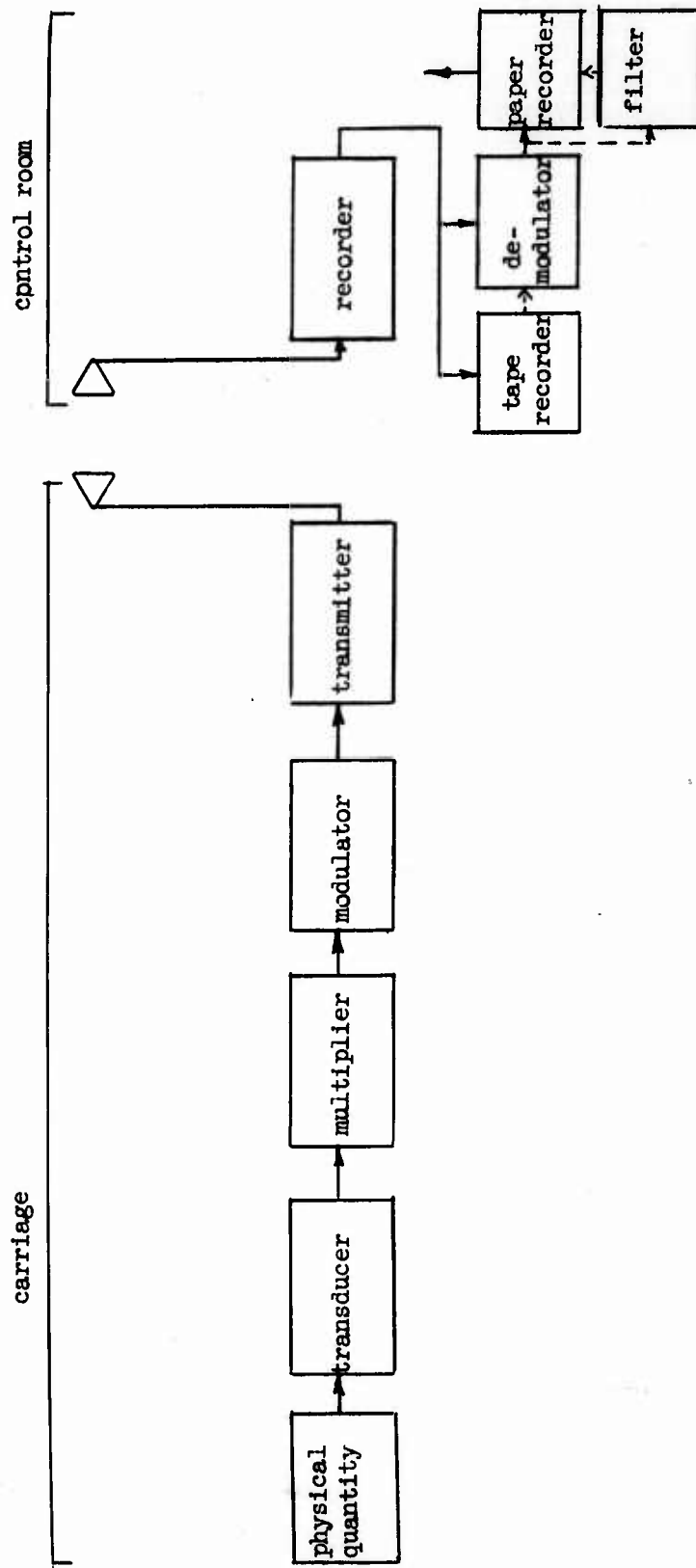


Figure 17 Block diagram of static and dynamic data gathering system

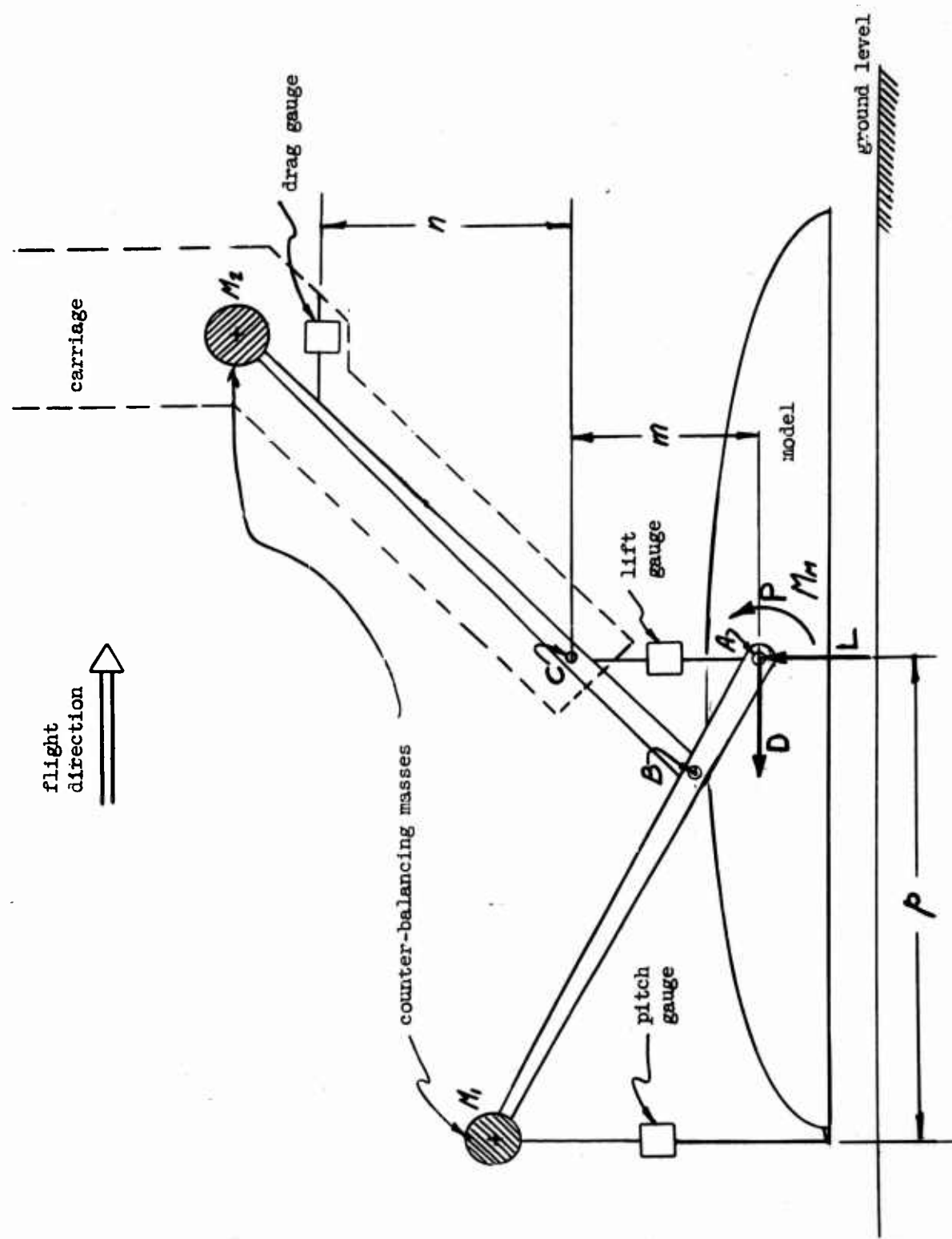
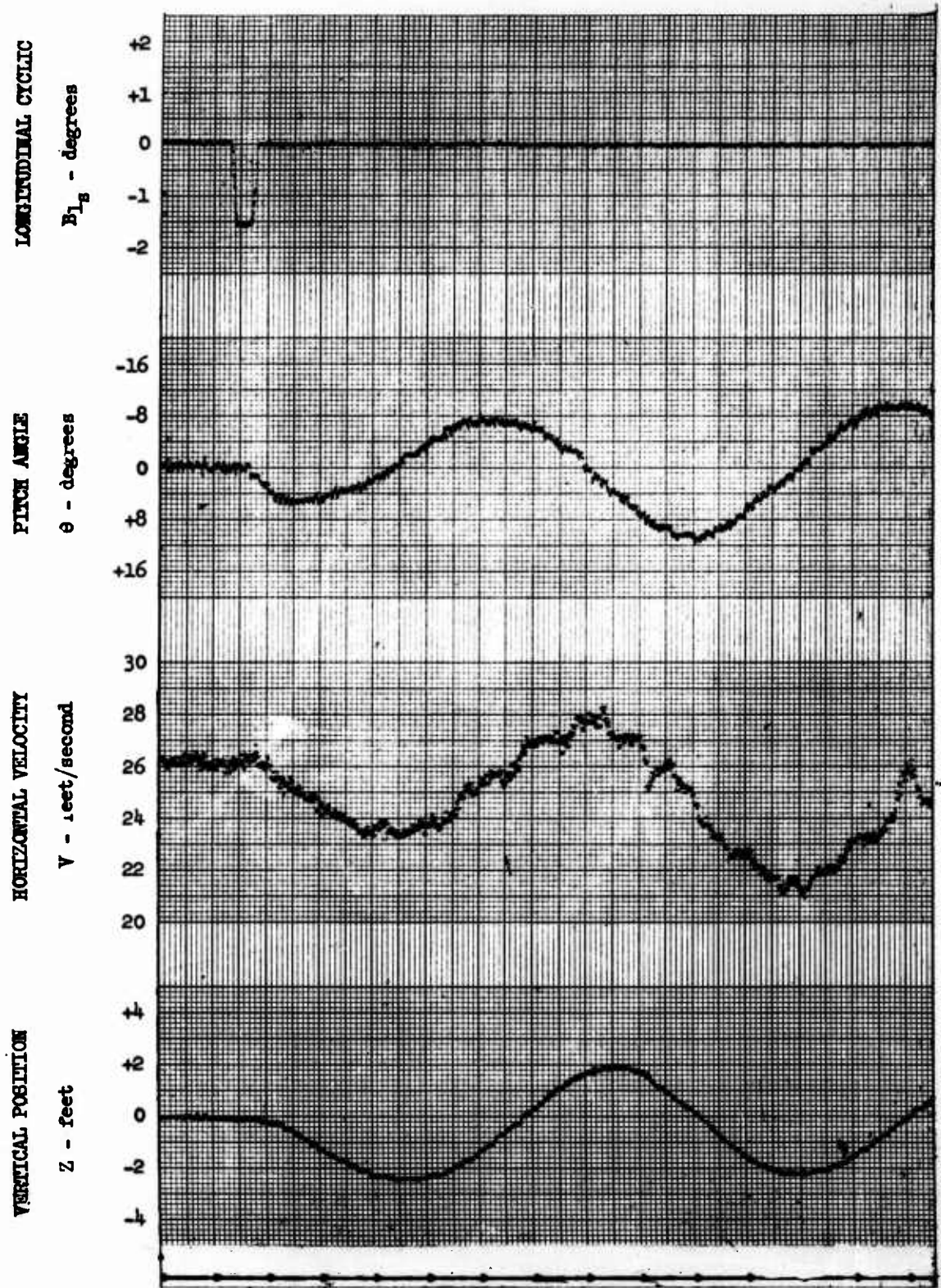


Figure 18 Schematic drawing of the three-component strain gauge balance for ground effect models

TYPICAL TRANSIENT RESPONSE OF HELICOPTER MODEL

ABOUT FORWARD FLIGHT TRIM CONDITION



TIME - seconds

FIG. 19

Figure 26

CARRIAGE AND TRACK -- GENERAL VIEW

1. Model
2. Error links
3. Horizontal boom and vertical carriage
4. Vertical track
5. Vertical brake
6. Vertical drive
7. Shock absorbers
8. Electric power rails
9. Power brush assembly
10. Top aluminum track
11. Steel rail support
12. Lower carriage guide rail

The carriage as it stands weighs approximately 750 pounds and the track is 750 feet long.

The carriage and track design was primarily dictated by the concept that a monorail system is the most suitable type for minimum maintenance and adjustment. To reduce electric noise generated at the brushes at higher speeds, a large number of brushes per rail are used.

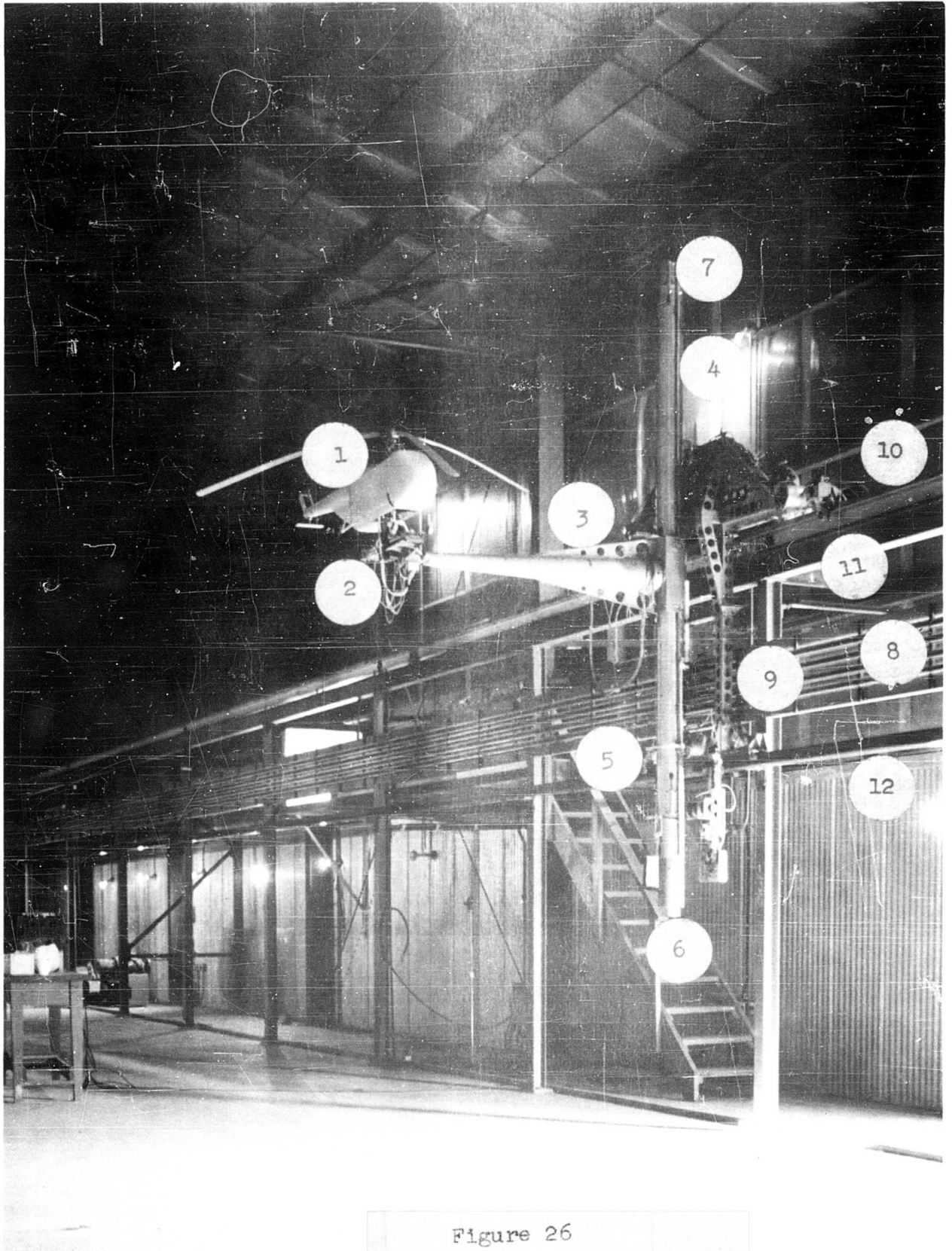


Figure 26

Figure 27

GENERAL REAR VIEW OF THE CARRIAGE

1. Error links
2. Vertical carriage with horizontal boom
3. Camera
4. Vertical track and chain drive

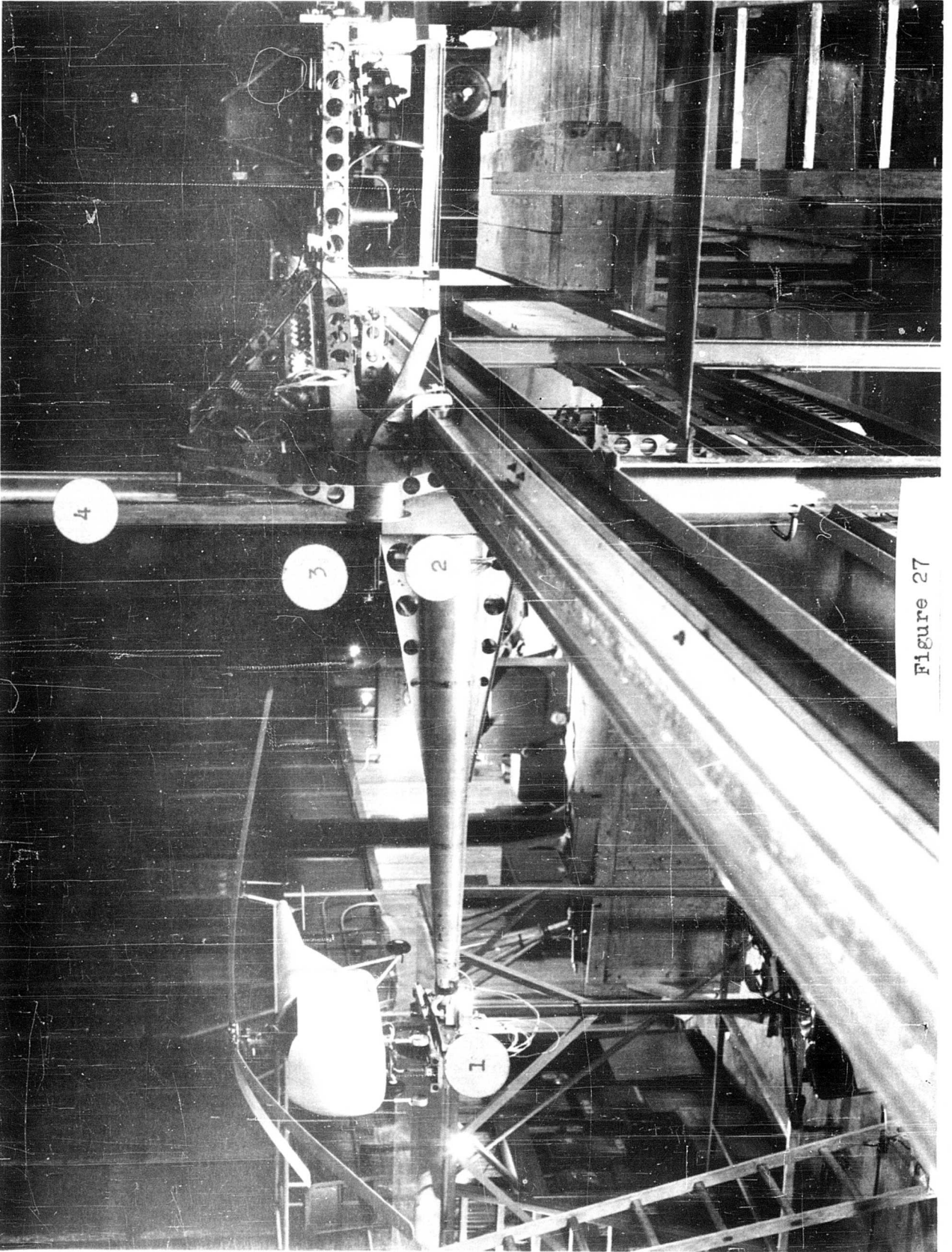


Figure 27

Figure 28

ERROR LINK

1. Horizontal freedom link
2. Error potentiometer and tachometer drive
3. Pneumatic and electrical lines
4. Shock absorbers and end locks
5. Model showing rotor hub with cyclic and collective controls

The error links sense the position of the carriage both horizontally and vertically. Not visible in the picture is the vertical link which is located inside the model. Also hidden by the model are the pneumatically operated locking and releasing devices that restrain the model horizontally, vertically, and in pitch rotation or any combination thereof, during part or all of a run.

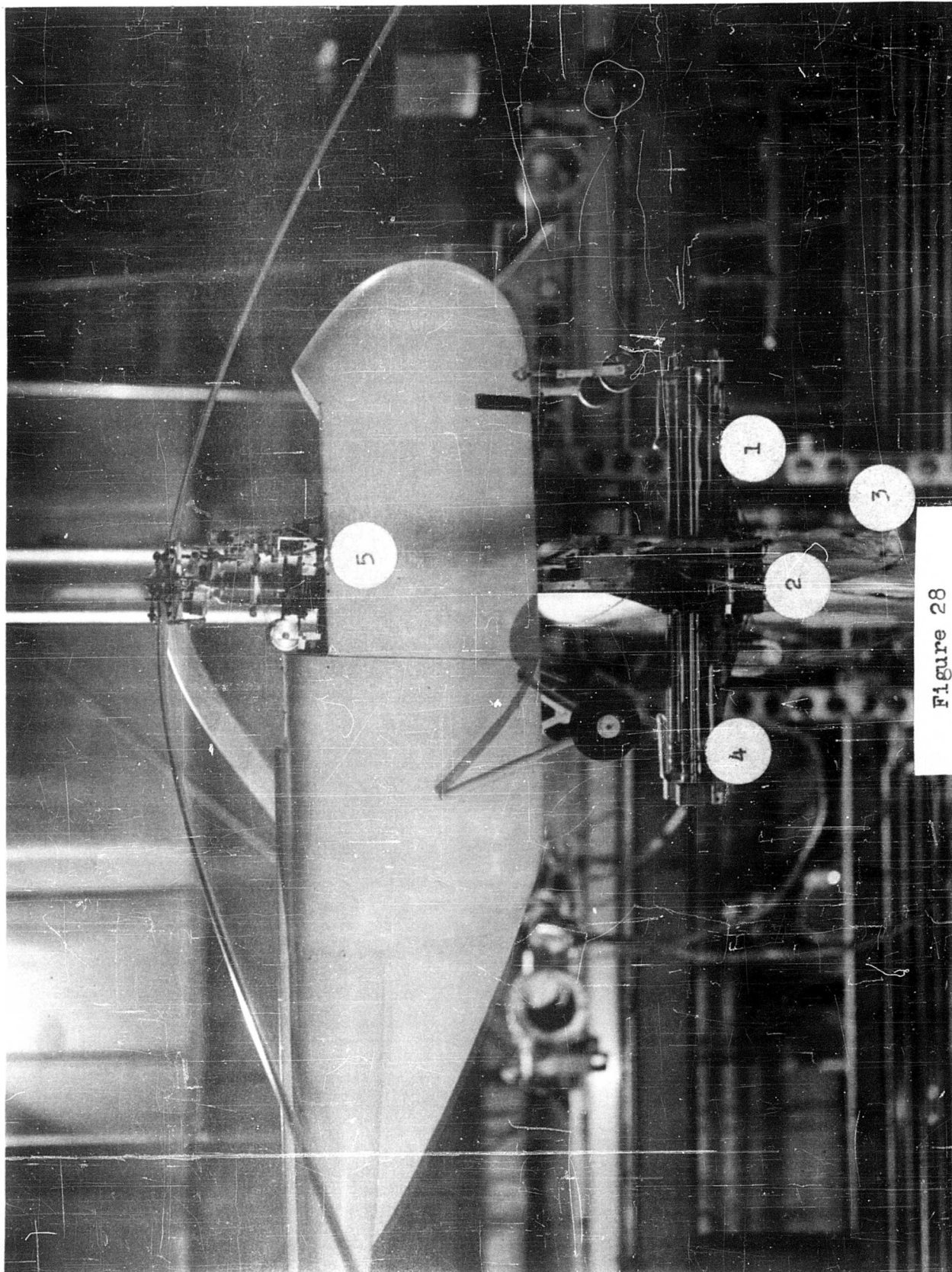


Figure 28

Figure 29

MODEL CONTROLS

1. Model motor Variac
2. Automatic pneumatic Variac control
3. Model cyclic control input generator
4. Model control box with manual cyclic and collective controls

The cyclic input generator consists of a series of programmed rotating cams that turn on the cyclic control motor, turn it off, then reverse it, returning the linkages to their original setting, thus producing a controlled magnitude impulse.

The input is started after a predetermined time delay from the instant of the complete release of the model.

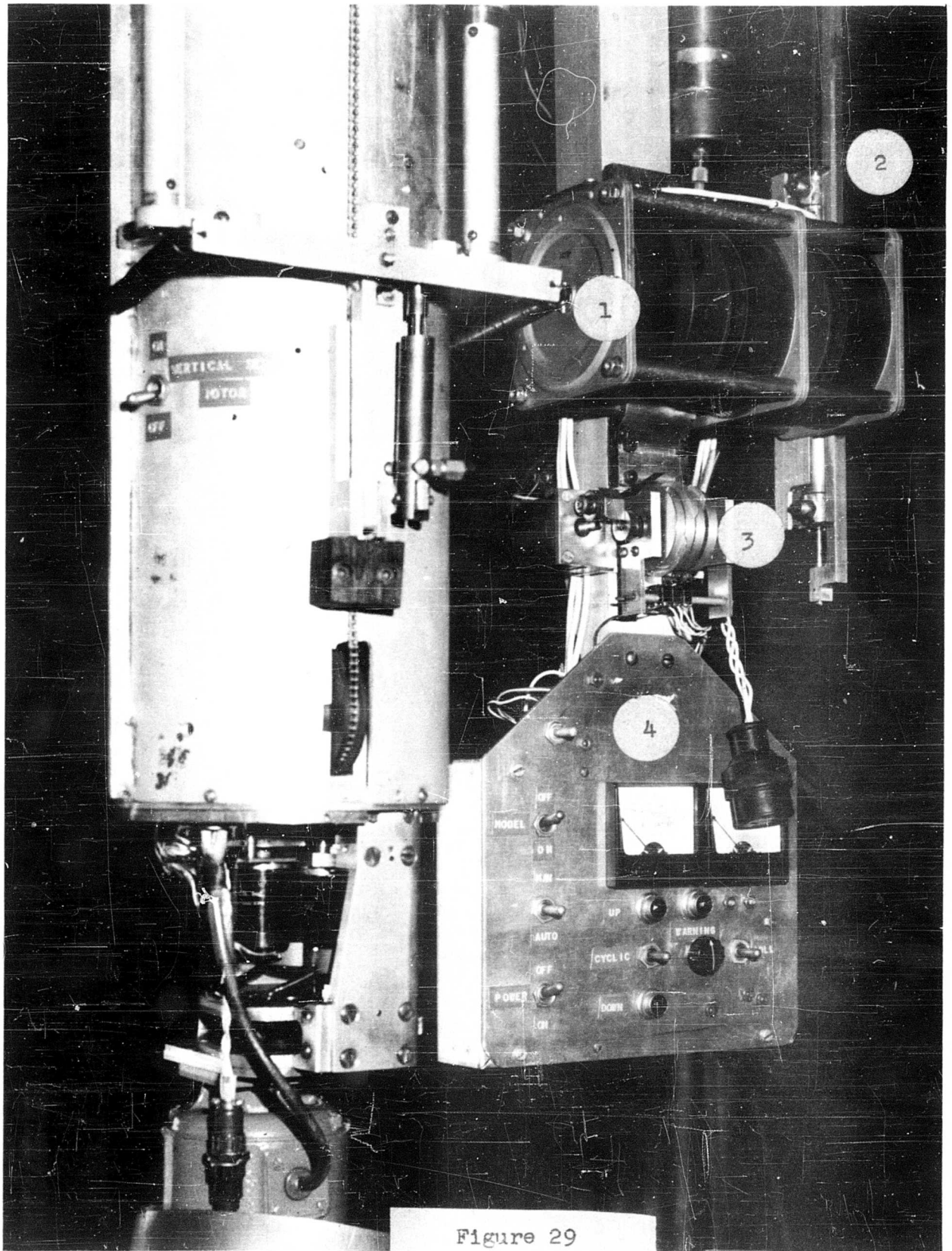


Figure 29

Figure 30

VERTICAL SERVO

1. Telemeter signal tachometer
2. Cover and cooling fan
3. Vertical track
4. Shock absorber
5. Drive chain
6. Locking device
7. Pneumatic lock release

The locking device holds the model at the required altitude during trim runs and during the acceleration phase at the start of a free flight experiment.

The pneumatic release disengages this lock at the moment the vertical servo comes into operation.

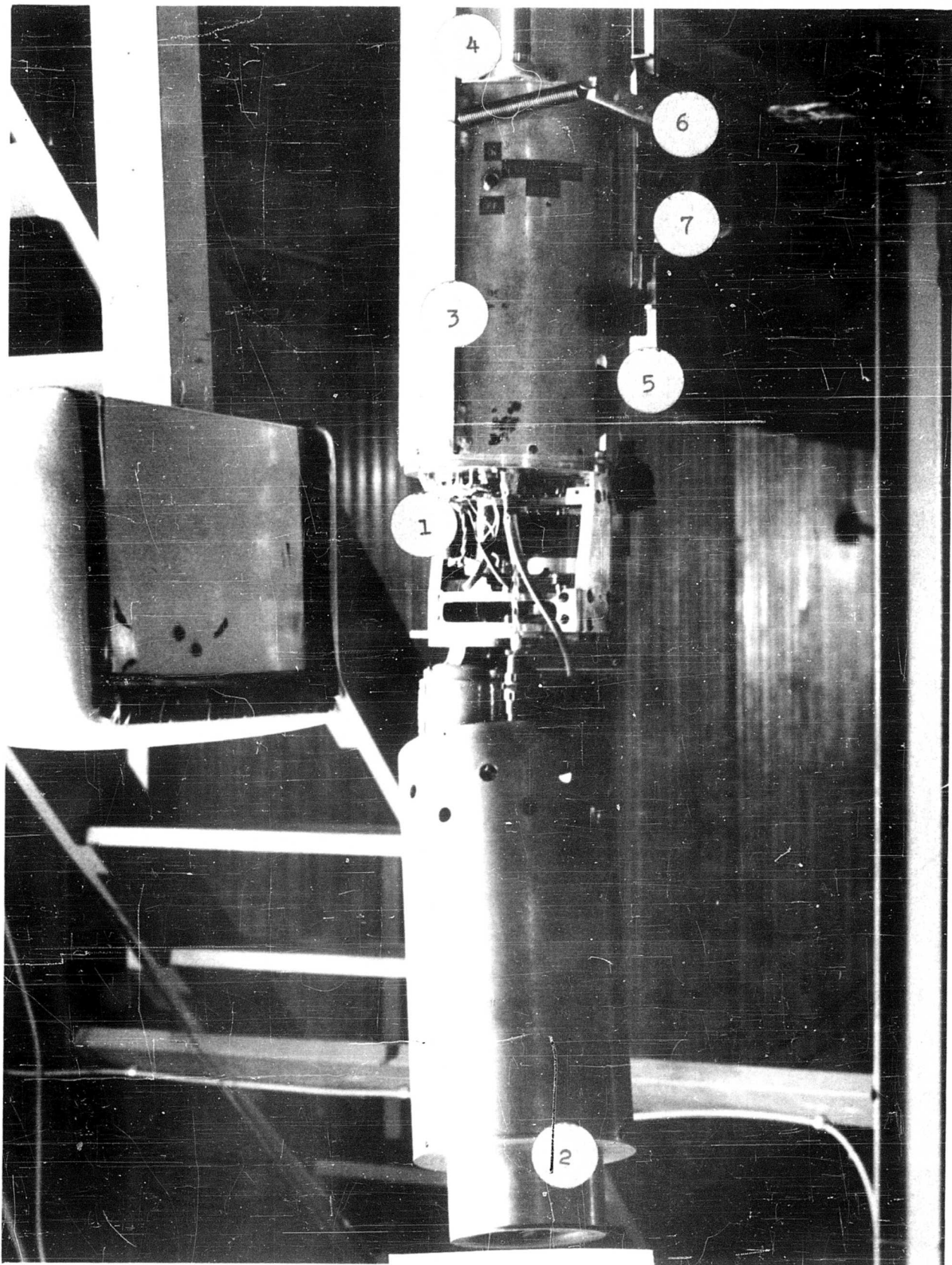


Figure 30

Figure 31

VERTICAL SERVO DRIVE AND CARRIAGE CONTROLS

1. Vertical servo drive prime mover: 1/4 horsepower U.S. Electrical motor, 115 volts, 400 cycle, 8000 rpm
2. Control component: Raymond Engineering Laboratories magnetic fluid clutch
3. Feedback tachometer
4. Sprocket output
5. Vertical position potentiometer drive
6. Carriage control box

The carriage control box contains the horizontal velocity potentiometer and the various switches to set the carriage in motion, return it at the end of the run, and a special purpose low velocity switch.

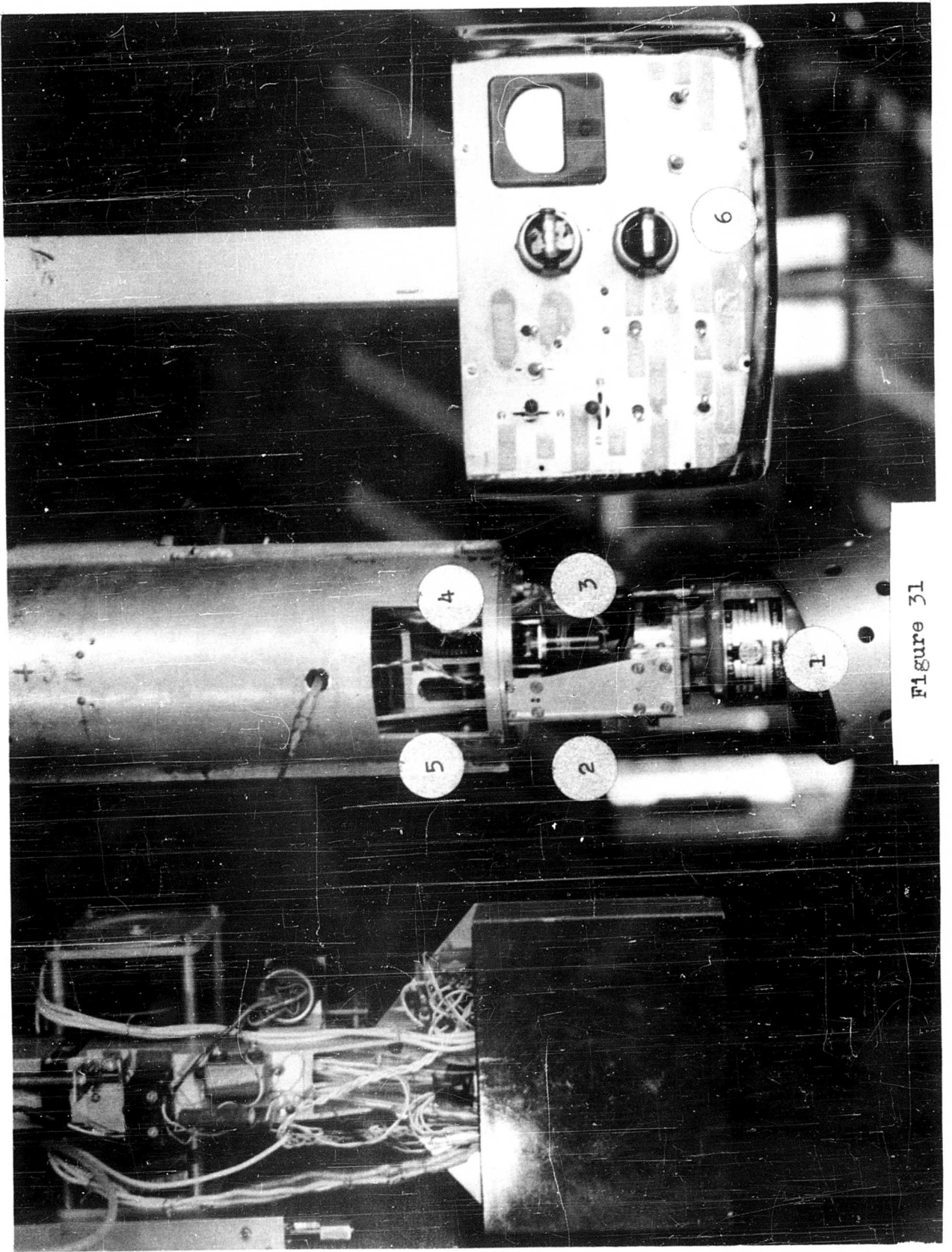


Figure 31

Figure 32

HYDRAULIC DRIVE INSTALLATION

1. Prime mover: 25 horsepower U.S. Electrical Motor, 115 volts, 400 cycles, 11,000 rpm
2. Pump input gearbox
3. Reservoir and pump inlet pressurization system
4. Oil cooler
5. Relief valve
6. Gearbox and drive wheel
7. Emergency brake-actuating light
8. Carriage guide rollers
9. Preloading springs

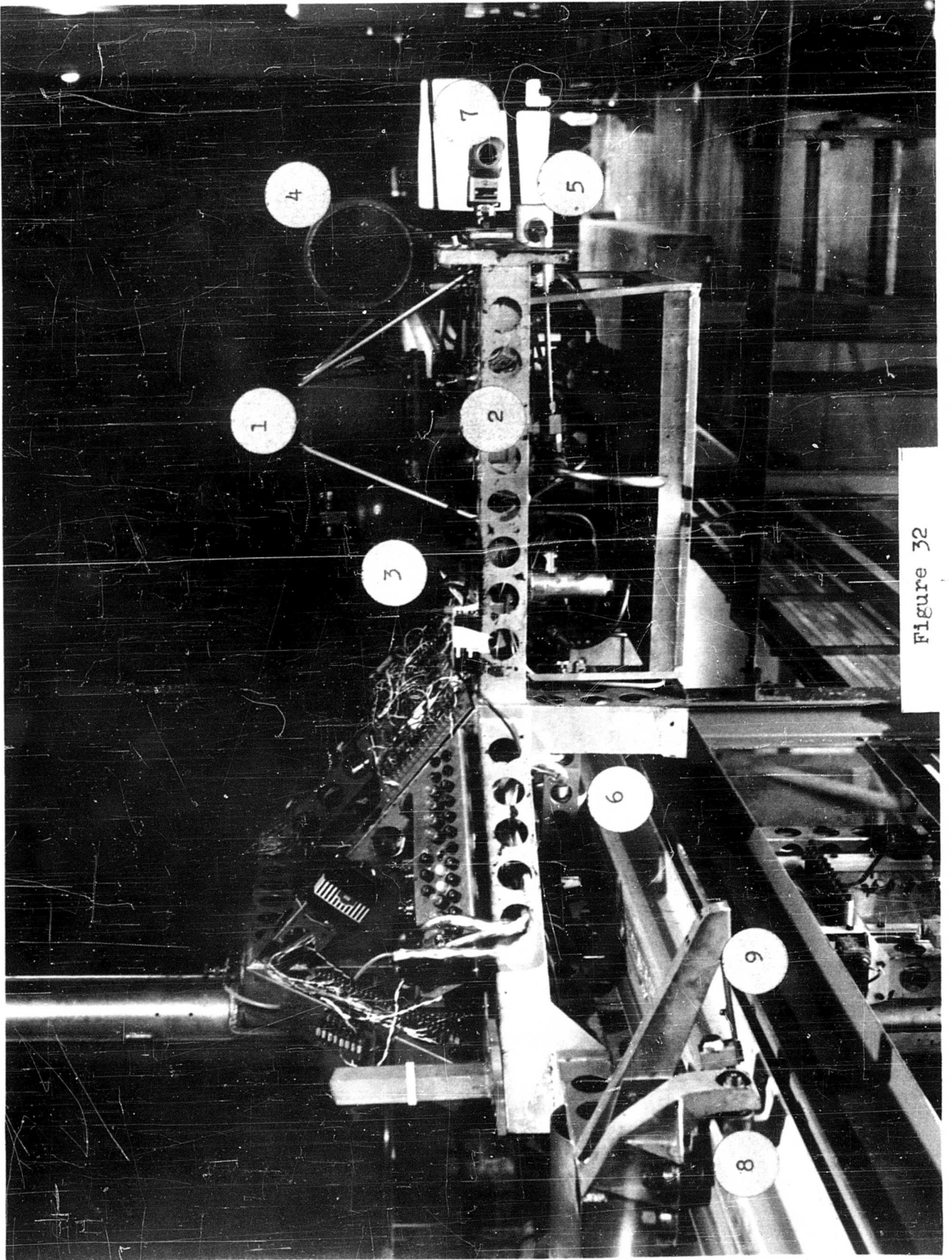


Figure 32

Figure 33

HYDRAULIC DRIVE INSTALLATION

1. Hydraulic pump
2. Hydraulic motor
3. Oil cooler fan and thermostatic control
4. Carriage velocity tachometer
5. Pneumatic solenoid control valves
6. Pump inlet pressure gauge

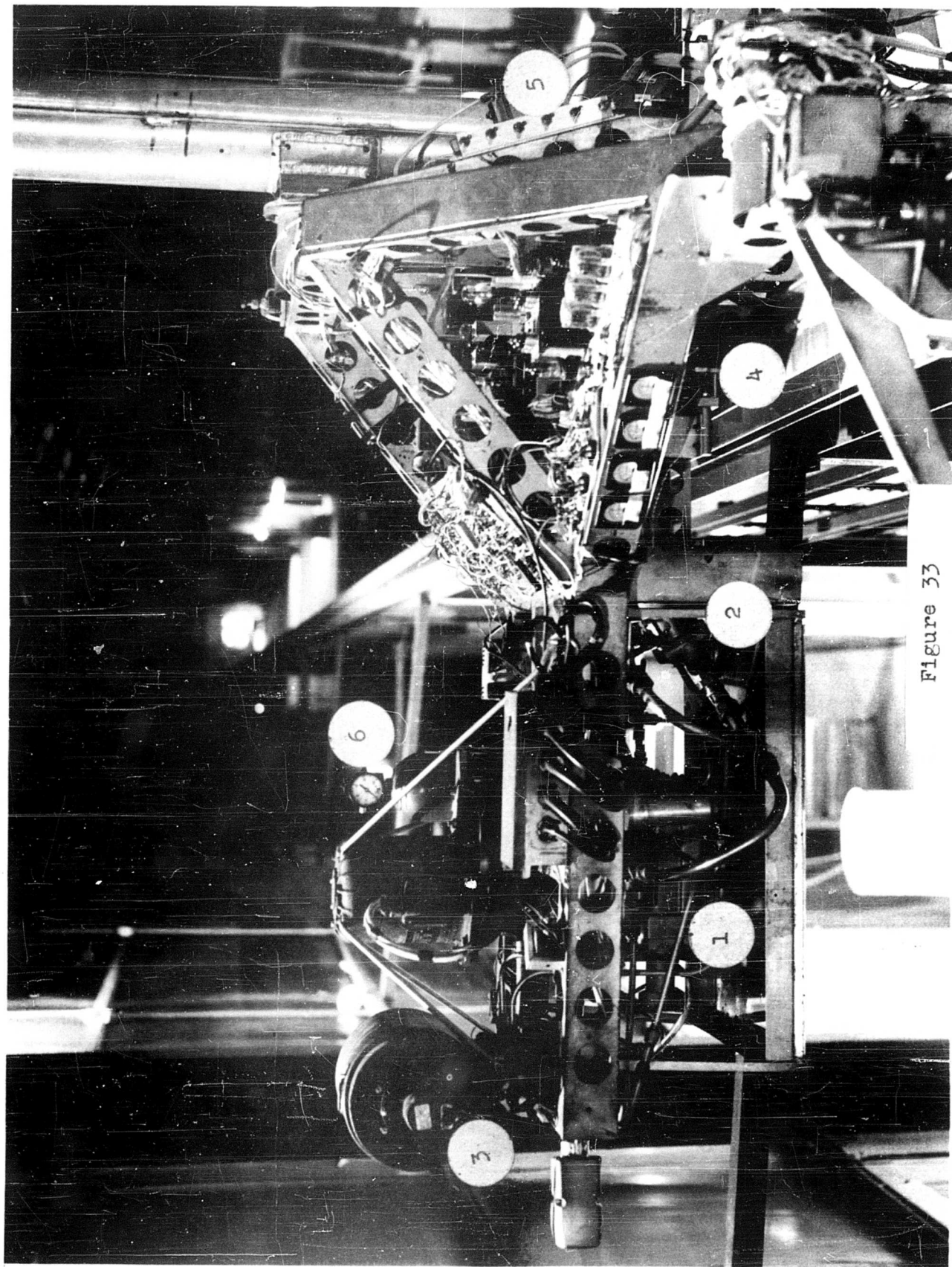


Figure 33

Figure 34

SERVO AMPLIFIERS

1. Vertical servo amplifier
2. Horizontal servo amplifier
3. Control relays
4. Horizontal amplifier output galvanometer and differential milliammeter
5. Vertical amplifier output galvanometer and differential milliammeter
6. Power supplies

Both servo amplifiers have been designed in a plug-in modular scheme for ease of replacement and maintenance. Experience with these amplifiers has shown they have outstanding long term stability.

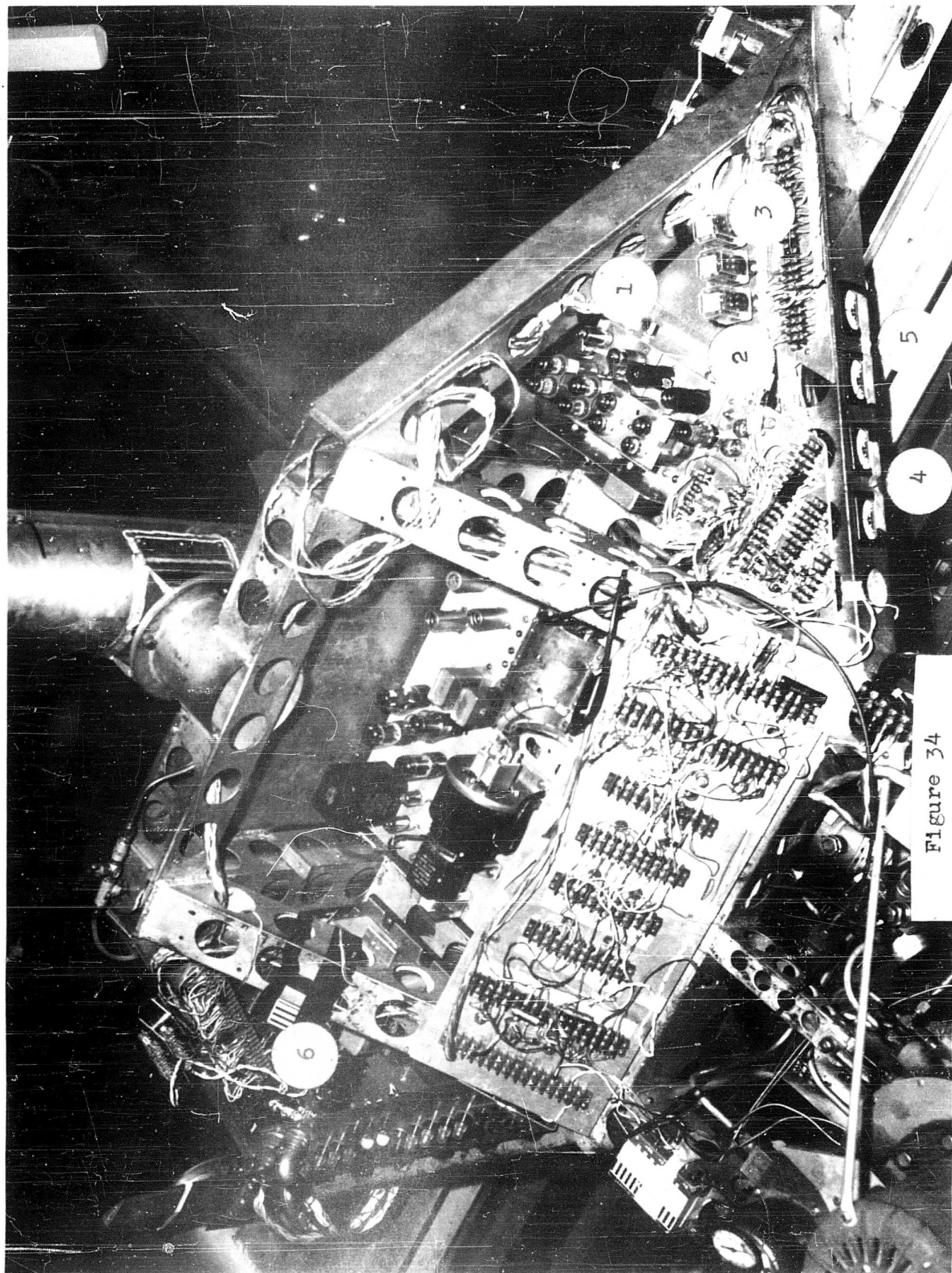


Figure 34

Figure 35

TELEMETER

1. Rotating commutator switch
2. Transmitter
3. Keyer
4. Patching board
5. Power supplies
6. Transmitter antenna

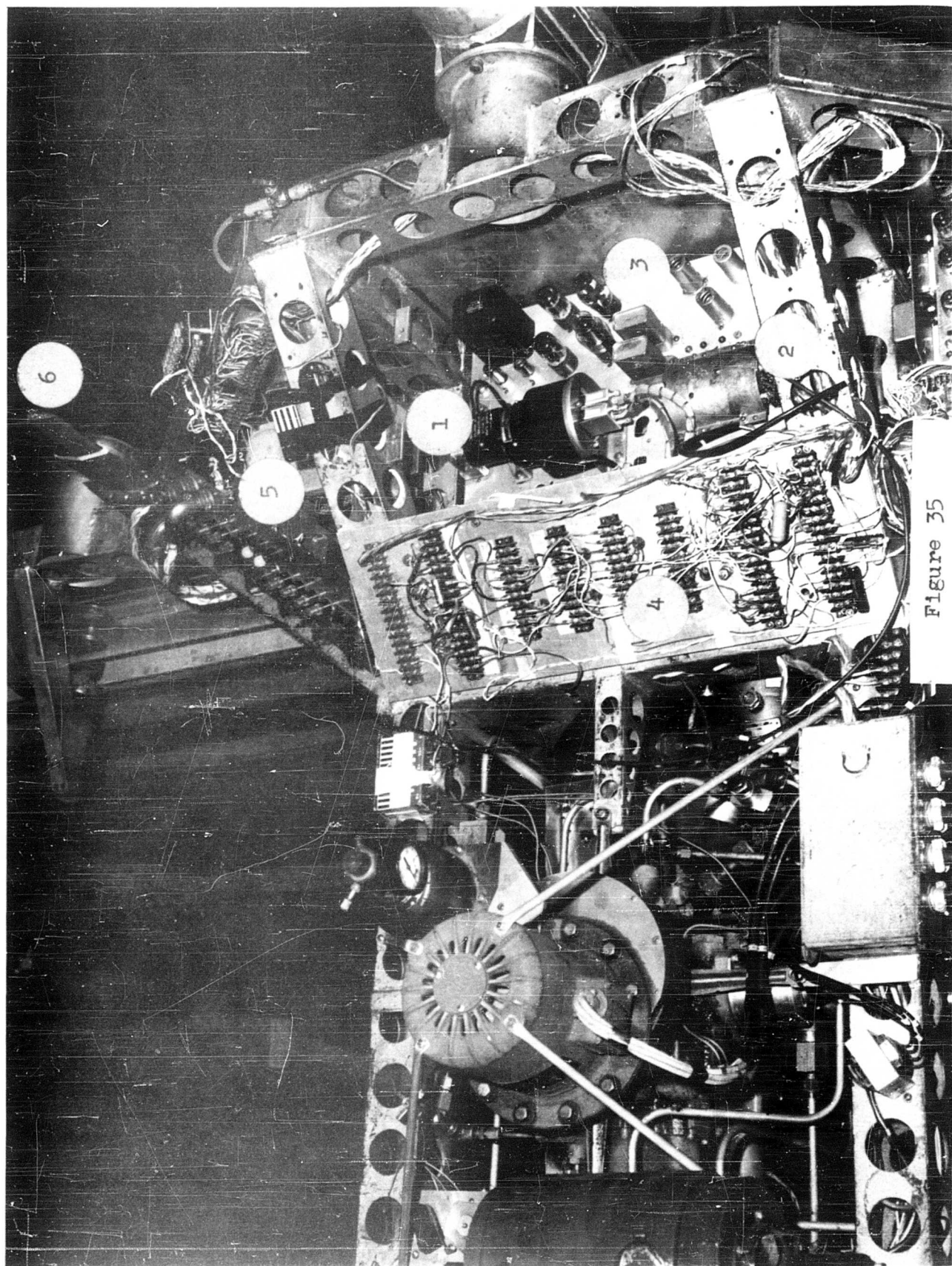


Figure 35

Figure 36

POWER SUPPLY INSTALLATION

1. Electric power supply
2. Fuses and warning lights
3. Pneumatic tank outlet

The integrated electric power supply furnishes the required different voltages for the servo operation and it also contains Zener diode regulated supplies for the instrumentation in general and for the excitation of various potentiometers.

24 volts D.C., 115 volts D.C. for power operations are available; 50 volts and 100 volts D.C. closely regulated are also available for instrumentation purposes.

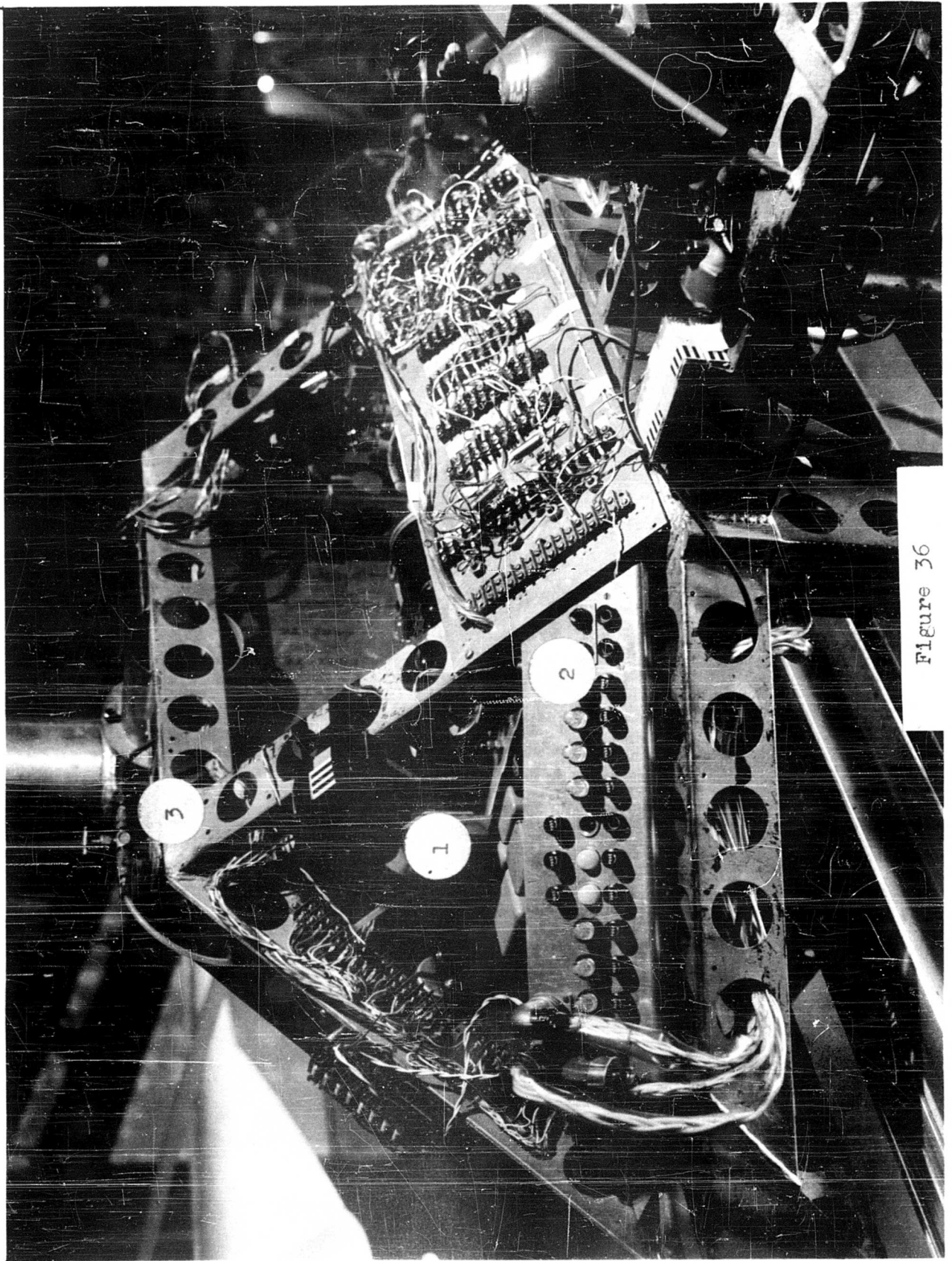


Figure 36

Figure 37

TWO DEGREE OF FREEDOM RIG

1. Support structure
2. Horizontal error link
3. Linear error potentiometer



Figure 37

Figure 38

CONTROL CONSOLE

1. Timing clocks
2. Telemetered data meter and scope presentation
3. Track atmospheric conditions instruments
4. Track controls

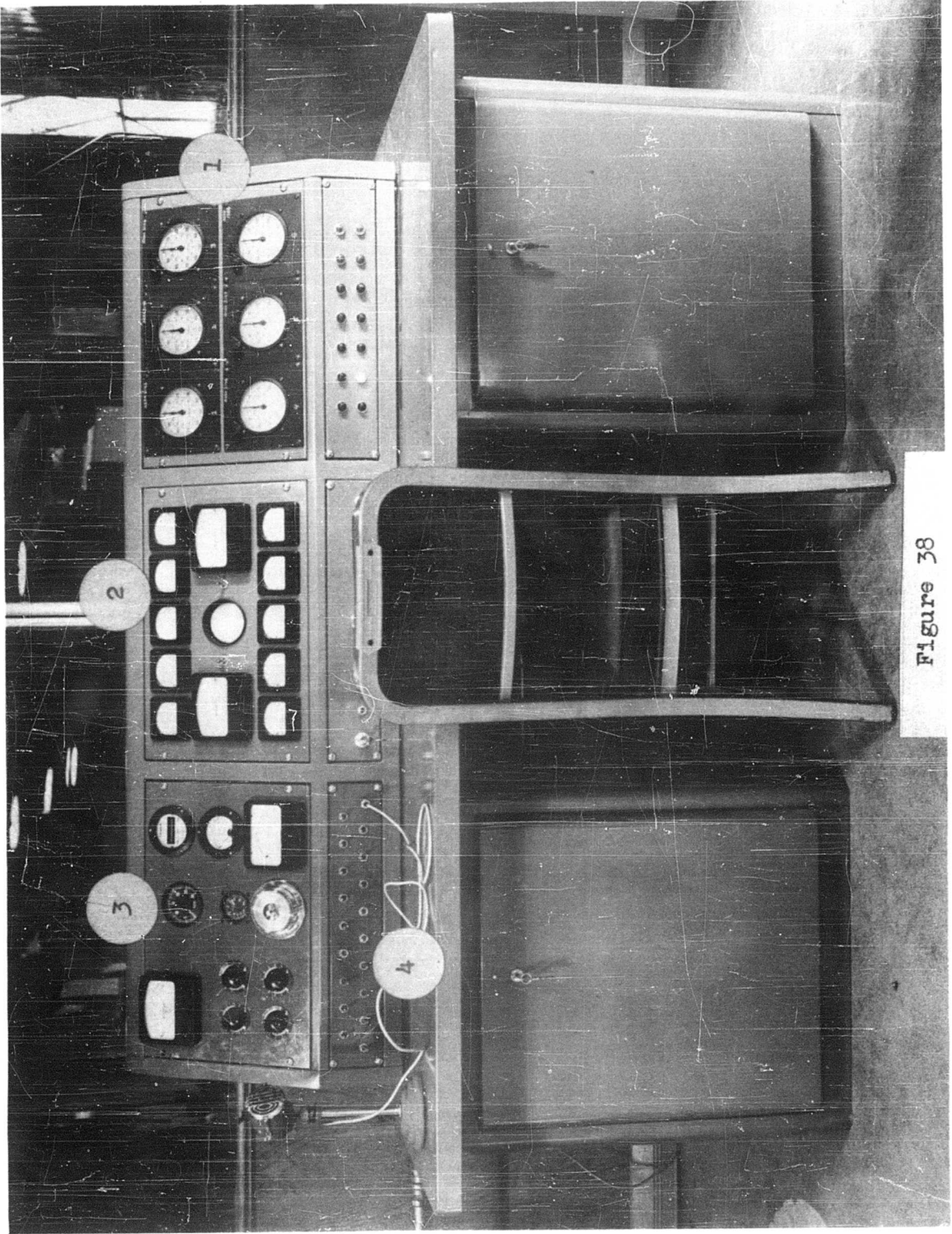


Figure 38

CONTROL CONSOLE

Figure 39

FORTY-FIVE CHANNEL SCOPE PRESENTATION
OF TEST DATA

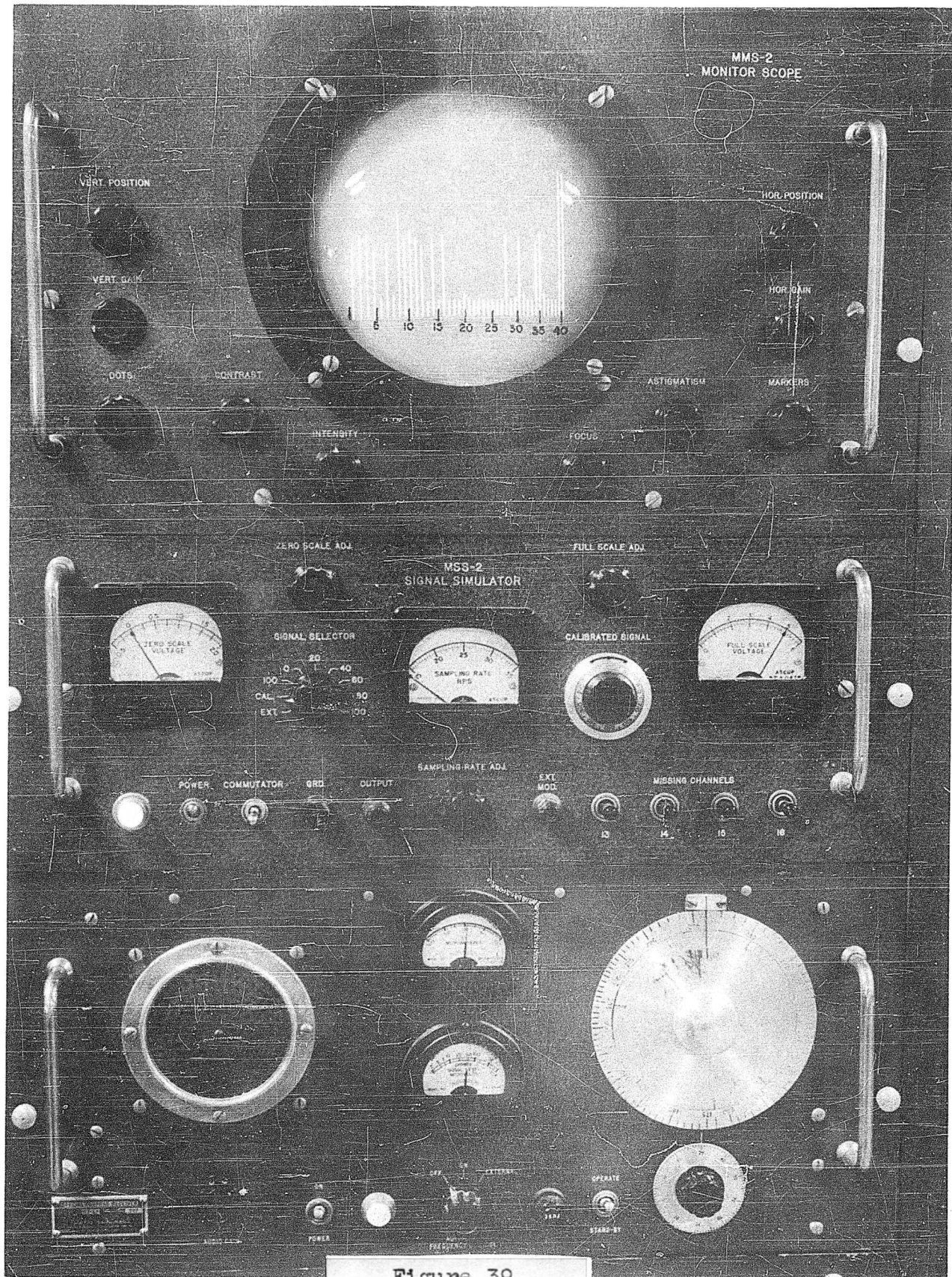


Figure 39

Figure 40

GROUND STATION
AND RECORDING EQUIPMENT

1. ASCOP Telemeter ground station
2. Ampex magnetic tape recorder
3. Sanborn paper recorder

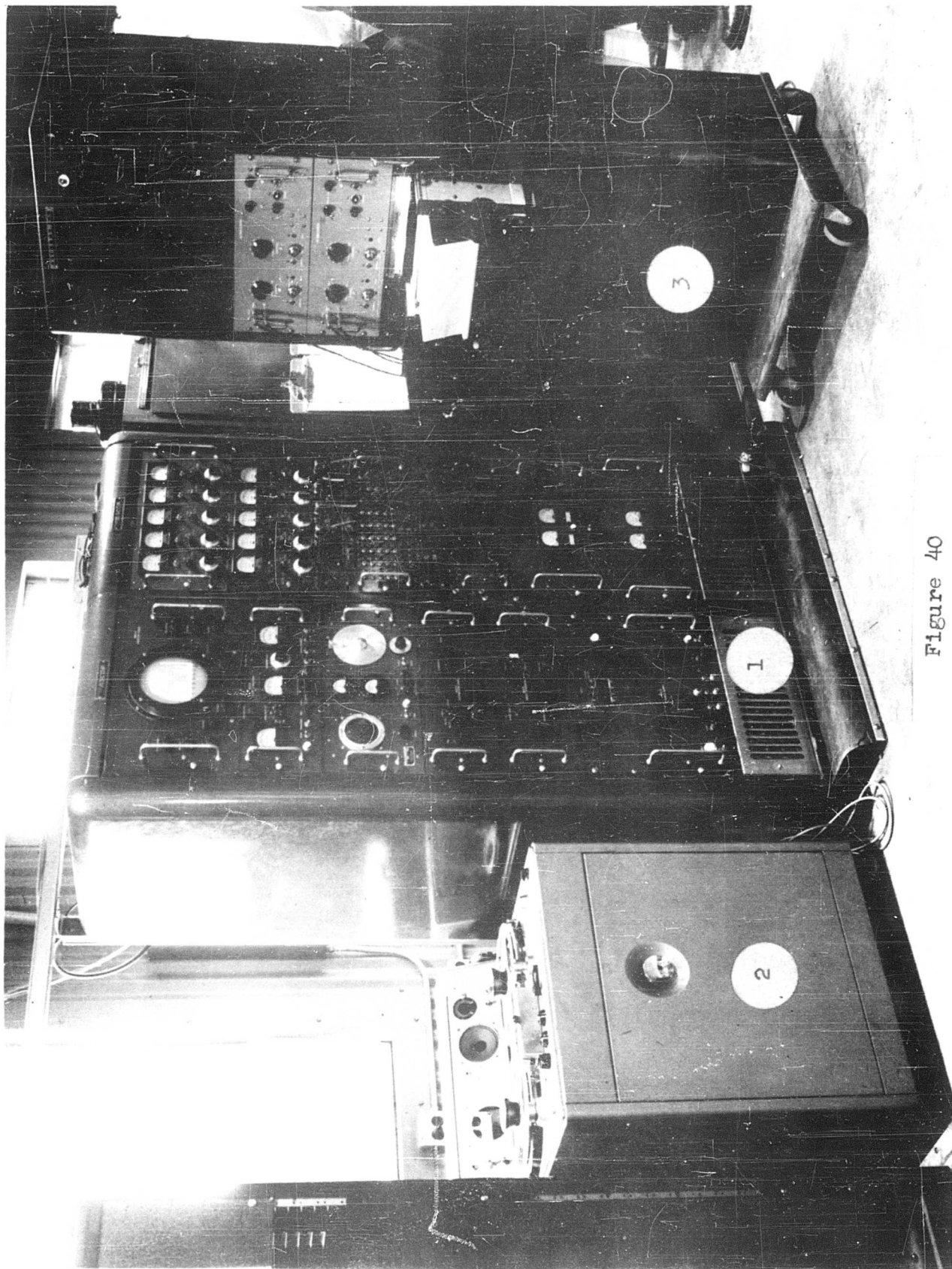


Figure 40

Figure 41

BOOST SYSTEM

1. Drive cable
2. Drum
3. Electric-powered clutch
4. Electric-powered brake
5. Limit switches
6. Boost speed feedback tachometer
7. Flywheel
8. Drive motor
9. Flywheel speed tachometer

The boost system is designed to accelerate the carriage up to 60 feet per second in a minimum track length. It overcomes the acceleration limitation of the carriage friction drive. It uses a 5 horsepower motor and a flywheel to deliver up to 35 horsepower.

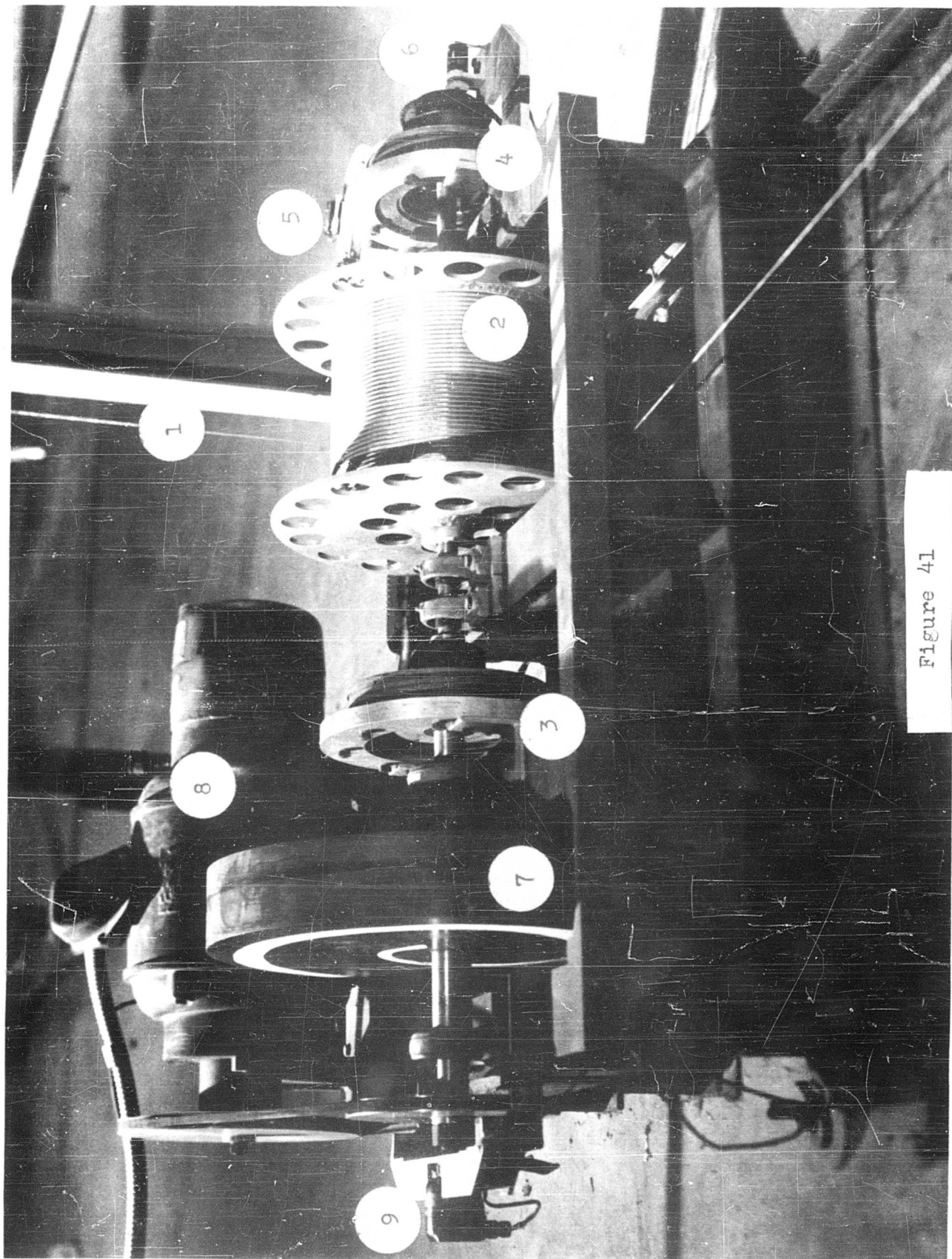


Figure 41

Figure 42

EMERGENCY MECHANICAL BRAKE

1. Brake cable
2. Drum
3. Electric brake
4. Rewind motor
5. Program cam
6. Velocity sensitive cutoff switch
7. Brake power supply
8. Photoelectric trigger

In the event of the failure of the normal built-in hydraulic brake, this emergency system will come into operation, first cutting off all power to the carriage, bringing the carriage to a stop before the end of the track, and then returning it to the normal braking area.

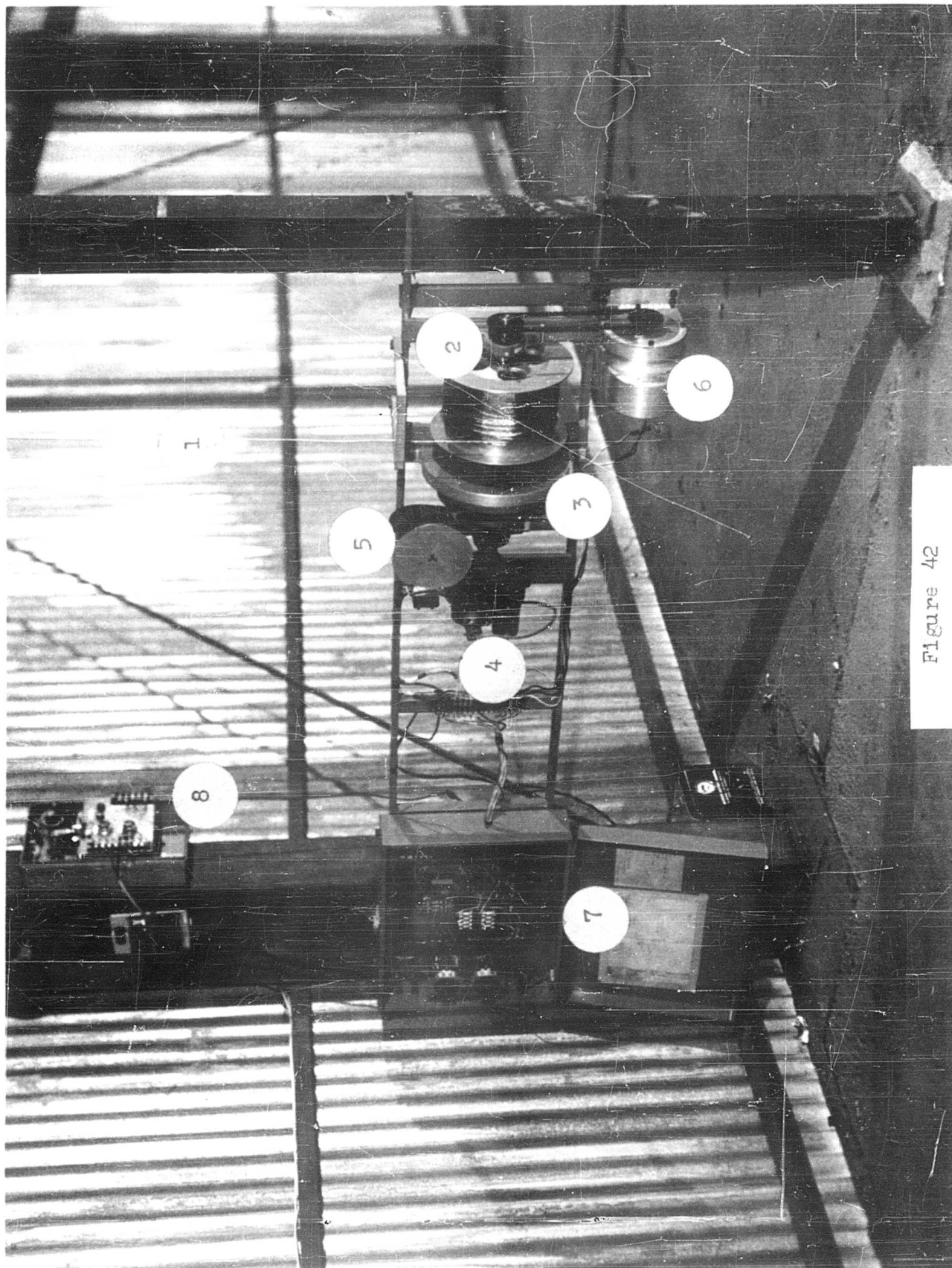


Figure 42

Figure 43

HOVERING TRACK -- SERVO CONTROLS

1. Electronic amplifier
2. Prime mover: General Electric 2 horsepower, 115 volts, 400 cycles, 11,000 rpm
3. Control elements: Four Raymond Laboratories magnetic fluid clutches.
4. Gearbox
5. Brake
6. Drive chain
7. Model motor Variac

The drive assembly is self-contained except for the model position signal. The signals for rate feedback and carriage velocity are obtained right at the output shaft of the drive.

Braking of the carriage at both ends of the track is also applied at the drive shaft and is controlled by a cam connected to it.

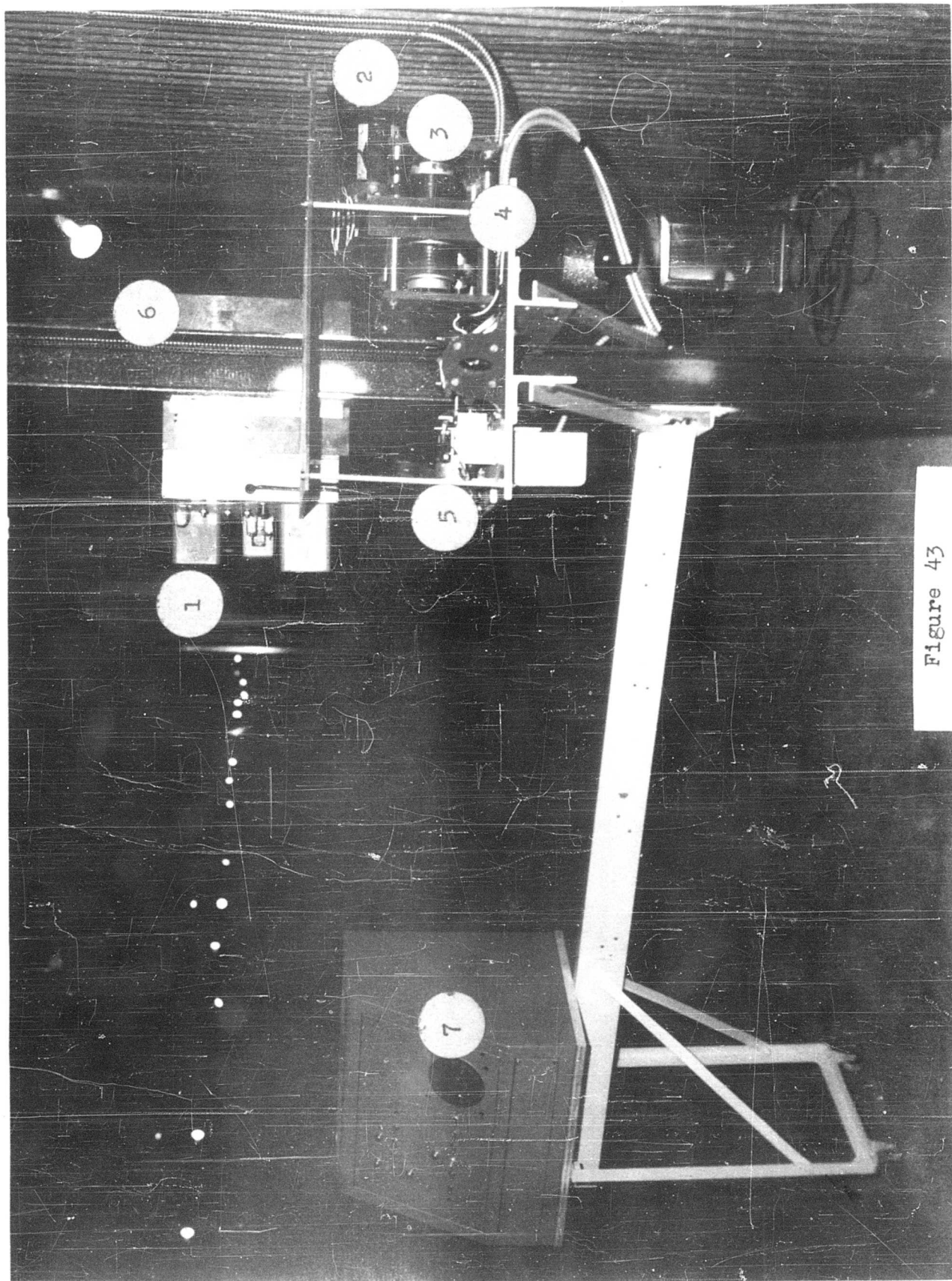


Figure 43

Figure 44

HOVERING TRACK -- GENERAL VIEW

1. Hovering carriage
2. Track
3. Error links
4. Drive chain
5. Servo amplifier
6. Fluid clutch servo drive
7. Control console

The hovering track is 50 feet long. The hovering carriage has an external drive and is moved by a drive chain. This permits an extremely light carriage structure, eliminating the friction drive limitations. Correspondingly high acceleration capabilities are obtained as required for the maximum time history of a hovering oscillation.

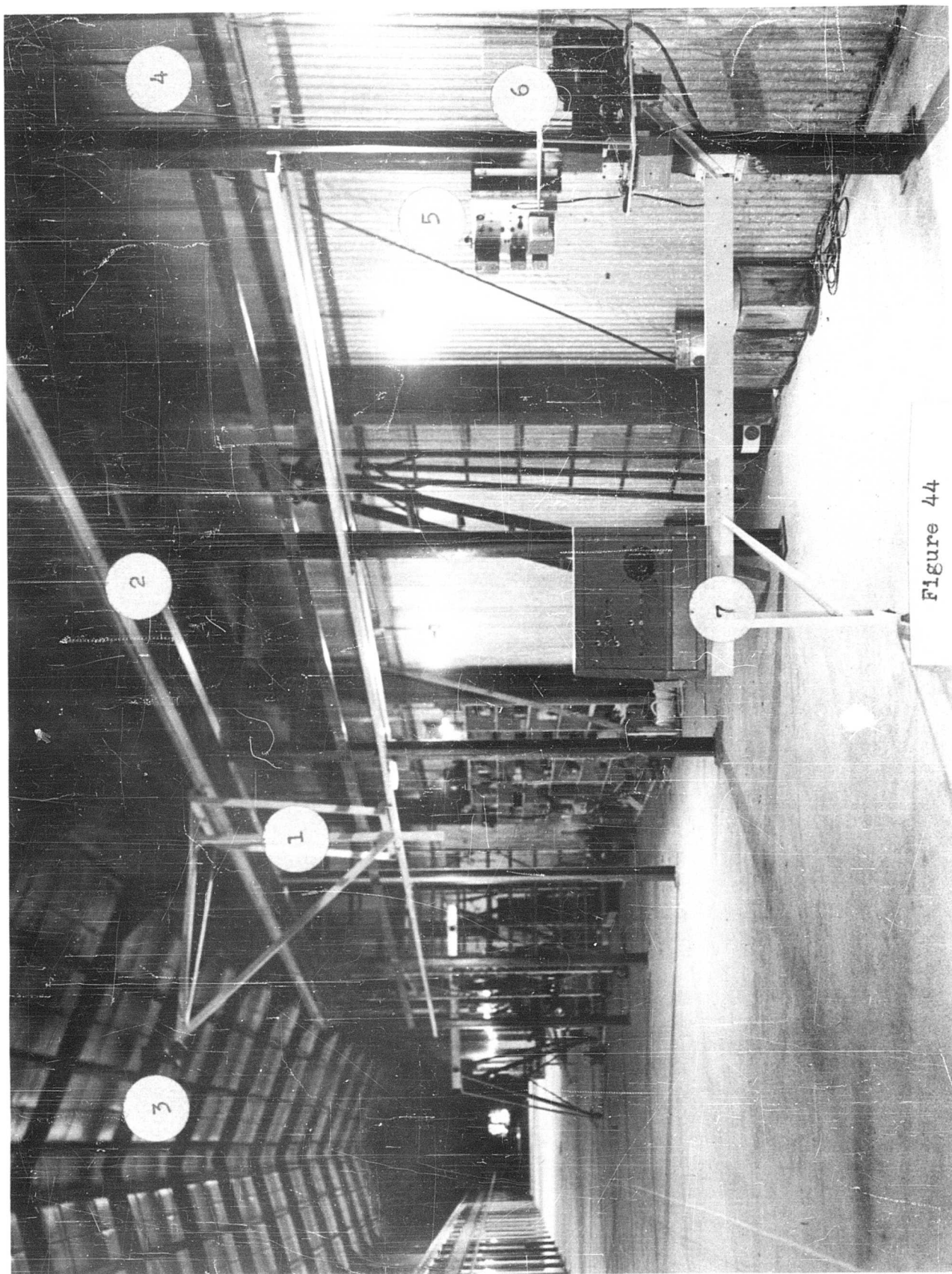


Figure 44

Figure 45

GROUND EFFECT MACHINE THREE DEGREE
OF FREEDOM RIG

1. Support structure
2. Horizontal and vertical freedom links
3. Ground effect machine model

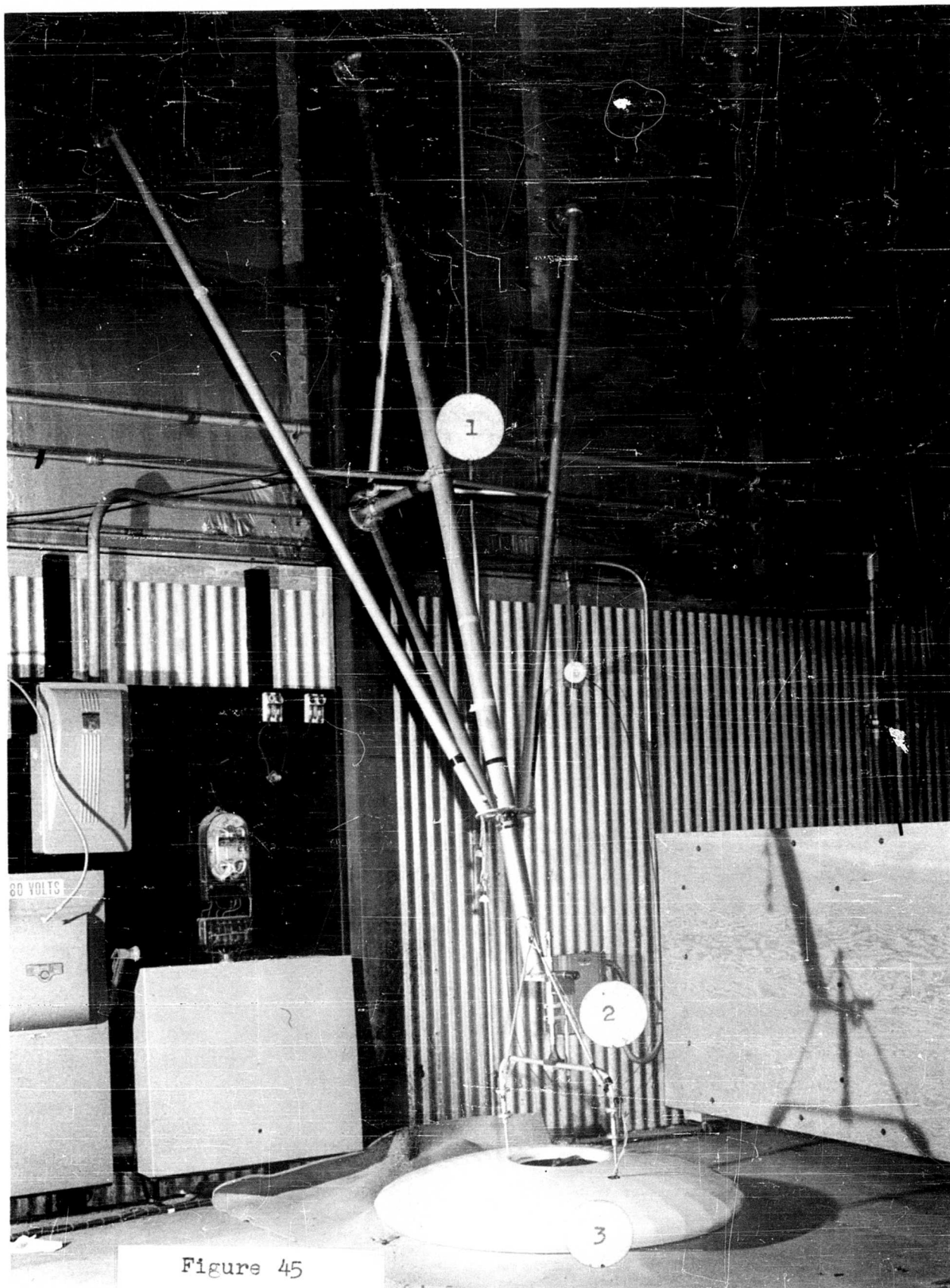


Figure 45

Figure 46

GROUND EFFECT MACHINE RIG — ERROR LINKS

1. Horizontal error link
2. Vertical error link
3. Error sending transducers: potentiometer and tachometer

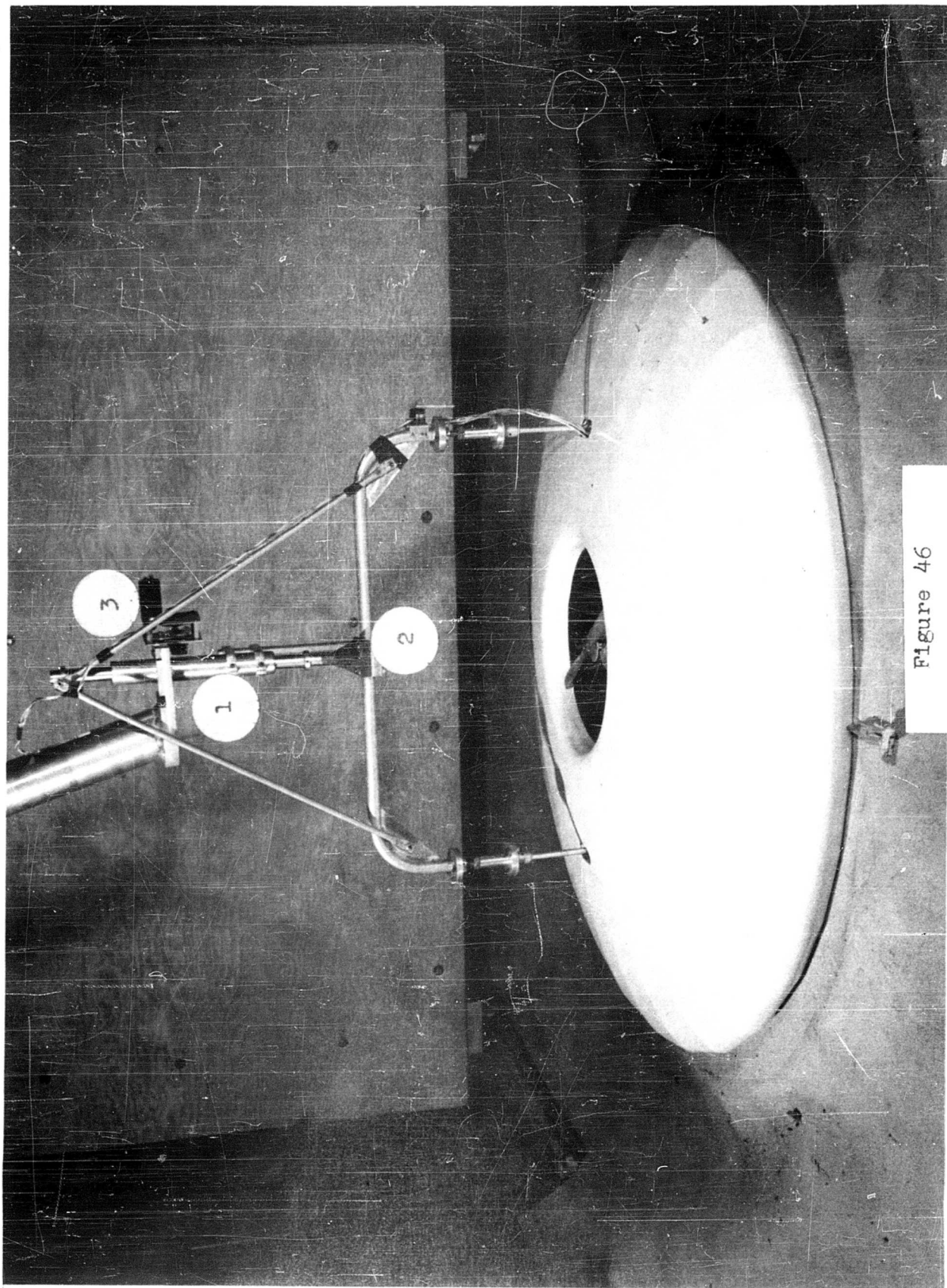


Figure 46

Figure 47

GENERAL VIEW OF CONTROL ROOM

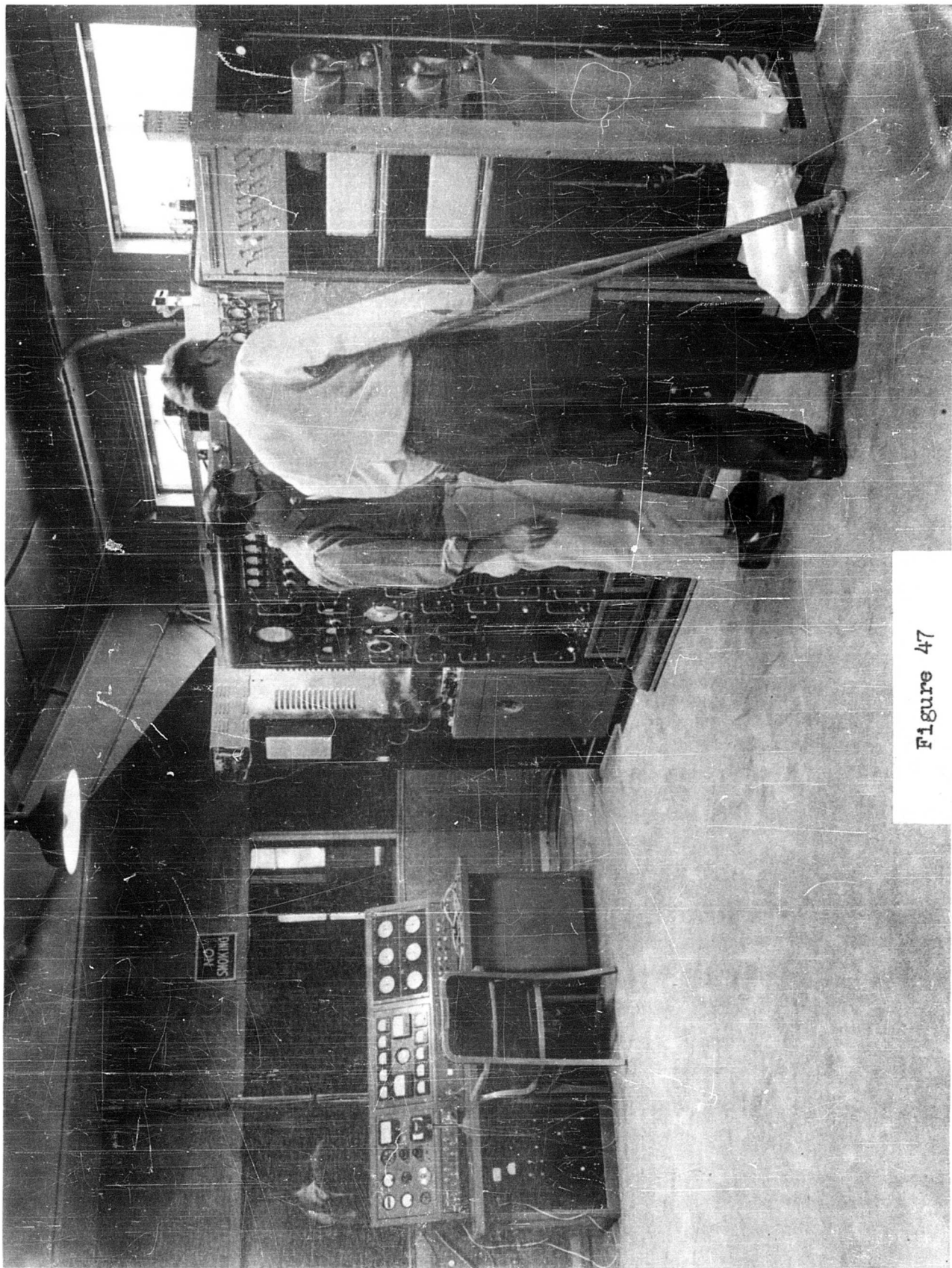


Figure 47

Figure 48

FLIGHT SIMULATION EQUIPMENT

1. GEDA analog computer -- model dynamics simulation board
2. Function generator
3. Sanborn recorder

The dynamics of the models developed by theoretical means can be conveniently set up in this analog computer. Arbitrary control inputs (such as a step function or an actual pilot control time history) can be applied to the simulated aircraft and its response is then obtained directly from the recorder.

Analog computer results are readily comparable with the experimental data furnished by the facility.

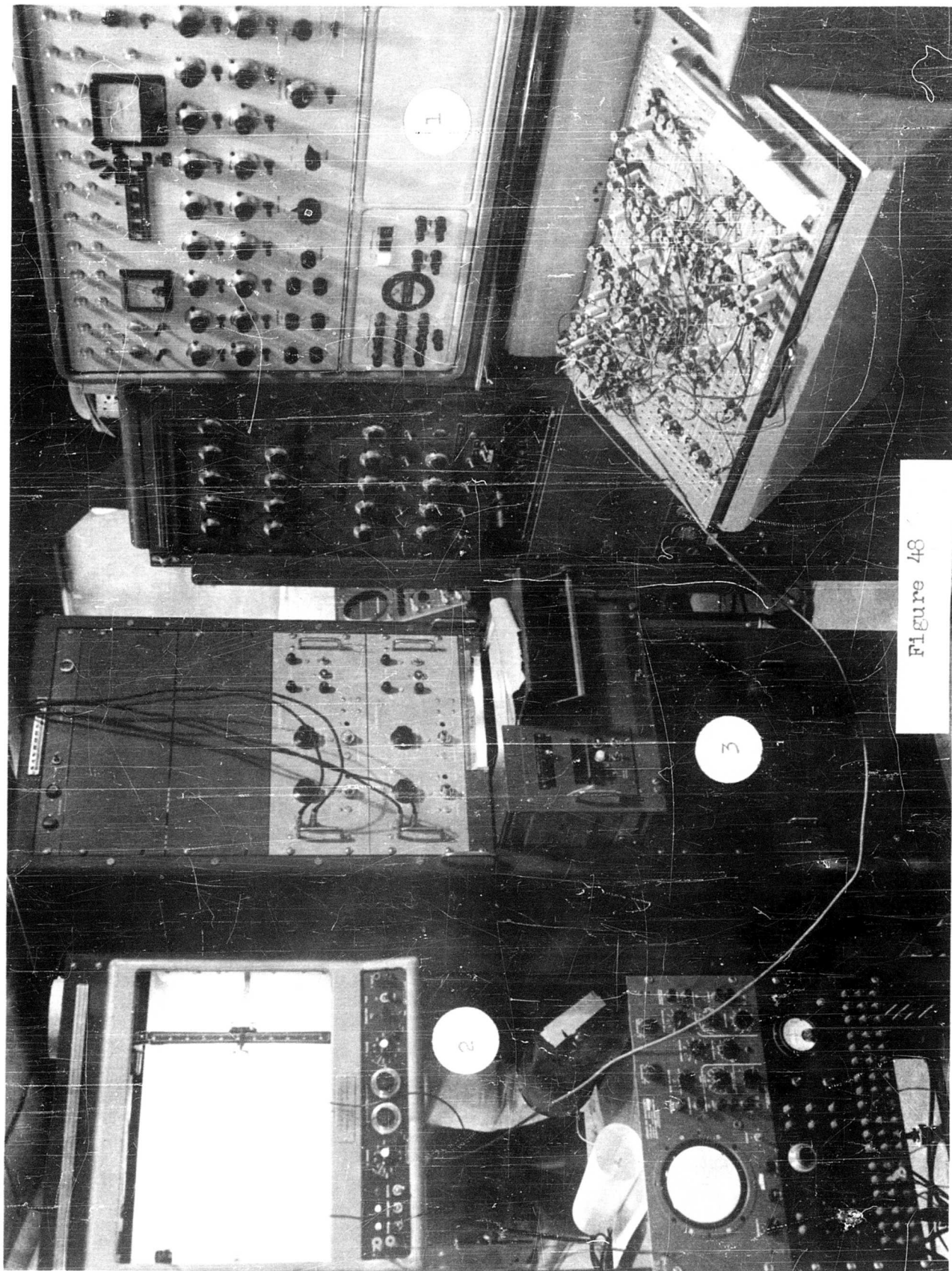


Figure 48

ALART PROGRAM
Technical Report
Distribution List

ADDRESS	NO. OF COPIES
1. Chief of Transportation Department of the Army Washington 25, D.C. ATTN: TCACR	2
2. Commander Wright Air Development Division Wright-Patterson Air Force Base, Ohio ATTN: WCLJA	2
3. Commanding Officer U.S. Army Transportation Research Command Fort Eustis, Virginia ATTN: Research Reference Center ATTN: Aviation Directorate	4 3
4. U.S. Army Representative HQ AFSC (SCR-LA) Andrews Air Force Base Washington 25, D.C.	1
5. Director Air University Library ATTN: AUL-8680 Maxwell Air Force Base, Alabama	1
6. Commanding Officer David Taylor Model Basin Aerodynamics Laboratory Washington 7, D.C.	1
7. Chief Bureau of Naval Weapons Department of the Navy Washington 25, D.C. ATTN: Airframe Design Division ATTN: Aircraft Division ATTN: Research Division	1 1 1
8. Chief of Naval Research Code 461 Washington 25, D.C. ATTN: ALO	1

	ADDRESS	NO. OF COPIES
9.	Director of Defense Research and Development Room 3E - 1065, The Pentagon Washington 25, D.C. ATTN: Technical Library	1
10.	U.S. Army Standardization Group, U.K. Box 65, U.S. Navy 100 FPO New York, New York	1
11.	National Aeronautics and Space Administration 1520 H Street, N.W. Washington 25, D.C. ATTN: Bertram A. Mulcahy Director of Technical Information	5
12.	Librarian Langley Research Center National Aeronautics & Space Administration Langley Field, Virginia	1
13.	Ames Research Center National Aeronautics and Space Agency Moffett Field, California ATTN: Library	1
14.	Armed Services Technical Information Agency Arlington Hall Station Arlington 12, Virginia	10
15.	Office of Chief of Research and Development Department of the Army Washington 25, D.C. ATTN: Mobility Division	1
16.	Senior Standardization Representative U.S. Army Standardization Group, Canada c/o Director of Weapons and Development Army Headquarters Ottawa, Canada	1
17.	Canadian Liaison Officer U.S. Army Transportation School Fort Eustis, Virginia	3

	ADDRESS	NO. OF COPIES
18.	British Joint Services Mission (Army Staff) DAQMG (Mov & Tn) 1800 K Street, N.W. Washington 6, D.C. ATTN: Lt. Col. R.J. Wade, R.E.	3
19.	Office of Technical Services Acquisition Section Department of Commerce Washington 25, D.C.	2
20.	Librarian Institute of the Aeronautical Sciences 2 East 64th Street New York 21, New York	2
21.	U.S. Army Research & Development Liaison Group APO 79 New York, New York ATTN: Mr. Robert R. Piper	1

AD _____	Accession No. _____	UNCLASSIFIED	AD _____	Accession No. _____	UNCLASSIFIED
Princeton University Aero. Eng. Dept., Princeton, N. J.		1. Helicopters, test facilities	Princeton University Aero. Eng. Dept., Princeton, N. J.		1. Helicopters, test facilities
A NEW FACILITY FOR THE STUDY OF AIRCRAFT DYNAMICS - E. Martinez		2. VTOL, Test methods	A NEW FACILITY FOR THE STUDY OF AIRCRAFT DYNAMICS - E. Martinez		2. VTOL, Test methods
Report No. 532, July 1961		3. Aircraft, Low speed, test facility	Report No. 532, July 1961		3. Aircraft, Low speed, test facility
Contract No. DA44-177-TC-524		4. Contract No. DA44-177 TC-524	Contract No. DA44-177-TC-524		4. Contract No. DA44-177 TC-524
Project No. 9-38-01-000, TK902			Project No. 9-38-01-000, TK902		
Unclassified Report			Unclassified Report		

AD _____	Accession No. _____	UNCLASSIFIED	AD _____	Accession No. _____	UNCLASSIFIED
Princeton University Aero. Eng. Dept., Princeton, N. J.		1. Helicopters, test facilities	Princeton University Aero. Eng. Dept., Princeton, N. J.		1. Helicopters, test facilities
A NEW FACILITY FOR THE STUDY OF AIRCRAFT DYNAMICS - E. Martinez		2. VTOL, Test methods	A NEW FACILITY FOR THE STUDY OF AIRCRAFT DYNAMICS - E. Martinez		2. VTOL, Test methods
Report No. 532, July 1961		3. Aircraft, Low speed, test facility	Report No. 532, July 1961		3. Aircraft, Low speed, test facility
Contract No. DA44-177-TC-524		4. Contract No. DA44-177 TC-524	Contract No. DA44-177-TC-524		4. Contract No. DA44-177 TC-524
Project No. 9-38-01-000, TK902			Project No. 9-38-01-000, TK902		
Unclassified Report			Unclassified Report		

This report describes a new facility for the study of the dynamic characteristics of helicopters, VTOL aircraft and ground effect machines by means of dynamically similar models. The test method consists of flying self-powered models in a protecting enclosure as a servo-carriage carrying the required instruments follows it closely. The information gathered by the instruments is transmitted to a ground station through a multi-channel telemeter link.

A discussion of the philosophy underlying the design and construction of the apparatus is included. Certain instrumentation problems peculiar to this type of facility are examined in detail. The data obtained from this facility shows remarkable repeatability and excellent correlation with the available full-scale information.

This report describes a new facility for the study of the dynamic characteristics of helicopters, VTOL aircraft and ground effect machines by means of dynamically similar models. The test method consists of flying self-powered models in a protecting enclosure as a servo-carriage carrying the required instruments follows it closely. The information gathered by the instruments is transmitted to a ground station through a multi-channel telemeter link.

A discussion of the philosophy underlying the design and construction of the apparatus is included. Certain instrumentation problems peculiar to this type of facility are examined in detail. The data obtained from this facility shows remarkable repeatability and excellent correlation with the available full-scale information.

This report describes a new facility for the study of the dynamic characteristics of helicopters, VTOL aircraft and ground effect machines by means of dynamically similar models. The test method consists of flying self-powered models in a protecting enclosure as a servo-carriage carrying the required instruments follows it closely. The information gathered by the instruments is transmitted to a ground station through a multi-channel telemeter link.

A discussion of the philosophy underlying the design and construction of the apparatus is included. Certain instrumentation problems peculiar to this type of facility are examined in detail. The data obtained from this facility shows remarkable repeatability and excellent correlation with the available full-scale information.

This report describes a new facility for the study of the dynamic characteristics of helicopters, VTOL aircraft and ground effect machines by means of dynamically similar models. The test method consists of flying self-powered models in a protecting enclosure as a servo-carriage carrying the required instruments follows it closely. The information gathered by the instruments is transmitted to a ground station through a multi-channel telemeter link.

A discussion of the philosophy underlying the design and construction of the apparatus is included. Certain instrumentation problems peculiar to this type of facility are examined in detail. The data obtained from this facility shows remarkable repeatability and excellent correlation with the available full-scale information.

UNCLASSIFIED

UNCLASSIFIED